2014 usa
dl 8/2018

NIH Public Access
Author Manuscript
Mol Aspects Med. Author manuscript; available in PMC 2015 April 01.

Published in final edited form as:
Mol Aspects Med. 2014 April ; 0: 1–55. doi:10.1016/j.mam.2013.08.002.

The Molecular Etiology and Prevention of Estrogen-Initiated Cancers

Ercole Cavalieri[*,1,2] and **Eleanor Rogan**[1,2]

[1]Eppley Institute for Research in Cancer and Allied Diseases, University of Nebraska Medical Center, 986805 Nebraska Medical Center, Omaha, Nebraska 68198-6805 USA

[2]Department of Environmental, Agricultural and Occupational Health, College of Public Health, University of Nebraska Medical Center, 984388 Nebraska Medical Center, Omaha, Nebraska 68198-4388 USA

Keywords

PAH radical cations; PAH diol epoxides; estrogen-3,4-quinones; depurinating PAH-DNA adducts; depurinating estrogen-DNA adducts; apurinic sites in DNA; preneoplastic mutations; mutations by error-prone repair; hormonal carcinogenesis; nonhormonal carcinogenesis; genotoxicity of estrogens; cytochrome P4501B1; 1,4-Michael addition mechanism; imbalance of estrogen homeostasis; carcinogenicity of 4-hydroxyestrogens; cancer prevention by N-acetylcysteine and resveratrol

1. Introduction

Exposure to estrogens has long been recognized as a risk factor for developing a variety of human cancers. To understand how estrogens can initiate the series of events leading to cancer, it is necessary to view estrogens as chemical carcinogens, rather than as hormones acting through receptor-mediated events.

Chemical carcinogens are characterized by a lack of common structural features. Most of them, approximately 95%, are metabolically activated to electrophilic forms that react covalently with the nucleophilic groups of DNA, RNA and protein (Miller and Miller, 1966, 1981a, 1981b). The remaining 5% are direct electrophilic alkylating agents that do not need metabolic activation. Thus, the common feature of chemical carcinogens is represented by their electrophilicity. Based on present knowledge and cellular functions, it is logical to assert that only the reaction of carcinogens with DNA generates the critical, irreversible mutations that lead to cancer initiation.

© 2013 Elsevier Ltd. All rights reserved.

[*]Corresponding author: Eppley Institute for Research in Cancer and Allied Diseases, University of Nebraska Medical Center, 986805 Nebraska Medical Center, Omaha, NE 68198-6805 USA, Telephone: 402-559-7237, Fax: 402-559-8068.

Publisher's Disclaimer: This is a PDF file of an unedited manuscript that has been accepted for publication. As a service to our customers we are providing this early version of the manuscript. The manuscript will undergo copyediting, typesetting, and review of the resulting proof before it is published in its final citable form. Please note that during the production process errors may be discovered which could affect the content, and all legal disclaimers that apply to the journal pertain.

Chemical Compounds:
estrone (PubChem CID: 5870); estradiol (PubChem CID: 5757); 2-hydroxyestradiol (PubChem CID: 247304); 4-hydroxyestradiol (PubChem CID: 5282360); estradiol-3,4-quinone (PubChem CID: 67402); benzo[*a*]pyrene (PubChem CID: 2336); 7,12-dimethylbenz[*a*]anthracene (PubChem CID: 6001); dibenzo[*a*,*l*]pyrene (PubChem CID: 9119); resveratrol (PubChem CID: 445154); N-acetylcysteine (PubChem CID: 12035)

NIH-PA Author Manuscript
NIH-PA Author Manuscript
NIH-PA Author Manuscript

NIH-PA Author Manuscript

NIH-PA Author Manuscript

NIH-PA Author Manuscript

Many fundamental principles of chemical carcinogenesis have been elucidated by studying polycyclic aromatic hydrocarbons (PAH), which are a class of chemicals that comprise very strong carcinogens. PAH were among the first compounds to be isolated from the environment and found to be carcinogenic (Cook et al., 1933; Hieger, 1930). Early on, theoretical studies suggested the K-region of PAH, which has a phenanthrene-like double bond, to be a critical reactive site (Pullman and Pullman, 1955). The K-region epoxides, however, showed little, if any, carcinogenic activity in laboratory animals (Sims, 1967) or ability to form DNA adducts (Baird et al., 1973), and this hypothesis was then disregarded.

The enhanced binding of a benzo[*a*]pyrene (BP) metabolite, the 7,8-dihydrodiol, to DNA, compared to the parent BP (Borgen et al., 1973), led Sims, Grover, Jerina and others in 1974 to propose the metabolic activation of PAH to ultimate carcinogenic metabolites by formation of the very electrophilic bay region diol epoxides (Jerina and Daly 1974, 1977; Sims et al., 1974; Sims and Grover, 1981). At the same time, it was determined that radical cations of BP and other potent PAH carcinogens were also capable of binding to DNA. Therefore, they were postulated to be ultimate carcinogenic metabolites of PAH (Cavalieri and Auerbach, 1974; Cavalieri and Roth 1976; Cavalieri et al., 1976; Fried, 1974; Fried and Schumm, 1967; Wilk et al., 1966; Wilk and Girke, 1972).

More recently, an extremely weak mechanism of metabolic activation for aromatic compounds has been determined for benzene (Cavalieri et al., 2002; Zahid et al., 2010b), the parent compound of aromatic chemistry, naphthalene (Saeed et al., 2007a, 2009a), and natural (Cavalieri et al., 1997; Li et al., 2004; Saeed et al., 2005b; Stack et al., 1996; Zahid et al., 2006) and synthetic (Jan et al., 1998; Saeed et al., 2005a, 2005b, 2009b) estrogens. In this mechanism, the aromatic compounds are metabolized to phenols; the phenols are further metabolized to catechols, which are then oxidized to the ultimate carcinogenic *ortho*-quinone metabolites. Reaction of the quinones with DNA produces specific adducts that generate mutations leading to initiation of cancer (see below Fig. 16) (Cavalieri and Rogan, 2011).

In this review, we will describe and discuss the mechanism of metabolic activation of estrogens that leads to the initiation of cancer, a mechanism that was discovered by building on the insights developed through studies of PAH carcinogenesis. Therefore, we will describe in detail the mechanism of metabolic activation by cytochrome P450, which catalyzes the oxidative metabolism of most carcinogens. Then, we will discuss the insights learned from studies of PAH carcinogenesis. These topics will set the stage for describing and discussing the mechanism of cancer initiation by estrogens. Finally, we will describe how knowledge of the mechanism of cancer initiation by estrogens provides the basis for approaches to the prevention of human cancer.

2. Cytochrome P450

a. Mechanism of oxygen transfer from cytochrome P450 to substrates as determined by using fluorobenzo[*a*]pyrenes

i. Fluorobenzo[*a*]pyrenes as probes for determining the mechanism of metabolic activation by cytochrome P450—BP consists of five condensed benzene rings, which afford 12 carbon atoms with different electron densities and double bonds displaying some ethylenic character (Fig. 1). The greatest reactivity of BP with electrophiles occurs at C-6, followed by C-1 and C-3 (Cavalieri and Calvin, 1971, 1972). In BP radical cation ($BP^{+\cdot}$), it is again C-6 that displays by far the major reactivity with nucleophiles (Blackburn et al., 1974; Caspary et al., 1973; Cavalieri and Auerbach, 1974; Cremonesi et al., 1989; Jeftic and Adams, 1970; Johnson and Calvin, 1973; Menger et al., 1976; Rochlitz, 1967; Stack et al., 1995; Wilk et al., 1966; Wilke and Girke, 1972). C-1 and C-3 follow in

NIH-PA Author Manuscript

NIH-PA Author Manuscript

NIH-PA Author Manuscript

decreasing order (Cavalieri and Calvin, 1971, 1972; Cremonesi et al, 1989). Experimental data indicate that the spin density in the high occupied molecular orbitals of $BP^{+\cdot}$, which follows the same pattern as the charge density, is greater at C-6, followed by C-1 and C-3 (Sullivan et al., 1985). These experiments are corroborated by molecular orbital calculations in BP (Loew, et al., 1978; Shipman, 1978) and $BP^{+\cdot}$ (Cavalieri et al., 1993; Mulder et al., 2003). The overall data suggest that electrophilic and nucleophilic substitution in BP and $BP^{+\cdot}$, respectively, should occur most easily at C-6, C-1 and C-3, in decreasing order. Furthermore, calculation of the bond orders of BP, 6-FBP, 1-FBP and 3-FBP display the highest electron density in the 4,5- double bond, followed by the 11,12-, 9,10- and 7,8- double bond (Cavalieri et al., 1993; Mulder et al., 2003).

When BP is metabolized by cytochrome P450, two classes of primary metabolites are obtained, BP phenols and BP dihydrodiols (Fig. 1) (Croy et al., 1976; Holder et al., 1974; Yang, et al., 1977). The major phenol obtained is 6-OHBP (Lesko et al., 1975; Lorentzen et al., 1975; Nagata et al., 1974). This metabolite is not isolated, however, because it is autoxidized to the secondary metabolites BP 1,6-, 3,6- and 6,12- quinone (Fig. 1). The other major phenol of BP is 3-OHBP, whereas the minor phenols obtained are 1-OHBP, 7-OHBP and 9-OHBP. The very small yield of 1-OHBP is presumably due to restrictions imposed by the binding site of the enzyme (Alpert and Cavalieri, 1980).

The second class of metabolites formed by BP is constituted by three dihydrodiols, BP - 4,5-, 7,8- and 9,10- dihydrodiol (Fig. 1). The dihydrodiols are obtained via two enzymatic steps, namely, formation of a BP epoxide, followed by hydrolysis catalyzed by epoxide hydrolase, to yield the dihydrodiol. The metabolic formation of dihydrodiols follows the same order as the calculated bond orders (see above), with the exception of the 11,12-dihydrodiol, which is not observed in the metabolism of BP, possibly due to hindrance of the binding site of the enzyme.

Fluorination of BP at C-6, C-1 and C-3 generated excellent probes for determining the mechanism by which the oxygen activated by cytochrome P450 is transferred from the enzyme to the substrate (Cavalieri et al., 1988b; Mulder et al., 2003). Combined studies of the chemistry of BP and 6-FBP, as well as the metabolism and molecular orbital calculations of BP, 6-FBP, 1-FBP and 3-FBP, enabled us to determine the mechanism of oxygen transfer by cytochrome P450 to BP to form 6-OHBP, 3-OHBP and 1-OHBP (Cavalieri et al., 1988b; Cremonesi et al., 1989; Mulder et al., 2003). Metabolism of 6-FBP by cytochrome P450 (Buhler et al., 1983; Cavalieri et al., 1988b), horseradish peroxidase (Cavalieri et al., 1988a) or prostaglandin H synthase (Cavalieri et al., 1988a) yielded the same metabolites as those obtained from BP (Cavalieri et al., 1988a, 1988b; Buhler et al., 1983). Displacement of the fluoro substituent from $6\text{-}FBP^{+\cdot}$ can occur only after attack by the activated nucleophilic oxygen (see below) of the enzyme. In fact, nucleophilic acetoxy substitution of $6\text{-}FBP^{+\cdot}$, obtained by oxidation of 6-FBP with manganic acetate, takes place exclusively at C-6, with displacement of the fluoro ion (Cremonesi et al., 1989). In addition, reaction of the synthesized BP radical cation perchlorate ($BP^{+\cdot}$ $C10_4^-$) with water yields the BP 1,6-, 3,6- and 6,12- quinones analogously to $BP^{+\cdot}$ formed in the metabolism of BP by cytochrome P450 (Cremonesi, P. et al., 1994). In contrast, typical electrophilic reactions of 6-FBP with the electrophiles trifluoro-deuteriated acetic acid (CF_3COOD) or pyridinium bromide perbromide yield 1,3-dideuteriated 6-FBP or a mixture of 1-Br-6-FBP and 3-Br-6-FBP, respectively, with retention of the fluoro substituent at C-6 (Cremonesi et al., 1989).

The calculated electron and charge densities in 6-FBP and $6\text{-}FBP^{+\cdot}$ resemble those of BP and $BP^{+\cdot}$, respectively, with the exception of C-6, which is positively charged in 6-FBP and even more so in $6\text{-}FBP^{+\cdot}$. This is due to the electron-withdrawing effect of the fluoro

NIH-PA Author Manuscript

NIH-PA Author Manuscript

NIH-PA Author Manuscript

substituent (Mulder et al., 2003). These values are in agreement with the electrophilic chemistry of 6-FBP and the nucleophilic chemistry of 6-$FBP^{+\cdot}$.

As previously suggested (Groves et al., 1981; Marnett et al., 1986), the remarkable reactivity of the activated oxygen of cytochrome P450 is attributed to an electrophilic oxo-Fe^{4+} porphyrin radical cation ($[Fe^{4+}=O]^{+\cdot}$, see Fig. 4 below) (Groves et al., 1981; Marnett et al., 1986). The first step in the metabolism of 6-FBP to produce the 1,6 - 3,6- and 6,12- quinone is the transfer of one electron from 6-FBP to $[Fe^{4+}=O]^{+\cdot}$ with formation of 6-$FBP^{+\cdot}$ and $Fe^{4+}=O$ (Fig. 2). The nucleophilic oxygen of $Fe^{4+}=O$ reacts at C-6 of 6-$FBP^{+\cdot}$ with subsequent removal of the fluoro ion. Then, the oxo-BP radical is oxidized by Fe^{4+}, with formation of an oxo-BP cation. Nucleophilic attack of water on the carbocation produces the 3,6-dihydroxyBP, which by autoxidation yields the corresponding BP-3,6-quinone. The BP-1,6-quinone and BP-6,12-quinone are formed analogously (not shown in Figure 2). Therefore, removal of the fluoro substituent from C-6 can occur only by formation of an intermediate 6-$FBP^{+\cdot}$ and attack of a nucleophilic oxygen of cytochrome P450. The fluoro substituent in 6-FBP cannot be removed by attack of an electrophilic oxygen of cytochrome P450 because the electrophilic oxygen cannot react with the positively charged C-6 in 6-FBP. Therefore, this demonstrates that the metabolite BP-3,6-quinone (and the BP-1,6- and 6,12-quinone, not shown in Figure 2) derive from attack of a nucleophilic oxygen in cytochrome P450 (Mulder et al., 2003).

Formation of the BP-1,6-quinone and BP-3,6-quinone from 1-FBP and 3-FBP, respectively, occurs by removal of the fluoro ion from C-1 or C-3, respectively (Mulder et al., 2003). This can occur only by an initial one-electron oxidation of 1-FBP or 3-FBP by the activated perferryl oxygen of cytochrome P450, with formation of 1-$FBP^{+\cdot}$ or 3-$FBP^{+\cdot}$, respectively. Analogously to 6-$FBP^{+\cdot}$ (Fig. 2), attack of the nucleophilic oxygen of cytochrome P450 on 1-$FBP^{+\cdot}$ or 3-$FBP^{+\cdot}$ yields BP-1,6-quinone or BP-3,6-quinone, respectively. Therefore, the minor metabolite 1-OHBP of BP and the abundant metabolite 3-OHBP of BP arise via oxygenation of 1-$BP^{+\cdot}$ and 3-$BP^{+\cdot}$, respectively.

Calculations of the bond orders of BP, 6-FBP, 3-FBP and 1-FBP show that the greatest electron density is in the 4,5- double bond, followed by the 11,12-, 7,8- and 9,10- in decreasing order (Mulder et al., 2003). The metabolic formation of dihydrodiols occurs at the same double bonds, with the exception of the 11,12-double bond, in which restriction is imposed by the enzyme binding site (Alpert and Cavalieri, 1980). These results lead us to hypothesize that the three dihydrodiols are obtained from abstraction of a π electron from one of these double bonds by the $[Fe^{4+}=O]^{+\cdot}$ of cytochrome P450, as illustrated for the formation of BP-7,8-dihydrodiol (Fig. 3). This is followed by a non-concerted oxygen rebound to the radical or cation of the double bond and subsequent closure, with formation of an epoxide. Hydrolysis of the epoxide, catalyzed by epoxide hydrolase, leads to the formation of BP-7,8-dihydrodiol (Fig. 3).

In summary, the metabolites formed by cytochrome P450-catalyzed oxidation of BP are obtained by abstraction of an initial π electron from BP by the $[Fe^{4+}=O]^{+\cdot}$ of cytochrome P450, with formation of $BP^{+\cdot}$ and $Fe^{4+}=O$. This is followed by transfer of the nucleophilic oxygen of $Fe^{4+}=O$ to C-6, C-3 and C-1, the most electropositive positions in $BP^{+\cdot}$, to form 6-OHBP (and then the three quinones formed by its autoxidation), 3-OHBP and 1-OHBP, respectively. Furthermore, if the $BP^{+\cdot}$ is located on the 4,5-, 7,8- or 9,10- double bond, the BP-4,5-, 7,8-, or 9,10-oxide is formed. Addition of water, catalyzed by epoxide hydrolase, yields the respective dihydrodiol.

ii. Mechanism of oxygen transfer from cytochrome P450 to substrates—

Characterization of the critical intermediates in the mechanism of oxygen transfer from

NIH-PA Author Manuscript

NIH-PA Author Manuscript

NIH-PA Author Manuscript

cytochrome P450s to specifically fluorinated BPs has enabled us to understand in a unified way the oxygenation of a variety of substrates. The overall reaction of cytochrome P450, monooxygenation, is represented as follows:

$$RH + O_2 \xrightarrow{2e,\ 2H^+} ROH + H_2O$$

where one oxygen atom of O_2 oxidizes the substrate RH and the other oxygen is reduced to H_2O. Two electrons and two protons are involved in the activation and cleavage of the O_2 to yield the oxygenated substrate and H_2O. The catalytic cycle presented in Figure 4 shows the mechanism of O_2 activation and the mechanism of oxygen transfer from cytochrome P450 to the substrate. The cycle begins with low-spin six-coordinate Fe^{3+} in the resting phase (**1**, Fig. 4), which has a cysteine thiolate and H_2O as axial ligands. The binding of the substrate RH gives rise to the high-spin five-coordinate derivative (**2**), with a higher reduction potential than (**1**). This is necessary to facilitate the electron transfer from cytochrome P450 reductase and yield the higher-spin five-coordinate Fe^{2+} (**3**). This intermediate is capable of binding O_2 to form the ternary $Fe^{2+}/RH/O_2$ complex (not shown in Fig. 4). Binding of O_2 presumably produces a low-spin six-coordinate Fe^{3+} intermediate, with a peroxy radical as the sixth ligand (**4**). One-electron reduction by cytochrome P450 reductase or cytochrome b_5 produces the peroxy anion (**5**). Addition of two protons leads to cleavage of the O-O bond to form H_2O and the perferryl Fe^{4+}. This reactive species, formally the Fe^{5+}, more likely corresponds to an Fe^{4+} porphyrin radical cation (Dawson, 1988; Groves et al., 1981; Marnett et al., 1986). An alternative pathway to produce directly the intermediate (**6**) from the high-spin Fe^{3+} (**2**), called the peroxide shunt, can occur in the presence of a peroxide cofactor that can donate an oxygen atom (Fig. 4).

The first step for substrates containing non-bonded or electrons consists of donation of an electron by the substrate RH to the perferryl oxygen radical cation (**6**), with formation of $RH^{+\cdot}$ and $Fe^{4+}=O$ (**7**, Fig. 4). This is followed by attack of the nucleophilic oxygen of (**7**) on $RH^{+\cdot}$ to yield (**8**) and subsequent formation of the oxygenated substrate ROH and the Fe^{3+} porphyrin (**9**).

When substrates, such as aliphatic compounds, contain only σ electrons, a mesomeric perferryl oxygen (**10**) is postulated, in which one electron of the $Fe^{4+}=O$ (**6**) neutralizes the radical cation and the other electron yields an oxygen radical (**10**). This oxygen radical intermediate, which is capable of abstracting a hydrogen atom from the substrate RH (Groves and McClusky, 1978), can be considered nucleophilic (Lewis et al., 1989). Oxygen rebound from the Fe^{4+}-OH (**11**) occurs with the carbon radical, $R^{\cdot}$, within a caged pair (Atkinson et al., 1994; Ortiz de Montellano and Stearns, 1987) to yield the oxygenated substrate ROH and the Fe^{3+} porphyrin (**9**).

In conclusion, for substrates containing non-bonded or π electrons, the electrophilic perferryl oxygen species (**6**) is converted to a nucleophilic oxygen species (**7**) by abstraction of one electron from the substrate. Instead, for compounds having only σ electrons, the cytochrome P450 oxygen species would be a mesomeric perferryl oxygen (**10**) capable of abstracting a hydrogen atom to form a carbon radical that leads to carbon hydroxylation.

b. Location of cytochrome P450 in the endoplasmic reticulum and nucleus of cells

The ultimate carcinogenic PAH radical cation metabolites are highly reactive and must be formed in close proximity to the nucleophiles with which they react. This requirement posed a problem for understanding how PAH radical cations might play a role in carcinogenesis. The problem was resolved, however, in the early 1970s, when cytochrome P450 activity was

NIH-PA Author Manuscript

NIH-PA Author Manuscript

NIH-PA Author Manuscript

detected in rat liver nuclei (Kasper, 1971; Khandwala and Kasper, 1973). Indeed, purified rat liver nuclei were found to have the capacity to covalently bind the PAH BP, 7,12-dimethylbenz[*a*]anthracene (DMBA) and 3-methylcholanthrene (MC) to DNA (Rogan and Cavalieri, 1974). Injection of the rats with MC to induce cytochrome P450 activity raised the level of binding of BP and DMBA to DNA approximately 4-fold (Rogan and Cavalieri, 1974) and that of MC, 7-methylbenz[*a*]anthracene, dibenz[*a*,*h*]anthracene or benz[*a*]anthracene (BA) 3 to 10-fold (Rogan et al., 1976). The enzymic binding activity was shown to be contained in the inner nuclear envelope (Rogan et al., 1976). The ability of the nuclei to bind PAH to DNA was subsequently confirmed in another laboratory (Vaught and Bresnick, 1976).

The amount of cytochrome P450 in the nucleus is about 10% of that present in microsomes prepared from the same rat liver cells (Rogan et al., 1976). Most of the PAH that enters a cell is likely to be metabolized to nonreactive, water-soluble products for excretion. These studies showed, however, that if PAH travel to the cell nucleus, the cytochrome P450 present there can catalyze formation of PAH metabolites that covalently bind to DNA. Metabolic activation by one-electron oxidation can occur because of the proximity between the DNA, PAH and nuclear cytochrome P450. This was demonstrated by identification of the depurinating DNA adduct BP-6-N7Gua after incubation of BP with purified rat liver nuclei (Cavalieri et al., 1990a).

Formation of a PAH-DNA adduct by one-electron oxidation requires the PAH to intercalate in the DNA and develop a physical complex with the DNA as a preliminary step to produce a covalent bond. The very low level of binding of BP, DMBA or dibenzo[*a*,*l*]pyrene (DB[*a*,*l*]P) to single-stranded DNA or RNA, compared to their binding to double-stranded DNA, demonstrates the requirement for this initial physical complex (Devanesan et al., 1993; Li et al., 1995; Rogan et al., 1993).

One can propose a model for the binding of PAH to DNA by one-electron oxidation. In this model, the PAH would bind to cytochrome P450 nearby in the nuclear envelope, and the cytochrome P450 would catalyze one-electron oxidation of the PAH to form its radical cation. This reactive intermediate would then diffuse toward the DNA, where it could be intercalated. Once there, reaction could occur at one of the nucleophilic sites of Ade or Gua. The much lower level of binding to denatured DNA or RNA, which are less well-structured nucleic acids than native DNA, would arise because the PAH radical cation could not achieve the proper orientation for a transition state that can yield the adducts observed with double-stranded DNA.

This mechanism is possible only if the radical cation can diffuse from the nuclear membrane-bound cytochrome P450 to the DNA binding site faster than the radical cation decays. The time required for diffusion can be estimated by taking into account typical diffusion coefficients of PAH and similar molecules in aqueous systems. By this method, the time required for a PAH radical cation to diffuse 1 micron would be on the order of 0.5×10^{-3}s (Cavalieri and Rogan, 1998). If a radical cation can survive that long, it could be generated at the cytochrome P450 binding site and react with the DNA. The radical cations of BP and 6-CH_3BP stabilized by anions such as perchlorate or fluoroborate in acetonitrile have half-lives ranging from less than 1 min to a few min, respectively (Cavalieri et al., 1985). Although radical cations generated in a cell nucleus would not be as stabilized as the ones above, it is reasonable to assume that they live long enough to travel from nuclear cytochrome P450 to DNA (Cavalieri and Rogan, 1998).

NIH-PA Author Manuscript

NIH-PA Author Manuscript

NIH-PA Author Manuscript

3. Ultimate carcinogenic metabolites of aromatic hydrocarbons

The approach to understanding the mechanisms of cancer initiation is based on several lines of investigation. These include metabolic studies, identification and quantification of DNA adducts, the relationship of DNA adducts to oncogenic mutations, and carcinogenicity experiments in various target organs.

The two major mechanisms of metabolic activation of PAH are formation of radical cations (Cavalieri and Auerbach, 1974; Cavalieri and Roth, 1976; Cavalieri, et al., 1976, 1990a, 2005; Devanesan et al., 1993; Fried, 1974; Fried and Schumm, 1967; Rogan et al., 1990, 1993; Wilk, et al., 1966; Wilk and Girke, 1972) and bay region diol epoxides (Conney, 1982; Dipple et al., 1984; Gelboin, 1980; Jerina and Daly, 1974, 1977; Sims and Grover, 1981; Sims et al., 1974). Some PAH are activated by both of these major mechanisms and some by only one of these two mechanisms. For example, activation of the very potent PAH DB[*a,l*]P proceeds via formation of both the radical cation and the diol epoxide (Fig. 5) (Cavalieri et al., 2005; Todorovic et al., 2005). DB[*a,l*]P is activated by cytochrome P450 or peroxidases to form radical cations with charge mainly localized at C-10. Reaction of this intermediate with DNA nucleophiles can lead to cancer initiation. In the diol epoxide pathway, DB[*a,l*]P proceeds via formation of an 11,12-epoxide, catalyzed by cytochrome P450, followed by hydrolysis catalyzed by epoxide hydrolase to the proximate carcinogenic metabolite, the 11,12-dihydrodiol. In turn, this metabolite is converted by cytochrome P450 to the ultimate carcinogenic metabolite DB[*a,l*]P-11,12-diol-13,14-epoxide. Covalent binding of this metabolite to DNA can lead to the initiation of cancer.

A third important mechanism of metabolic activation of the aromatic hydrocarbons benzene, naphthalene and estrogens is due to the formation of ultimate carcinogenic electrophilic *o*-quinones (see Section 9) (Cavalieri and Rogan, 2011)

a. PAH radical cations

Development of the chemistry of PAH radical cations has provided evidence that these intermediates play a very important role in cancer initiation by the most potent PAH (Cavalieri and Rogan, 1985, 1992, 1998). Radical cations of unsubstituted and methyl-substituted PAH have been generated by iodine oxidation (Cavalieri and Roth, 1976; Cavalieri et al., 1976; Hanson et al., 1998), manganic acetate oxidation (Cremonesi et al., 1989, 1992a; Rogan et al., 1980), and electrochemical oxidation (RamaKrishna et al., 1992a, 1992b, 1993a, 1993b; Rogan et al., 1988), with subsequent binding to a nucleophile. Furthermore, radical cations of BP and derivatives have been isolated as radical cation perchlorates after oxidation with iodine in the presence of silver perchlorate (Cremonesi et al., 1994; Stack et al., 1995).

Removal of one electron from the π system generates a radical cation (Fig. 6), in which the positive charge can be mainly localized at an unsubstituted carbon atom (Path 1) or adjacent to a methyl group (Path 2). Nucleophilic attack at the position of highest charge density in Path 1 produces an intermediate radical that is further oxidized to an arenium ion to complete the substitution reaction. When the charge is localized adjacent to the methyl group (Path 2), loss of a methyl proton generates a benzylic radical intermediate, which is rapidly oxidized to a benzylic carbenium ion with subsequent trapping by a nucleophile.

The physico-chemical properties of PAH radical cations are very important for demonstrating that these intermediates play a major role in the covalent binding to DNA catalyzed by cytochrome P450 and peroxidases. The rationale for asserting that radical cations play a primary role in metabolic activation of PAH derives from common features that belong to the most potent carcinogenic PAH, such as BP, DB[*a,l*]P, DMBA and MC.

NIH-PA Author Manuscript

NIH-PA Author Manuscript

NIH-PA Author Manuscript

These common characteristics are (1) a relatively low ionization potential (IP), which allows easy removal of one electron with formation of a relatively stable radical cation; (2) charge localization in the radical cation that renders this intermediate specifically and efficiently reactive toward nucleophiles; and (3) optimal geometric configuration that allows formation of appropriate intercalating physical complexes with DNA, thus favoring formation of covalent bonds with DNA.

i. Ionization potential—The ease of formation and relative stability of PAH radical cations is related to their IP. Above a certain IP, the radical cation is unstable due to the more difficult removal of one electron by cytochrome P450 or peroxidase, and it is unable to react with nucleophilic groups in DNA. In contrast, for PAH with lower IP, the radical cations are sufficiently stable to undergo reaction with cellular nucleophiles. Approximately 7.35 eV is the cut-off IP above which a radical cation is not sufficiently stable for reaction. This value is based on the level of DNA binding for a series of PAH with IP ranging from 8.19 eV (phenanthrene) to 6.68 eV (6,12-dimethylanthanthrene), catalyzed by horseradish peroxidase or prostaglandin H synthase (Cavalieri et al., 1983; Devanesan, et al., 1987). A similar cut-off IP for cytochrome P450 can be assumed. Therefore, the IP of a PAH serves as one guideline as to whether or not a PAH can be metabolically activated to a radical cation ultimate carcinogenic metabolite.

ii. Charge localization—A relatively low IP is a necessary, but not sufficient, prerequisite for activation of a PAH to its ultimate radical cation. Another important factor that must be considered is the localization of charge in the PAH radical cation. Condensation of benzene rings to form PAH reduces the delocalization of the π electrons found in benzene, resulting in positions of unequal charge localization. The extent of unequal distribution depends also on the symmetry of the condensed benzene rings. For example, the PAH perylene, which has a low IP but is highly symmetric, is not carcinogenic because the charge is not localized in its radical cation and the molecule does not react with nucleophiles. Typically, the *meso*-anthracenic positions in PAH have high electron charge. When one electron is removed to form a radical cation, the *meso*-anthracenic position with the highest charge density in the neutral molecule will have the highest positive charge in the radical cation. For example, in BP, C-6 is the position with the greatest electron density and the highest reactivity with electrophiles in the neutral molecule (Cavalieri and Calvin, 1971). In BP radical cation, C-6 has the lowest electron density and the highest reactivity with nucleophiles (Cavalieri and Auerbach, 1974; Cremonesi et al., 1989; Jeftic and Adams, 1970; Rochlitz, 1967; Wilk et al., 1966; Wilke and Girke, 1972). Therefore, the relatively low IP for BP, 7.23 eV, and charge localization at C-6 render this molecule susceptible to forming a BP radical cation with reactivity to nucleophiles.

Radical cations of unsubstituted- and methyl-substituted PAH have been obtained by oxidation of the PAH with iodine, manganic acetate or electrochemical oxidation and subsequent trapping with nucleophiles (see above). Specificity of the reactivity of radical cations derives from charge localization in one or a few carbon atoms of the PAH that are, in general, the *meso*-anthracenic position(s). Development of the radical cation chemistry of PAH has allowed designation of the position(s) of specific reactivity of PAH radical cations. For BP and DB[*a*,*l*]P, the charge in the radical cation is mainly at C-6 and C-10, respectively (Cremonesi et al., 1989, 1992a). Nucleophilic substitution occurs regiospecifically at those positions with subsequent formation of an intermediate radical (Fig. 6, Path 1). This intermediate is rapidly oxidized to an arenium ion with loss of a proton to complete the substitution reaction.

When the charge is mainly localized at a carbon atom adjacent to a methyl group, as in 6-methylBP, loss of a methyl proton is favored by the partial alignment of the C-H bond with

NIH-PA Author Manuscript

NIH-PA Author Manuscript

NIH-PA Author Manuscript

the adjacent *p*-orbital (Fig. 6, Path 2, and Fig. 7). The benzylic radical formed is rapidly oxidized to a carbenium ion that reacts with a nucleophile (Cremonesi et al., 1989). When the positive charge in the radical cation is located adjacent to an ethyl group, such as in 6-ethylBP (Fig. 7), reaction cannot occur at the benzylic methylene because the C-H bond is much less favorably aligned with the adjacent *p*-orbital than the C-H bond of 6-methylBP. This less favorable alignment does not cause deprotonation, and subsequently nucleophilic attack cannot occur at the benzylic methylene group (Cavalieri and Roth, 1976; Tolbert et al., 1990). On the contrary, perfect alignment between the methylene group and the *p*-orbital occurs in the strong carcinogen MC, because the condensation of cyclopentadiene to the BA moiety forces the CH_2 to align optimally with the *p*-orbital at the *meso*-anthracenic position (Fig. 7). The fact that *meso*-anthracenic ethyl-substituted PAH are not carcinogenic (Pataki and Balic, 1972), whereas the corresponding methyl derivatives are carcinogenic, provides further evidence that radical cations of these compounds play the primary role in their metabolic activation.

iii. Optimal geometric configuration—An important factor for PAH to display carcinogenic activity is related to the geometry of the molecule. In general, carcinogenic activity is found in PAH containing three to seven condensed rings (Arcos and Argus, 1974). A more precise requirement concerning the geometric characteristics of PAH is the presence of an angular ring, for example, in the BA series. This ring is essential for eliciting carcinogenic activity, regardless of whether it is aromatic or aliphatic (Arcos and Argus, 1974; Cavalieri et al., 1990b). Optimal geometric configuration of PAH is essential for forming the preliminary, appropriate intercalation complexes with DNA that are a prerequisite for the formation of a covalent bond with nucleophilic groups (Lesko et al., 1968). A strong piece of evidence for the formation of these intercalation physical complexes was derived from the demonstration that depurinating DNA adducts formed from radical cations of BP, DMBA or DB[*a*,*l*]P can be observed with double-stranded DNA, but not with single-stranded DNA or RNA (Cavalieri et al., 2005; Devanesan et al., 1993; Li et al., 1995; Rogan et al., 1993).

b. PAH diol epoxides

Formation of bay region diol epoxides is the second major mechanism of metabolic activation of PAH (Fig. 5). We report here some of the data concerning three moderately potent carcinogens, namely, 5-methylchrysene, BA and dibenz[*a*,*h*]anthracene (Fig. 8). The experimental data for these compounds are consistent with activation through the diol epoxide pathway.

All of the experimental data concerning the mechanism of cancer initiation by 5-methylchrysene are consistent with activation by the diol epoxide pathway. This compound has an IP too high to be activated via the radical cation pathway (Table 1). Studies of the metabolism, mutagenicity and carcinogenicity of 5-methylchrysene and its monofluorinated derivatives (Amin et al., 1985, 1987; Hecht et al., 1978a, 1978b, 1979a, 1979b) clearly indicate that the 1,2-diol-3,4-epoxide of 5-methylchrysene is the key ultimate carcinogenic metabolite of this compound. Characterization of the DNA adducts of 5-methylchrysene formed *in vitro* and *in vivo* was also consistent with the diol epoxide mechanism of activation (Melikian et al., 1982, 1983; Peltonen et al., 1991; Reardon et al., 1987).

Dibenz[*a*,*h*]anthracene also has an IP too high for this compound to be activated via the radical cation pathway (Table 1). This symmetrical compound can form not only the bay-region 3,4-diol-1,2-epoxide, but also the 3,4:10,11-bis-diol-1,2-epoxide (Carmichael et al., 1993; Fuchs et al., 1993a, 1993b). When the metabolism, mutagenicity, carcinogenicity and formation of DNA adducts of this compound were studied, all of the results indicated that it

NIH-PA Author Manuscript

NIH-PA Author Manuscript

NIH-PA Author Manuscript

is activated via the diol epoxide pathway (Fuchs et al., 1993a, 1993b; Lecoq et al., 1991, 1992; Platt, et al., 1990). One study suggests that the 3,4:10,11-bis-diol-1,2-epoxide is the most important for the carcinogenicity of this compound (Carmichael et al., 1993).

For BA, its IP is high and precludes activation of this compound via the radical cation pathway (Table 1). BA is activated metabolically by the diol epoxide mechanism at the bay region (C1-C4) by mouse skin and rat liver microsomes (MacNicoll et al., 1980; Thakker et al., 1979a, 1979b). The major DNA adduct formed in mouse skin treated with BA was derived from the *anti*-3,4-diol-1,2-epoxide metabolite (Cooper et al., 1980). The *anti*-BA-3,4-diol-1,2-epoxide had greater tumor-initiating activity or carcinogenicity in mouse skin and mouse lung than BA-3,4-diol, which had greater activity than that of the parent compound, BA (Levin et al., 1978; Wislocki et al., 1979). Other types of data, for example, on genotoxicity and mutagenicity, are consistent with metabolic activation by the diol epoxide pathway.

4. PAH-DNA adducts in target organs

Carcinogens react with DNA to form two types of adducts: stable adducts and depurinating adducts. Investigators in chemical carcinogenesis have always considered only stable adducts, which remain in DNA unless removed by repair. These adducts are usually detected by the ^{32}P-postlabeling technique (Reddy and Randerath, 1986), but they have not always been identified. The stable adducts are formed when the activated PAH reacts at the exocyclic amino group of Ade or Gua. Instead, when reaction occurs at the N3 or N7 of Ade or the N7 or sometimes C8 of Gua, the glycosyl bond becomes destabilized and subsequent depurination occurs (Cavalieri et al., 1990a; Rogan et al., 1988).

In the Watson-Crick model of DNA (Fig. 9), the Gua is hydrogen-bonded to cytosine and Ade is hydrogen-bonded to thymine. The backbone of the DNA is composed of deoxyribose and phosphate groups. The Gua has an exocyclic 2-NH_2 nucleophilic group that can react with electrophilic groups of carcinogens to form stable adducts (Fig. 9, hollow arrow). For Ade, reaction of an electrophile with the nucleophilic exocyclic 6-NH_2 group also forms a stable adduct (Fig. 9, hollow arrow); however, if reaction occurs at N7 or sometimes C8 of Gua, or at the N3 or N7 of Ade, depurinating adducts are obtained (Fig. 9, solid arrows). Following the reaction at the N3 of Ade, destabilization of the glycosyl bond occurs via formation of an intermediate oxocarbenium ion, with subsequent depurination and generation of an apurinic site in the DNA (Fig. 9). To determine the role of DNA adducts in cancer initiation, it is essential to identify and quantify the stable and depurinating adducts formed in target tissues.

a. Benzo[*a*]pyrene

The first PAH-DNA adducts to be identified were the adducts of BP. One of the major pieces of evidence for the diol epoxide mechanism of activation of PAH was the identification of the stable adducts formed *in vitro* and in mouse skin by reaction of BP diol epoxide (BPDE) with the 2-NH_2 group of Gua (Koreeda et al., 1978; Sims et al., 1974). Formation of adducts by one-electron oxidation was demonstrated by identification of the depurinating adduct BP-6-N7Gua after activation of BP in the presence of DNA by horseradish peroxidase (Rogan et al., 1988) or cytochrome P450 in rat liver microsomes or nuclei (Cavalieri et al., 1990a). Subsequently, complete profiles of the depurinating and stable BP-DNA adducts formed by rat liver microsomes or rat liver nuclei, or in mouse skin were determined (Fig. 10) (Chen et al., 1996; Devanesan et al., 1992, 1996; Rogan et al., 1993).

NIH-PA Author Manuscript

NIH-PA Author Manuscript

NIH-PA Author Manuscript

When BP was activated by rat liver microsomes in the presence of DNA, 68% of the total adducts were depurinating adducts, with only 4% of them arising via the diol epoxide pathway (Fig. 10) (Chen et al., 1996). Of the 32% stable adducts, 26% was the BPDE-10-N^2dG adduct and 6% were unidentified stable adducts. When BP-7,8-dihydrodiol was activated by microsomes, 93% of the adducts were stable adducts, with 90% being BPDE-10-N^2dG and 3% were unidentified. When *anti*-BPDE was reacted with DNA *in vitro*, 98% of the adducts were stable adducts, almost exclusively the BPDE-10-N^2dG (Fig. 10) (Chen et al., 1996).

Qualitative and quantitative comparison of the adducts was obtained by treating mouse skin with BP, its proximate carcinogenic metabolite BP-7,8-dihydrodiol or the ultimate carcinogenic metabolite BPDE (Fig. 10). This comparison had several purposes, which included discovering the relative amounts of stable vs depurinating adducts and the relative abundance of depurinating Ade vs Gua adducts. BP forms both stable (29%) and depurinating (71%) adducts in mouse skin (Chen et al., 1996). The depurinating adducts are BP-6-C8Gua (34%), BP-6-N7Gua (10%), BP-6-N7Ade (22%), BPDE-10-N7Gua (2%) and BPDE-10-N7Ade (3%), whereas the stable BPDE-10-N^2dG adduct constitutes 23%, and the remaining 6% are unidentified stable adducts (Fig. 10). Most of the adducts after treatment with BP are depurinating adducts formed by one-electron oxidation (66%), whereas the stable adducts are mostly formed by the diol epoxide, with the major one being BPDE-10-N^2dG (23%).

BP-7,8-dihydrodiol forms more stable adducts (63%) in mouse skin than depurinating adducts (37%, Fig. 10) (Chen et al., 1996), but the amount of depurinating adducts (1.17 μmol/mol DNA-P) is very similar to the amount of depurinating adducts formed after treatment with BP (1.47 μmol/mol DNA-P). Treatment of mouse skin with *anti*-BPDE yields fewer depurinating adducts (0.62 μmol/mol DNA-P) than with its precursor BP or BP-7,8-dihydrodiol. The stable adducts formed by BP, BP-7,8-dihydrodiol and *anti*-BPDE are mainly BPDE-10-N^2dG, and the ratio of the amount of total stable adducts is 1 (0.62, BP):3 (1.97, BP-7,8-dihydrodiol):80 (46.9, BPDE), respectively. The carcinogenicity of these three compounds is proportional to the amount of depurinating adducts formed in mouse skin, with BP and BP-7,8-dihydrodiol displaying similar potency in mouse skin, and *anti*-BPDE much less active (Cavalieri et al., 1980; Chouroulinkov et al., 1976; Levin et al., 1976a, 1976b, 1977a, 1977b; Slaga et al., 1976, 1977). In contrast, the carcinogenicity bears no relationship to the amount of total stable adducts, since the less carcinogenic *anti*-BPDE forms much higher levels of stable adducts than BP or BP-7,8-dihydrodiol (Fig. 10) (Chen et al., 1996).

b. Dibenzo[*a,l*]pyrene

Analysis of the adducts formed by DB[*a,l*]P after activation by rat liver microsomal cytochrome P450 (Fig. 11) serves as a guideline for studies of adducts formed in the target organs mouse skin and rat mammary gland. Analogously to BP, the major adducts obtained (85%) are depurinating adducts (Li et al., 1995). In contrast to BP, in which the depurinating adducts arise almost exclusively from BP radical cation, the depurinating adducts of DB[*a,l*]P are formed almost equally from the radical cation and diol epoxides. A second difference, compared to BP, is that with DB[*a,l*]P the predominant depurinating adducts are Ade adducts, whereas BP forms twice as much Gua as Ade depurinating adducts (Figs. 10 and 11) (Chen et al., 1996; Li et al., 1995).

Microsomal activation of DB[*a,l*]P-11,12-dihydrodiol produces (±)-*syn*-DB[*a,l*]PDE-14-N7Ade as the predominant depurinating adduct (18%) (Fig. 11) and 81% stable adducts (Li et al., 1995). The level of stable DB[*a,l*]P adducts was 16-fold higher than the level of stable adducts formed by DB[*a,l*]P itself (112 vs 6.8 μmol/mol DNA-P, Fig. 11) (Li et al., 1995).

NIH-PA Author Manuscript

NIH-PA Author Manuscript

NIH-PA Author Manuscript

Similar results were obtained when (±)-*syn*-DB[*a,l*]PDE was reacted with DNA (Fig. 11), 21% (±)-*syn*-DB[*a,l*]PDE-14-N7Ade and 78% stable adducts. Instead, the (±)-*anti*-DB[*a,l*]PDE produced 99.5% stable adducts (Fig. 11). The (±)-*anti*-DB[*a,l*]PDE formed six-fold more stable adducts than the (±)-*syn*-DB[*a,l*]PDE did.

The DNA adducts formed in mouse skin treated with DB[*a,l*]P, DB[*a,l*]P-11,12-dihydrodiol, (±)-*syn*-DB[*a,l*]PDE, or (±)-*anti*-DB[*a,l*]PDE have also been analyzed (Fig. 12). DB[*a,l*]P forms virtually only depurinating adducts (99%), of which 81% are Ade adducts (Cavalieri et al., 2005). The DB[*a,l*]P radical cation forms 75% of the depurinating adducts, and 24% are depurinating adducts formed by the diol epoxide. When mouse skin is treated with DB[*a,l*]P-11,12-dihydrodiol, a similar total amount of adducts (23.8 μmol/mol DNA-P) is formed, but the stable adducts are 20% and their level is 24 times higher than from the parent compound (Fig. 12). The major depurinating adduct formed by DB[*a,l*]P-11,12-dihydrodiol is (±)-*syn*-DB[*a,l*]PDE-14-N7Ade (69%) and the (±)-*anti*-DB[*a,l*]PDE-14-N7Ade is 6%, while the N7Gua adducts total 5%. Treatment of mouse skin with (±)-*syn*-DB[*a,l*]PDE produces twice as many total adducts, of which 68% are stable adducts and 25% is the (±)-*syn*-DB[*a,l*]PDE-14-N7Ade and 7% is the (±)-*syn*-DB[*a,l*]PDE-14-N7Gua (Cavalieri et al., 2005). A similar amount of total adducts (42.9 μmol/mol DNA-P) is obtained in mouse skin treated with (±)-*anti*-DB[*a,l*]PDE. In this case, 97% are stable adducts, 2% are (±)-*anti*-DB[*a,l*]PDE-14-N7Ade and 1% the (±)-*anti*-DB[*a,l*]PDE-14-N7Gua (Cavalieri et al., 2005).

When rat mammary gland is treated with DB[*a,l*]P, a smaller amount of adducts (8.6 μmol/mol DNA-P) is obtained. Of these, 2% are stable adducts and the depurinating adducts formed by DB[*a,l*]P radical cation are 75% of total adducts, with 57% Ade adducts. In addition, 23% of the total adducts is (±)-*syn*-DB[*a,l*]PDE-14-N7Ade (Fig. 12) (Cavalieri et al., 2005). The stable adducts formed by DB[*a,l*]P activated by rat liver microsomes and in both mouse skin and rat mammary gland treated with DB[*a,l*]P have been identified (Todorovic et al., 2005). In both of the target organs, mouse skin and rat mammary gland, DB[*a,l*]P forms predominantly depurinating adducts with 1–2% stable adducts. The depurinating adducts are formed by both the radical cation and diol epoxide, but 75% of the adducts arise from the radical cation.

c. 7,12-Dimethylbenz[*a*]anthracene

Activation of DMBA by rat liver microsomes in the presence of DNA produces 89–99% depurinating adducts formed by one-electron oxidation (Devanesan et al., 1993; RamaKrishna et al., 1992b). The depurinating adducts are regiospecific at the 12-methyl group, with four times as much 7-methylbenz[*a*]anthracene (MBA)-12-CH_2-N7Ade formed as 7-MBA-12-CH_2-N7Gua (Devanesan et al., 1993; RamaKrishna et al., 1992b). When the *trans*-3,4-dihydrodiol metabolite of DMBA is activated by rat liver microsomes in the presence of DNA, the major adduct is formed by the diol epoxide of DMBA (Bigger et al., 1978; Devanesan et al., 1993). When mouse skin is treated with DMBA, 99% of the adducts are depurinating adducts formed by oneelectron oxidation (Fig. 13) (Devanesan et al., 1993), and 79% of these depurinating adducts have the DMBA bound to the N7 of Ade, whereas 20% have DMBA bound to the N7 of Gua (Devanesan et al., 1993). The major stable adduct formed in mouse skin treated with DMBA corresponds to an adduct formed by the diol epoxide metabolite of DMBA (Devanesan et al., 1993). Stable adducts, however, constitute less than 1% of the total adducts formed in mouse skin. Thus, the predominant DMBA adducts derive from the radical cation of DMBA, with regiospecific reactivity at the 12-methyl group.

NIH-PA Author Manuscript

NIH-PA Author Manuscript

NIH-PA Author Manuscript

5. Correlation of depurinating PAH-DNA adducts with oncogenic mutations

The profiles of DNA adducts determined for BP, DB[*a,l*]P and DMBA (Figs. 10–13) suggest that the oncogenic mutations formed in mouse skin papillomas induced by these PAH are generated by mis-repair of apurinic sites derived from the loss of depurinating adducts (Table 2). Mouse skin papillomas initiated with DMBA, DB[*a,l*]P, DB[*a,l*]P-11,12-dihydrodiol, (±)-*anti*-DB[*a,l*]PDE or BP were harvested, and mutations in exons 1 and 2 of the c-Harvey (H)-*ras* oncogene were investigated (Chakravarti et al., 1995). DMBA induces the c-H-*ras* codon 61 A → T mutation (CAA → CTA) (Brown et al., 1990; Chakravarti et al., 1995; Quintanilla et al., 1986). This correlates with the predominant formation of the N7Ade depurinating adduct of DMBA (Fig. 13). After initiation by DB[*a,l*]P, papillomas have the A → T mutation at codon 61, and all of the papillomas initiated by DB[*a,l*]P-11,12-dihydrodiol or (±)-*anti*-DB[*a,l*]PDE contain the same mutation (Chakravarti et al., 1995). As seen in Figures 11 and 12, N7Ade and N3Ade adducts are the predominant depurinating adducts of DB[*a,l*]P, and the N7Ade adducts are the predominant depurinating adducts of DB[*a,l*]P-11,12-dihydrodiol. In contrast, BP forms more depurinating Gua (46%) than Ade (25%) adducts (Fig. 10). This PAH produces twice as many G → T mutations at codon 13 as A → T mutations at codon 61 in the c-H-*ras* oncogene (Table 2) (Chakravarti et al., 1995).

Bulky stable adducts have low mutagenic potential and are estimated to induce 1–3% mutations at the site of adduction (Rodriquez and Loechler, 1993; Shibutani et al., 1993). Apurinic sites were postulated to be important mutagenic DNA lesions that can initiate carcinogenesis (Loeb and Preston, 1986), although it was not known then that bulky carcinogens like PAH can form high proportions of depurinating adducts. Mutagenesis by noncoding lesions produces G → T and A → T transversions (Miller, 1983). These mutations occur by DNA mis-replication across apurinic sites with most frequent insertion of A opposite the lesion (Schaaper et al., 1983; Strauss, 1985). For example, BP mostly produces G → T transversions in codon 13 of the c-H-*ras* oncogene in mouse skin tumors (Table 2) (Chakravarti et al., 1995; Colapietro et al., 1993). Based on the greater formation of depurinating Gua (46%) compared to Ade (25%) adducts of BP (Chen et al., 1996), the G → T transversions can be attributed to loss of the depurinating Gua adducts, generation of apurinic sites and mis-replication at these sites (Fig. 14). In depurination, the glycosyl bond between the adducts and deoxyribose is cleaved (Fig. 9), leading to loss of the adduct and formation of an apurinic site. In the next round of DNA replication, the most likely base to be inserted opposite the apurinic site is Ade, as demonstrated with bacterial and some mammalian DNA polymerases (Cai et al., 1993; Ide et al., 1992; Klinedinst and Drinkwater, 1992; Loeb and Preston, 1986; Sagher and Strauss, 1983). When the coding strand of DNA is then replicated, a T is often inserted opposite the new A. This results in the G → T transversion observed in codon 13 of the c-H-*ras* oncogene. When an Ade adduct is lost by depurination, leaving an apurinic site in the DNA, the preferential insertion of Ade in the opposite DNA strand leads to an A → T transversion at the site of the adduct.

Other results support this hypothesis. In *Drosophila melanogaster*, methyl methanesulfonate produced A → T and G → T transversions caused by depurination of 3-methylAde and 7-methylGua, followed by mis-replication at the resulting apurinic sites (Nivard et al., 1992). Mutations in the lacI gene of *Escherichia coli* treated with (±)-*anti*-BPDE have also been investigated. The predominant G → T transversions were attributed to formation of the depurinating BPDE-N7Gua adduct and mis-replication at apurinic sites (Bernelot-Moens et al., 1990). Six stereoisomers of the stable BPDE-N^6dA adduct were inserted at position 2 of the human N-*ras* codon 61 (CAA) in an 11-base oligonucleotide. In *E. coli*, these adducts induced only A → G mutations (Chary et al., 1995)) and not the A → T transversions found in codon 61 in mouse skin tumors initiated with BP (Table 2) (Chakravarti et al., 1995;

NIH-PA Author Manuscript

NIH-PA Author Manuscript

NIH-PA Author Manuscript

Colapietro et al., 1993). This result supports the view that the codon 61 A → T mutation in PAH-induced tumors does not derive from a stable deoxyadenosine adduct.

About 10,000 apurinic sites are formed spontaneously per cell per day or ca. 1,700 in 4 h (Lindahl and Nyberg, 1972). The amount of depurinating adducts detected in mouse skin treated with BP, DMBA or DB[*a*,*l*]P, along with the estimated number of cells in the treated area of skin, provide conservative estimates of apurinic sites of ca. 25,000 for BP, ca. 40,000 for DMBA and ca. 200,000 for DB[*a*,*l*]P formed during the 4 h of treatment with the PAH (Figs. 10–13) (Cavalieri et al., 2005; Chen et al., 1996; Devanesan et al., 1993; Rogan et al., 1993). Hence, depurinating BP, DMBA or DB[*a*,*l*]P adducts generate 10–100 times more apurinic sites than those spontaneously formed per cell during the 4 h.

The apparent nonrepair may be due to excessive apurinic sites beyond the repair capacity of the cells or to the presence of stable adducts interfering with error-free repair. Translesional replication studies of stable adducts (Rodriguez and Loechler, 1993; Shibutani et al., 1993) and abasic sites (Sagher and Strauss, 1983) *in vitro*, and the correspondence between misincorporated bases and mutations identified *in vivo* with stable adducts (Eisenstad et al., 1982) and abasic sites (Klinedinst and Drinkwater, 1992) suggest that mis-replication could play a critical role in the induction of mutations by DNA adducts.

The correlation between depurinating adducts and mutations has also been observed in preneoplastic tissue (Chakravarti et al., 2000). Preneoplastic mutations have been detected by PCR amplification of the c-H-*ras* gene in PAH-treated mouse skin. For example, 81% of the adducts formed in mouse skin treated with DB[*a*,*l*]P are depurinating Ade adducts (Cavalieri et al., 2005). These adducts are converted within 12 h into preneoplastic mutations (Chakravarti et al., 2000), which are overwhelmingly (90%) A → G transitions. The rapid induction of preneoplastic mutations occurs while replication is repressed and base excision repair is induced by the treatment of the skin with the PAH (Gill et al., 1991; Sawyer et al., 1988). Therefore, these mutations appear to be induced by error-prone repair (Chakravarti et al., 2000).

Error-prone repair of apurinic sites can occur much more quickly than mis-replication of apurinic sites (Fig. 14). In mis-replication, two rounds of DNA replication must occur for the mutation to be fixed in the DNA (Fig. 14, left). In error-prone repair, only one round of replication is needed to fix a mutation (Fig. 14, right). Therefore, depending on their cell cycle, cells can undergo one round of DNA replication and cell division within 12–24 h, thereby fixing a mutation generated by error-prone repair of an apurinic site.

Qualitative and quantitative study of various carcinogen adducts and mutations induced in *ras* oncogenes should yield further insight into the role of apurinic sites in cancer initiation.

6. Carcinogenicity of PAH and derivatives in the target organs mouse skin and rat mammary gland

Identification and quantification of DNA adducts formed by PAH and their correlation with oncogenic mutations (see above) can provide some orientation in delineating the mechanism(s) of tumor initiation of PAH and their derivatives. Carcinogenicity experiments with PAH can also provide very useful guidelines on the mechanism(s) of metabolic activation of various PAH. Such studies can suggest, for example, whether or not the diol epoxide pathway plays a role in the metabolic activation of a certain PAH.

One avenue to obtain information on the mechanism of metabolic activation is to compare the carcinogenicity of the parent compound to its dihydrodiol that leads to the bay region

NIH-PA Author Manuscript

NIH-PA Author Manuscript

NIH-PA Author Manuscript

diol epoxide and to the diol epoxide itself. The assumption is that the diol epoxide should be more carcinogenic than the proximate dihydrodiol and, in turn, the dihydrodiol more potent than the parent compound in dose-response carcinogenicity studies.

A second method to obtain critical information consists of comparing the parent compound to a fluoro-substituted PAH in which the fluoro group occupies one of the sites of the diol epoxide, thereby blocking this pathway of activation. If the diol epoxide pathway is the exclusive mechanism of activation, the fluoro compound should be inactive.

A third approach consists of comparing the carcinogenicity of PAH and derivatives in the two target organs mouse skin and rat mammary gland (Table 1). The assumption in these studies is that activation by radical cations is predominant in the rat mammary gland because peroxidases catalyzing this mechanism of activation are very abundant there.

Following the first approach, when BP and BP-7,8-dihydrodiol were compared in mouse skin by initiation-promotion and repeated application, the two compounds had similar activity (Cavalieri et al., 1980; Chouroulinkov et al., 1976; Levin et al., 1976a, 1976b, 1977b; Slaga et al., 1976). The (-)-BP-7,8-dihydrodiol enantiomer that leads to the most active *anti*-BPDE is no more potent than BP in mouse skin (Levin et al., 1977b; Slaga et al., 1977). In turn, the BPDEs are less carcinogenic than the parent BP or BP-7,8-dihydrodiol (Slaga et al., 1976, 1977).

DB[*a*,*l*]P is the most potent carcinogen among the dibenzo[*a*]pyrene isomers (Cavalieri et al., 1989) and is the most potent PAH (Higginbotham, et al., 1993). At high doses, the tumor-initiating activity of DB[*a*,*l*]P and DB[*a*,*l*]P-11,12-dihydrodiol, the proximate metabolite leading to the bay region diol epoxide, are similar in mouse skin (Cavalieri et al., 1991), but at low doses the 11,12-dihydrodiol is much less active than DB[*a*,*l*]P (Cavalieri et al., 1994; Gill et al., 1994; Higginbotham et al., 1993). The diol epoxides, *syn*- and *anti*-DB[*a*,*l*]PDE, are much weaker than DB[*a*,*l*]P and its 11,12-dihydrodiol (Cavalieri et al., 1994; Gill et al., 1994). Furthermore, *syn*-DB[*a*,*l*]PDE is a stronger tumor initiator than its congener, *anti*-DB[*a*,*l*]PDE (Cavalieri et al., 1994; Gill et al., 1994). Thus, these experiments clearly indicate that the diol epoxide pathway is not the exclusive pathway of activation for BP and DB[*a*,*l*]P.

The second approach, in which a fluoro substituent in the bay region blocks formation of the diol epoxide, has been applied to BP, DMBA and MC. The moderate-weak activity of 7-FBP, 8-FBP and 10-FBP in mouse skin and rat mammary gland indicates that other mechanisms are involved in the metabolic activation of these compounds (Cavalieri et al., 1988c). In fact, these derivatives of BP are not metabolized to their dihydrodiols at the double bond in which the fluoro group is substituted. Metabolism of 8-FBP and 9-FBP yields the same metabolites as BP, with the exception of the 7,8-dihydrodiol from 8-FBP and the 9,10-dihydrodiol from 9-FBP (Chou and Fu, 1984). Thus, the carcinogenic activation of these fluoro compounds is not initiated by the diol epoxide pathway.

The tumorigenicity experiment of DMBA versus DMBA-3,4-dihydrodiol, the proximate metabolite in the diol epoxide pathway of activation, indicates that the latter is a more potent initiator than the parent compound (Slaga et al., 1979). This result would suggest that the diol epoxide plays a major role in the activation of DMBA. The DMBA-3,4-dihydrodiol, however, can also be activated via a radical cation. Therefore, the tumorigenic effect of the 3,4-dihydrodiol could arise from both mechanisms of activation, formation of a diol epoxide and a radical cation. Saturation of the angular benzo ring in which the diol epoxide of DMBA is formed leads to 1,2,3,4-tetrahydroDMBA (Table 1). This compound is a relatively potent carcinogen (Cavalieri et al., 1990b; DiGiovanni et al., 1982), indicating that its

NIH-PA Author Manuscript

NIH-PA Author Manuscript

NIH-PA Author Manuscript

activation does not occur via the bay-region diol epoxide pathway. Furthermore, the diol epoxide mechanism cannot play a role in the weak carcinogenic activity of 1-FDMBA, 2-FDMBA or 4-FDMBA, in which formation of the diol epoxide is hindered by the fluoro substituent (Cavalieri et al., 1990b; DiGiovanni et al., 1982; Harvey and Dunne, 1978). By the same rationale, the carcinogenicity of 8-FMC and 10-FMC in rat mammary grand (Table 1) (Cavalieri et al., 1988c) suggests that diol epoxides do not play a role in the metabolic activation of these compounds.

The third approach is to compare carcinogenic activity in the two target organs mouse skin and rat mammary gland. In these studies, the assumption is that rat mammary gland tissue has abundant peroxidases and little cytochrome P450, whereas mouse skin has more cytochrome P450. Another factor plays an important role in assessing the mechanism of carcinogenic activation of the PAH listed in Table 1, namely the IP. Above a certain IP, activation by radical cations is not operative, due to the more difficult removal of one electron and the formation of a less stable radical cation. The cut-off IP above which activation by radical cations is not operative has been proposed to be about 7.35 eV (Cavalieri et al., 1983). This value was generated based on the level of binding to DNA of a series of PAH with IP ranging from 8.19 to 6.68 eV catalyzed by horseradish peroxidase (Cavalieri et al., 1983) or prostaglandin H synthase (Devanesan et al., 1987). Thus, in these carcinogenicity experiments, PAH with high IP should be activated by the diol epoxide and should be active only in mouse skin. In contrast, PAH with IP below 7.35 eV can be activated by both mechanisms and should be carcinogenic in both mouse skin and rat mammary gland.

The PAH 5-methylchrysene and dibenz[*a*,*h*]anthracene are potent carcinogens in mouse skin (Hecht et al., 1974; Hoffman, 1974; IARC, 1973, 1983), but are inactive in rat mammary gland (Cavalieri et al., 1988d), as predicted by their relatively high IP (Table 1). BA, which has a relatively high IP and is a borderline carcinogen in mouse skin, is inactive in rat mammary gland (Cavalieri et al., 1988d; IARC, 1973, 1983). 7-Methylbenz[*a*]anthracene, which has an IP value near the cut-off of 7.35eV (Table 1), is a potent carcinogen in mouse skin (Stevenson and Von Haam, 1965; Wislocki et al., 1982) and very weakly active in rat mammary gland (Cavalieri et al., 1988d). BP-7,8-dihydrodiol and DB[*a*,*l*]P-11,12-dihydrodiol, which have relatively high IP of 7.49 and 7.79 eV, respectively, are activated by monooxygenation to form diol epoxides and would be expected to be non-carcinogenic or weakly carcinogenic in the rat mammary gland, in which cytochrome P450 is at a very low concentration or not present. BP-7,8-dihydrodiol has been found to be a mammary carcinogen in the rat, although weaker than the parent BP (Cavalieri et al., 1988c). This effect could be due to the ability of peroxidases to catalyze epoxidation at the bay region double bond (Dix and Marnett, 1983; Marnett, 1990). Thus, the carcinogenic activity of the dihydrodiol in the mammary gland does not contradict the proposed cut-off of about 7.35 eV, above which PAH cannot be activated to effective radical cations. In summary, carcinogenicity experiments in mouse skin and rat mammary gland can provide some orientation in delineating the mechanisms of cancer initiation by PAH and their derivatives.

7. Mechanism of cancer initiation by the most potent PAH carcinogens

Determination of the mechanisms of cancer initiation by the most potent PAH carcinogens BP, DB[*a*,*l*]P, DMBA and MC is based on several lines of investigation, which include metabolism studies, dose-response carcinogenicity experiments, identification and quantification of DNA adducts, and the relationship of these adducts to oncogenic mutations.

NIH-PA Author Manuscript

NIH-PA Author Manuscript

NIH-PA Author Manuscript

a. Benzo[*a*]pyrene

Metabolism of BP *in vitro* and *in vivo* has established that the bay region diol epoxide is involved in the formation of DNA adducts of BP. BP forms three types of metabolites (Fig. 1). The phenols, of which the 3-OHBP is the major one, followed by the 9-OHBP, 7-OHBP and 1-OHBP; the quinones BP-1,6-, BP-3,6-, and BP-6,12-quinone; and the BP-4,5-, BP-7,8- and BP-9,10-dihydrodiol (Alpert and Cavalieri, 1980; Holder et al., 1974; Selkirk et al., 1974; Yang, 1977). The presence of the metabolite BP-7,8-dihydrodiol led various investigators to propose that the ultimate carcinogenic metabolite of BP was the BP-7,8-dihydrodiol-9,10-epoxide, which yielded both *in vitro* and *in vivo* BPDE-10-N^2dG as a major adduct (Sims et al., 1974). Tumorigenicity data do not support the hypothesis that the diol epoxide pathway is the exclusive mechanism of activation because the proximate BP-7,8-dihydrodiol stereoisomers, in particular the (−)enantiomer, are not more carcinogenic in mouse skin than the parent compound. Furthermore, the most active ultimate carcinogenic metabolite, (+)-*anti*-BPDE, is much less carcinogenic than BP and BP-7,8-dihydrodiol (Cavalieri et al., 1980; Chouroulinkov et al., 1976; Levin et al., 1976a, 1976b, 1977a, 1977b; Slaga et al., 1976, 1977). Therefore, other mechanisms of metabolic activation must be involved.

The electrophilic radical cations of BP can play a role in the metabolic activation of BP because it has a relatively low IP (7.23 eV, Table 1). In addition, the radical cation has charge localized at C-6 (Cavalieri and Auerbach, 1974; Cremonesi et al., 1989; Jeftic and Adams, 1970; Rochlitz, 1967; Wilk et al., 1966; Wilk and Girke, 1972) that renders this position reactive toward the nucleophilic groups of Ade and Gua (RamaKrishna et al., 1992c; Rogan et al., 1988). After having synthesized the DNA adducts of BP formed both by both the radical cation and the diol epoxide (Chen et al., 1996; RamaKrishna et al., 1992c; Rogan et al., 1988), a thorough analysis of these adducts formed in mouse skin has led to the determination that most of the adducts are depurinating adducts (71%) and only 29% are stable adducts, of which 23% are BPDE-10-N^2dG (Fig. 10) (Chen et al., 1996).

Among the depurinating adducts, 66% are formed by the radical cation and only 5% by the diol epoxide pathway. When mouse skin is treated with *anti*-BPDE, a smaller amount of depurinating adducts than with BP, 0.6 μmol/mol DNA-P vs. 1.5 μmol/mol DNA-P, respectively, but a much larger amount of stable adducts is formed, 47 μmol/mol DNA-P vs 0.6 μmol/mol DNA-P, respectively (Chen et al., 1996). Since *anti*-BPDE is much less carcinogenic than BP, these results clearly indicate that the level of stable adducts is not related to the carcinogenic activity.

The relevance of depurinating adducts to the mechanism of tumor initiation is seen in the correlation of these adducts with mutations formed in the H-*ras* oncogene in mouse skin papillomas initiated with BP (Table 2) (Chakravarti et al., 1995; Colapietro et al., 1993). Depurinating Gua and Ade adducts comprise 46% and 25%, respectively, of the total BP-DNA adducts formed in mouse skin (Fig. 10). *Ras* mutations formed in DNA from 54% of the papillomas display G → T transversions in codon 13, while 15% of the papillomas exhibit A → T transversions in codon 61) (Chakravarti et al., 1995; Colapietro et al., 1993). Thus, the mutations correlate with the depurinating adducts, but have no relationship to the stable adducts formed by BP.

In conclusion, the mechanism of tumor initiation by BP is dictated by the depurinating adducts of Gua and Ade, predominantly formed by the BP radical cation (Fig. 10). The correlation of depurinating adducts and mutation data for BP suggests that the tumor-initiating activity of BP-7,8-dihydrodiol and *anti*-BPDE could be also based on their depurinating Ade and Gua adducts (Fig. 10), but the demonstration of this hypothesis can be obtained only by correlating these adducts with oncogenic mutations.

NIH-PA Author Manuscript

NIH-PA Author Manuscript

NIH-PA Author Manuscript

b. Dibenzo[*a,l*]pyrene

Metabolism of DB[*a,l*]P produces three major metabolites, and one of them is DB[*a,l*]P-11,12-dihydrodiol, a proximate carcinogenic metabolite in the diol epoxide pathway (Devanesan et al., 1990). One-electron oxidation of DB[*a,l*]P by manganic acetate (Cremonesi et al., 1992a) or by electrochemical oxidation in the presence of dG or dA (RamaKrishna et al., 1993b) affords a radical cation with charge localization at C-10, followed by specific reaction with nucleophiles at this carbon atom. Identification and quantification of the depurinating and stable adducts have been pivotal for understanding the pathways of activation of DB[*a,l*]P. In fact, *in vitro*, in mouse skin and in the rat mammary gland, the preponderant adducts are the depurinating ones (Figs. 11 and 12), and among these adducts loss of Ade represents the predominant event with DB[*a,l*]P, DB[*a,l*]P-11,12-dihydrodiol and the DB[*a,l*]P diol epoxides (Cavalieri et al., 2005; Li et al., 1995).

Studies of the H-*ras* oncogene mutations in mouse skin papillomas induced by DB[*a,l*]P, DB[*a,l*]P-11,12-dihydrodiol or *anti*-DB[*a,l*]PDE indicate that these compounds produce exclusively A → T mutations at codon 61 (Table 2) (Chakravarti et al., 1995). Thus, a correlation between *ras* mutations and Ade depurinating adducts suggests that these mutations arise from unrepaired apurinic sites.

Comparative tumorigenicity studies of DB[*a,l*]P, DB[*a,l*]P-11,12-dihydrodiol, *syn*-DB[*a,l*]PDE and *anti*-DB[*a,l*]PDE indicate that DB[*a,l*]P is slightly more potent than the 11,12-dihydrodiol and much more potent than the two diol epoxides (Cavalieri et al., 1991, 1994; Gill et al, 1994; Higginbotham et al., 1993). Therefore, the diol epoxide pathway does not appear to play a major role in the carcinogenicity of DB[*a,l*]P. Furthermore, the least tumorigenic metabolite, *anti*-DB[*a,l*]PDE, forms by far the greatest amount of stable adducts both *in vitro* (Li et al., 1995) and *in vivo* (Cavalieri et al., 2005), suggesting that these adducts do not play a significant role in tumor initiation. While the stable adducts are mainly formed by the diol epoxide pathway (Li et al., 1995; Todorovic et al., 2005), the depurinating adducts arise mainly in mouse skin and rat mammary gland via the radical cation pathway. Thus, tumor initiation by DB[*a,l*]P is mainly due to depurinating Ade adducts formed by DB[*a,l*]P radical cation and by the diol epoxide pathway.

c. 7,12-Dimethylbenz[*a*]anthracene

Evidence for the predominant metabolic activation of DMBA via the radical cation pathway derives in part from observations concerning the carcinogenic activities of BA and its alkylated derivatives, and the physico-chemical properties of their radical cations (Cavalieri and Roth, 1976; RamaKrishna et al., 1992a, 1992b). The parent compound BA is a borderline carcinogen (Dipple et al., 1976), but substitution of a methyl group at C-7 leads to substantially increased carcinogenicity (Dunning and Curtis, 1960; Stevenson and Von Haam, 1965; Wislocki et al., 1982). Among the methyl-substituted BA, the 7-methyl and 12-methyl are the most active, followed by the 6-methyl and 8-methyl derivatives. The remaining methyl derivatives are inactive. Substitution of BA with two methyl groups at the 7- and 12-*meso*-anthracenic positions leads to DMBA, one of the most potent carcinogens (Dipple et al., 1976). Although less potent than DMBA, 1,2,3,4-tetrahydroDMBA is also a strong carcinogen, despite being fully saturated in the angular ring and, thus, unable to be activated by the diol epoxide pathway (Cavalieri et al., 1990b; DiGiovanni et al., 1982). Electrochemical oxidation of 1,2,3,4-tetrahydroDMBA in the presence of dG or dA yields numerous adducts, which include the ones at the 12-methyl and 7-methyl groups that are similar to those obtained with DMBA under similar conditions (Mulder et al., 1996).

Both *in vitro* and in mouse skin, 99% of the DMBA-DNA adducts formed are depurinating adducts, in which DMBA is regiospecifically bound through the 12-methyl to the N-7 of

NIH-PA Author Manuscript

NIH-PA Author Manuscript

NIH-PA Author Manuscript

Ade (79%) or Gua (20%) (Fig. 13) (Devanesan et al., 1993; RamaKrishna et al., 1992b). The stable adducts contribute a very minor proportion (1%); and are mostly formed via the diol epoxide pathway (Cheng et al., 1988a, 1988b; Vericat et al., 1991). The specificity of binding of DMBA at the 12-methyl group to the DNA bases correlates well with the results of carcinogenicity experiments. When the two methyl groups of DMBA are substituted with ethyl groups, the resulting 7,12-$(C_2H_5)_2$BA is not carcinogenic (Pataki and Balic, 1972). The inactivity of the ethyl-substituted compound is consistent with the lack of nucleophilic substitution at the benzylic methylene group of the radical cation of an ethyl PAH (Fig. 7) (Tolbert et al., 1990). Furthermore, 7-CH_3-12-C_2H_5BA is a much weaker carcinogen than DMBA, whereas 7-C_2H_5-12-CH_3BA displays a carcinogenic activity similar to that of DMBA (Pataki and Balic, 1972). These data clearly suggest that the 12-methyl group plays the major role in the carcinogenic activity of DMBA.

DMBA-3,4-dihydrodiol, precursor to the bay region diol epoxide, has been found among the numerous metabolites of DMBA (Chou et al., 1981) and has been shown to be a more potent tumor initiator in mouse skin than the parent DMBA (Slaga et al., 1979). The tumorigenicity of the 3,4-dihydrodiol can be attributed to adducts formed by both its diol epoxide and radical cation (since this compound has chemical properties similar to 1,2,3,4-tetrahydroDMBA).

DMBA consistently produces A → T transversions in codon 61 of the H-*ras* oncogene in mouse skin tumors (Table 2) (Brown et al., 1990; Chakravarti et al., 1995; Quintanilla et al., 1986). Based on the preponderant formation of the N7Ade adduct of DMBA (79%) (Devanesan et al., 1993), the A → T transversions can be attributed to loss of the N7Ade adducts, generation of apurinic sites, and error-prone repair at these sites. The same A → T transversion in codon 61 is observed in papillomas induced by 1,2,3,4-tetrahydroDMBA (Chakravarti et al., 1995). The adducts formed by this carcinogen have not been identified, but, as stated above, electrochemical oxidation of 1,2,3,4-tetrahydroDMBA in the presence of dG and dA yields methyl-substituted depurinating adducts similar to those obtained with DMBA (Mulder et al., 1996). Thus, it is anticipated that 1,2,3,4-tetrahydroDMBA, which cannot form a bay region diol epoxide, is metabolically activated mostly by the radical cation at the 12-methyl group, like DMBA, forming a preponderance of N7Ade adducts that generate apurinic sites in DNA.

In conclusion, based on the several lines of evidence described above, DMBA initiates tumors by forming radical cations that bind specifically at the 12-methyl group preponderantly to the N7 of Ade.

d. 3-Methylcholanthrene

MC is a very potent carcinogen in mouse skin and rat mammary gland (Cavalieri et al., 1978, 1988c, 1988d). This compound has a relatively low IP (Table 1). The charge localization in its radical cation at position 12b (Fig. 15) causes it to react specifically at C-1 with various nucleophiles (Cavalieri and Roth, 1976), including Ade, dA and dG (Li et al., 1996). The specific reaction at C-1 competes successfully with the reaction at the *meso*-anthracenic position C-6, due to the complete alignment of the C-H bond of the C-1 methylene with the adjacent aromatic *p*-orbital as a result of geometric constraints (Fig. 7). This molecular characteristic, which is unique to the MC radical cation, is responsible for the mechanism of cancer initiation by this compound.

In the metabolism of MC by rat liver microsomes, MC is not converted to the proximate metabolite MC-9,10-dihydrodiol, precursor to the bay region diol epoxide. Only the major metabolites of MC, 1-hydroxyMC and 2-hydroxyMC, yield metabolically the 9,10-dihydrodiol (Shou and Yang, 1990; Thakker et al., 1978a, 1978b). These results imply that

NIH-PA Author Manuscript

NIH-PA Author Manuscript

NIH-PA Author Manuscript

formation of the ultimate bay region diol epoxide from MC requires four distinct steps, namely hydroxylation at C-1, epoxidation at the 9,10-double bond, enzymatic hydrolysis to form the 9,10-dihydrodiol, and, finally, epoxidation at the 7,8-double bond.

Tumor-initiating activity in mouse skin shows that the activity of the two diastereomeric 1-hydroxyMC-9,10-dihydrodiols is no greater than that of the parent compound MC (Chouroulinkov et al., 1979; Levin et al., 1979), while 1-hydroxyMC is less active than MC and the two 1-hydroxyMC-9,10-dihydrodiols. The proximate metabolite 1-hydroxyMC is also consistently much less carcinogenic than MC in mouse skin (Cavalieri et al., 1978; Sims, 1967) and rat mammary gland (Cavalieri et al., 1988d). Furthermore, the 8-FMC and 10-FMC, which cannot be activated by the diol epoxide pathway, are carcinogenic in the rat mammary gland (Gill et al., 1994).

Activation of MC by rat liver microsomes yielded 91% depurinating adducts, of which 87% were MC-1-N7Ade, 4% MC-1-N3Ade and 3% MC-1-N7Gua (Li et al., 1996). The remaining 6% were unidentified stable adducts. These results clearly indicate that the predominant depurinating adducts arise from the MC radical cation and most of the adducts contain Ade.

All of the results obtained suggest that the main molecular characteristic in the initiation of cancer by MC is the activation of C-1 in MC radical cation and reaction with the nucleophilic groups of Ade and Gua to form depurinating adducts.

8. Conclusions on PAH

The most significant research on PAH has been centered around initiation, the process involving the reaction of ultimate carcinogenic PAH metabolites with DNA. The two major types of carcinogenic metabolites are PAH radical cations and diol epoxides.

A key aspect of understanding PAH carcinogenesis has been to elucidate the mechanism of oxygen transfer by cytochrome P450. Specific PAH, in particular fluorinated BPs, have been critical in determining how this oxygen transfer occurs. Development of the PAH radical cation chemistry revealed that radical cation intermediates are the precursors of PAH oxygenated metabolites, such as the diol epoxides. Whether ultimate carcinogenic PAH radical cations or PAH diol epoxides are metabolically formed depends on the physico-chemical properties of the PAH and the enzymes involved. Among the PAH radical cations and diol epoxides, the radical cations are the ultimate carcinogenic metabolites that play the predominant role in the initiation of cancer by the very potent carcinogens BP, DB[*a,l*]P, DMBA and MC.

Cancer initiation by PAH occurs when PAH radical cations and/or diol epoxides react with DNA to form specific adducts. In general, PAH diol epoxides tend to form stable adducts that remain in DNA unless removed by repair. In contrast, PAH radical cations predominantly form depurinating adducts that are lost from DNA, leaving mutagenic apurinic sites. The resulting mutations can lead to the initiation of cancer. The depurinating PAH-DNA adducts are the critical adducts in the initiation of cancer by BP, DB[*a,l*]P, DMBA and MC. This insight was revealed by the correlation between depurinating PAH-DNA adducts and cancer-causing mutations in the target organs mouse skin and rat mammary gland.

Detailed knowledge of the mechanism of cancer initiation by PAH has provided the information necessary to understand how natural estrogens can become chemical carcinogens and initiate various types of human cancer.

NIH-PA Author Manuscript

NIH-PA Author Manuscript

NIH-PA Author Manuscript

9. Hormonal and nonhormonal mechanisms of estrogen carcinogenesis

Two mechanisms have been hypothesized for the role of estrogens in the induction of cancer: one is hormonal and the other is nonhormonal. In the hormonal mechanism, which occurs in hormone-dependent organs, estrogens bind to the estrogen receptor (ER) to generate a variety of signals that stimulate cell proliferation (Nandi et al., 1995; Preston-Martin et al., 1990). This event takes place during cancer promotion and progression. Although hormonal effects can mediate cell proliferation, a genotoxic event is necessary to produce mutations, the permanent genetic change at the origin of cancer. In a nonhormonal mechanism, estrogens can act as chemical carcinogens and initiate mutations and cancer via formation of estrogen-DNA adducts (Cavalieri et al., 2000, Cavalieri and Rogan, 2010, 2011).

The scientific community does not accept estrogens as chemical carcinogens, mostly because these compounds were not found to induce mutations in bacterial and mammalian test systems, presumably because the reactive estrogen quinones either were not formed or could not reach the target DNA (Drevon et al., 1981; Lang and Redmann, 1979, 1993; Li, 1993; Nandi, 1978). These results have led scientists to classify estrone (E_1) and estradiol (E_2) as epigenetic carcinogens that function mainly by stimulating abnormal cell proliferation via ER-mediated processes (Dickson and Stancel, 2000; Feigelson and Henderson, 1996; Furth, 1982; Li, 1993; Li and Li, 1990; Nandi et al., 1995). The stimulated cell proliferation would create more opportunities for mutations leading to carcinogenesis (Feigelson and Henderson, 1996; Hahn and Weinberg, 2002; Li and Li, 1990). The ER-mediated events can be involved in accelerating the process of carcinogenesis, but they do not play a critical role in cancer initiation, because the hypothetical mutations obtained during cell proliferation are random. The discovery that specific oxidative metabolites of estrogens, catechol estrogen quinones (see below), react with DNA led to and supports the hypothesis that estrogens can become endogenous chemical carcinogens by generating the mutations leading to the initiation of cancer (Cavalieri and Rogan, 2010, 2011). This paradigm suggests that specific, critical mutations generate abnormal cell proliferation leading to cancer, rather than ER-mediated abnormal cell proliferation giving rise to random mutations (Dickson and Stancel, 2000; Feigelson and Henderson, 1996; Furth, 1982; Li and Li, 1990; Nandi, 1978; Nandi et al., 1995). The specificity of the critical mutations derives from the preliminary intercalating physical complex between estrogen and DNA before formation of a covalent bond between them. This has been demonstrated by studying the mechanism of cancer initiation of the human carcinogen diethylstilbestrol (DES) (Saeed et al., 2009b).

10. Common mechanism of cancer initiation by estrogens and other compounds containing one or two benzene rings

A mechanism of metabolic activation, which produces extremely weak ultimate carcinogens, involves estrogens and other aromatic compounds with one or two benzene rings. In this mechanism, the benzene ring of the compounds is enzymatically oxidized to yield a phenol (Fig. 16). A second hydroxylation leads to production of a catechol, followed by a third oxidation to afford the electrophilic ultimate carcinogenic *ortho*-quinone metabolite. This metabolite can react with DNA by Michael addition to form predominantly the depurinating DNA adducts at the N-3 of Ade and N-7 of Gua (Fig. 16). These adducts detach from DNA, leaving behind a DNA with apurinic sites. Erroneous repair of the apurinic sites gives rise to mutations that could initiate cancer. Evidence has been provided that this unifying mechanism of activation occurs with benzene (Cavalieri et al., 2002b; Zahid et al., 2010b), naphthalene (Saeed et al., 2007a, Saeed et al., 2009a), the natural estrogens E_1 and E_2 (Cavalieri et al., 1997; Dwivedy et al., 1992; Li et al., 2004; Saeed et

NIH-PA Author Manuscript

NIH-PA Author Manuscript

NIH-PA Author Manuscript

al., 2005b, 2007b; Stack, et al., 1996; Zahid et al., 2006), the synthetic estrogens DES (Hinrichs et al., 2011; Saeed et al., 2009b) and hexestrol (HES) (Jan et al., 1998; Saeed et al., 2005a, 2005b), and dopamine (Cavalieri et al., 2002b; Zahid et al., 2010b; 2011b) (Fig. 16).

a. Natural and synthetic estrogens

Oxidation of catechol estrogens to semiquinones and then to quinones is a pathway that can initiate cancer by natural estrogens, as well as synthetic estrogens such as the human carcinogen DES (Herbst et al., 1971) and its hydrogenated derivative HES. These compounds, similarly to the natural estrogens, are carcinogenic in the kidney of Syrian golden hamsters (Li et al., 1983; Liehr et al., 1985); the major metabolites are their catechols (Blaich et al., 1990; Haaf and Metzler, 1985; Liehr et al., 1985; Metzler and McLachlan, 1981). The catechols are easily oxidized to catechol quinones. The catechol quinones of DES and HES have chemical and biochemical properties similar to those of $E_1(E_2)$-3,4-Q; namely, they form N3Ade and N7Gua adducts after reaction with DNA (Fig. 16), and depurination of the N7Gua adduct occurs rather slowly, analogously to the respective adducts of the natural $E_1(E_2)$-3,4-Q (Hinrichs et al., 2011; Jan et al., 1998; Saeed et al., 2005a, 2005b, 2009b).

Therefore, the catechol quinones of DES and HES appear to be the critical initiators of cancer by these synthetic estrogens. In turn, these results support the hypothesis that $E_1(E_2)$-3,4-Q may be endogenous cancer initiators.

b. Benzene and naphthalene

Oxidation of catechols to semiquinones and quinones is not only the mechanism of cancer initiation for natural and synthetic estrogens, but could also be the mechanism of cancer initiation for the leukemogen benzene. It has long been known that benzene causes acute myelogenous leukemia in humans (Paxton, 1996; Rinsky et al., 1987). Metabolites of benzene include catechol (1,2-dihydroxybenzene, CAT) and hydroquinone (1,4-dihydroxybenzene) (Sabourin et al., 1989; Snyder and Kalf, 1994). CAT and hydroquinone can accumulate in bone marrow (Greenlee et al., 1981; Rickert et al., 1979), where they can be oxidized by peroxidases, including myeloperoxidase and prostaglandin H synthase (Sadler et al., 1988). The resulting CAT quinone can produce DNA adducts. In fact, oxidation of CAT by horseradish peroxidase, tyrosinase, or phenobarbital-induced rat liver microsomes in the presence of DNA yields the depurinating adducts CAT-4-N7Gua and CAT-4-N3Ade (Fig. 16) (Cavalieri et al., 2002b; Zahid et al., 2010b). Thus, formation of depurinating adducts specifically at the N-7 position of Gua and N-3 position of Ade by 1,4-Michael addition of benzene-1,2-quinone to DNA suggests that benzene-1,2-quinone may play a critical role in cancer initiation by benzene.

Inhalation of naphthalene has been found to induce olfactory epithelial neuroblastomas in 5–10% of male and female rats chronically exposed to naphthalene for two years (NTP, 2000). The only logical mechanism of activation of naphthalene is analogous to the one described above for natural and synthetic estrogens, and benzene. In fact, naphthalene-1,2-quinone reacts with DNA to yield analogous depurinating N3Ade and N7Gua adducts *in vitro* and *in vivo* (Fig. 16) (Saeed et al., 2007a; Saeed et al., 2009a).

In conclusion, the catechol quinones of natural and synthetic estrogens, benzene and naphthalene react with DNA by 1,4-Michael addition to form predominantly depurinating N3Ade and N7Gua adducts. With all of these compounds, the N3Ade adduct depurinates instantaneously from DNA, whereas the N7Gua adduct depurinates slowly, with a half-life

NIH-PA Author Manuscript

NIH-PA Author Manuscript

NIH-PA Author Manuscript

of a few hours. These common features may lead to the initiation of cancer by these compounds.

11. Metabolism and genotoxicity of estrogens

In addition to the evidence of a common mechanism of metabolic activation of estrogens with other weak carcinogens (Fig. 16), experiments on estrogen metabolism, formation and analysis of DNA adducts, mutagenicity, cell transformation and carcinogenicity have led to and support the hypothesis that the reaction of specific estrogen metabolites, preponderantly the electrophilic catechol estrogen-3,4-quinones, with DNA can generate the critical mutations to initiate breast, prostate and other human cancers (Cavalieri and Rogan, 2010, 2011).

Metabolic formation of estrogens derives from aromatization of androstendione and testosterone, catalyzed by CYP19 (aromatase), to afford E_1 and E_2, respectively (Fig. 17). E_1 and E_2 are interconverted by 17β-hydroxy steroid dehydrogenase. The excess of estrogens obtained is stored as estrone sulfate (Fig. 17). Estrogens are metabolized by two main pathways: formation of the 16α-$OHE_1(E_2)$ (not shown in Fig. 17) and formation of the catechol estrogens 2-$OHE_1(E_2)$ and 4-$OHE_1(E_2)$ (Fig. 17) (Zhu and Conney, 1998). CYP1A1 catalyzes hydroxylation of E_1 and E_2 preferentially at C-2, whereas CYP1B1 catalyzes hydroxylation almost exclusively at C-4 (Hayes et al., 1996; Spink et al., 1994, 1998). The two catechol estrogens can be inactivated by conjugation to glucuronides and sulfates, especially in the liver (not shown in Fig. 17). In extrahepatic tissues, the most common path of conjugation of catechol estrogens is *O*-methylation catalyzed by catechol-*O*-methyltransferase (COMT) (Männistö and Kaakkola, 1999; Yager, 2013). Oxidation of the catechol estrogens to $E_1(E_2)$-2,3-quinone (Q) and $E_1(E_2)$-3,4-Q catalyzed by cytochrome P450 or peroxidase (Fig. 17) becomes more competitive when the activity of COMT is low.

Oxidation of semiquinones to quinones can also be obtained by molecular oxygen (Fig. 17). Reduction of estrogen quinones to semiquinones by cytochrome P450 reductase completes the redox cycle (Fig. 17). In this process, the molecular oxygen is reduced to superoxide anion radical, and then converted by superoxide dismutase to hydrogen peroxide. In the presence of Fe^{2+} the hydrogen peroxide is transformed to hydroxyl radical. Reaction of the hydroxyl radical with lipids affords lipid hydroperoxides (Kappus, 1985), which can act as unregulated cofactors for the oxidation of catechol estrogens by cytochrome P450. Thus, redox cycling can be a major contributor to the formation of catechol estrogen quinones, which are the ultimate carcinogenic metabolites of estrogens.

4-$OHE_1(E_2)$ are more potent carcinogens than 2-$OHE_1(E_2)$ (Li and Li, 1987; Liehr et al., 1986; Newbold and Liehr, 2000). This property cannot be attributed to formation of hydroxyl radicals from redox cycling, because the 2-OHE_2 and 4-OHE_2 have the same redox potential (Cavalieri, 1994; Mobley et al., 1999). The greater carcinogenic activity of 4-OHE_2 is related to the much higher levels of depurinating DNA adducts formed by the E_2-3,4-Q compared to the E_2-2,3-Q (Fig. 18) (Zahid et al., 2006). Different mechanisms of adduction are responsible for the different reactivity. E_2-3,4-Q reacts via a proton-assisted 1,4-Michael addition (Stack et al., 2008), whereas the E_2-2,3-Q rearranges to *para*-quinone methide, which reacts then via a 1,6-Michael addition (Bolton and Shen, 1998).

Following the formation of catechol estrogen quinones (Fig. 17), they can be inactivated by conjugation with glutathione (GSH). A second inactivating pathway for the quinones is reduction to their respective catechols by quinone reductase (Gaikwad et al., 2007; Gaikwad et al., 2009c), a protective enzyme that can be induced by a variety of compounds (Talalay

NIH-PA Author Manuscript

NIH-PA Author Manuscript

NIH-PA Author Manuscript

et al., 2003). If all the protective processes are insufficient, the catechol estrogen quinones can react with DNA to form predominantly depurinating adducts.

12. Depurinating estrogen-DNA adducts in the etiology of cancer

Carcinogens react with DNA to yield two types of adducts: stable adducts and depurinating adducts. Investigators in chemical carcinogenesis have always considered only stable adducts, which remain in DNA unless removed by repair. These adducts are usually detected by the ^{32}P-postlabeling technique, but their structure has not always been identified. In general, metabolically activated PAH and estrogens predominantly produce adducts with DNA at the N-7 of Gua and N-3 and N-7 of Ade, the most nucleophilic sites of Gua and Ade (Pullman and Pullman, 1981) with destabilization of the glycosyl bond and subsequent depurination.

The first evidence that depurinating DNA adducts play a major critical role in cancer initiation was obtained from a correlation between the level of depurinating PAH-DNA adducts and oncogenic H-*ras* mutations in mouse skin papillomas (Chakravarti et al., 1995). The potent carcinogens DMBA (Devanesan et al., 1993) and DB[*a*,*l*]P (Cavalieri et al., 2005; Todorovic et al., 2005) yield predominantly depurinating Ade adducts that induce A to T transversions in codon 61 (Chakravarti et al., 1995). Instead BP produces twice as many Gua depurinating adducts as Ade depurinating adducts (Rogan et al., 1993), corresponding to twice as many codon 13 G to T transversions as codon 61 A to T transversions (Chakravarti et al., 1995), respectively.

A similar correlation between the sites of formation of depurinating DNA adducts and H-*ras* mutations was found in mouse skin and rat mammary gland treated with the ultimate carcinogenic metabolite E_2-3,4-Q (Chakravarti et al., 2001; Mailander et al., 2006). When $E_1(E_2)$-3,4-Q react with DNA, they form 99% depurinating adducts, 4-$OHE_1(E_2)$-1-N3Ade and 4-$OHE_1(E_2)$-1-N7Gua, by the 1,4-Michael addition mechanism (Fig. 17) (Cavalieri et al., 1997, Li et al., 2004; Stack et al., 1996; Zahid et al., 2006), whereas $E_1(E_2)$-2,3-Q yield much lower levels of 2-$OHE_1(E_2)$-6-N3Ade (Fig. 18) by the 1,6-Michael addition mechanism that occurs after tautomerization of the $E_1(E_2)$-2,3-Q to the $E_1(E_2)$-2,3-Q methide (Bolton and Shen, 1998; Zahid et al., 2006). The levels of DNA adducts formed by the two catechol estrogen quinones are in agreement with the greater carcinogenicity of 4-$OHE_1(E_2)$ compared with the borderline carcinogenic activity of 2-$OHE_1(E_2)$ (Li and Li, 1987; Liehr et al., 1986; Newbold and Liehr, 2000).

The major cancer initiating pathway is presented in Figure 19. E_1 and E_2 can be metabolically converted to 4-$OHE_1(E_2)$ by CYP1B1. Oxidation of the catechol estrogens yields the corresponding $E_1(E_2)$-3,4-Q, which react with DNA to form small amounts of stable adducts (~1%), which remain in the DNA unless removed by repair, and predominant amounts of the depurinating adducts 4-$OHE_1(E_2)$-1-N3Ade and 4-$OHE_1(E_2)$-N7Gua (99%) (Fig. 19), which detach from DNA, leaving behind apurinic sites. Errors in the repair of these sites can lead to the critical mutations that initiate cancer.

13. Estrogens as mutagens

The ability of depurinating DNA adducts to generate mutations that can initiate cancer was discovered by correlating the sites of H-*ras* mutations in mouse skin treated with one of three potent carcinogenic PAH with the DNA base bonded to the PAH in adducts formed in the skin (Chakravarti et al., 1995). This seminal discovery laid the groundwork for investigating estrogens as mutagens.

NIH-PA Author Manuscript

NIH-PA Author Manuscript

NIH-PA Author Manuscript

Early studies of E_2 in *in vitro* mutagenesis assays failed to detect any activity, and the estrogens were classified as epigenetic carcinogens (Liehr, 2000). Subsequently, more appropriate and more sensitive assays have demonstrated that E_2 and 4-OHE_2 are, indeed, mutagenic in mammalian cells. The clearest demonstration of mutagenicity by 4-OHE_2 was achieved by using the Big Blue® (BB®) rat2 embryonic cell line, which is transfected with the lambda-LIZ vector. This enables the BB rat2 cells to detect mutations in the *lac*I and/or *c*II genes. With multiple treatments of the cells with 4-OHE_2, a dose-dependent, statistically significant increase in mutant fraction (mutants/10^5 pfu) was observed, with 2.6 ± 1.3 in controls to 4.5 ± 0.7 and 5.8 ± 0.3 at 100 and 200 nM, respectively (Zhao et al., 2006). The reactive quinone formed from 4-OHE_2, E_2-3,4-Q, was similarly mutagenic. In contrast, no mutagenicity was detected when the cells were treated with 2-OHE_2. The spectrum of mutations induced by 4-OHE_2 in the BB rat2 cells contained a higher percentage of mutations at A:T base pairs (ca. 24%) than the mutation spectrum in the controls (6%) (Zhao et al., 2006). The mutagenic activity of 4-OHE_2 provides additional evidence that genotoxicity plays a role in estrogen-induced carcinogenesis.

The mutagenicity of E_2-3,4-Q was first demonstrated in female SENCAR mice by treating a shaved area of dorsal skin, excising the treated skin and determining the H-*ras* mutations induced and the estrogen-DNA adducts formed (Table 3) (Chakravarti et al., 2001). Equal amounts of the depurinating 4-OHE_2-1-N3Ade and 4-OHE_2-1-N7Gua adducts were identified in the skin, representing more than 99% of the total adducts formed (Chakravarti et al., 2001). Mutations were observed in the H-*ras* oncogene within 6–12 h after treatment. A.T to G.C mutations predominated. The rapid appearance of mutations indicated that they arose by error-prone repair of the apurinic sites generated by the depurinating estrogen-DNA adducts.

Similar mutations were observed when female ACI rats were treated by intramammillary injection of E_2-3,4-Q (Table 3) (Mailander et al., 2006). Once again, the two depurinating adducts, 4-OHE_2-1-N3Ade and 4-OHE_2-1-N7Gua, were formed in equal amounts and represented more than 99% of the total adducts. H-*ras* mutations, mainly A.T to G.C, were detected by 6–12 h. The abundant formation of depurinating adducts and early induction of base excision repair (BER) genes following treatment with a carcinogen suggest that error-prone BER could be the mechanism of induction of the mutations.

The mutagenicity of E_2 and 4-OHE_2 was investigated in female BB® rats, which carry the lambda-LIZ vector in every cell, but are not affected biochemically or physiologically by it. Following implantation of E_2, 4-OHE_2, or E_2 plus 4-OHE_2, the rats were sacrificed after 20 weeks and DNA from the inguinal mammary fat pads was analyzed for mutations in the *c*II gene. The mutation spectrum of the rats receiving 4-OHE_2 was different from that in the group receiving E_2 or the untreated group. The rats treated with 4-OHE_2 exhibited a higher fraction of mutations at A.T base pairs. Presumably, the level of mutations was so low that mutations induced by the parent E_2 could not be detected. Only the rats receiving 4-OHE_2 had a significant number of A.T to G.C. mutations, while other mutations were observed in all four treatment groups (Cavalieri et al. 2006). These results are consistent with the hypothesis that 4-OHE_2 contributes to mutagenesis in BB® rat mammary tissue.

In summary, 4-OHE_2 and E_2-3,4-Q have now been demonstrated to be mutagenic in vitro and/or in vivo, whereas the marginally carcinogenic 2-OHE_2 was not found to be mutagenic. The mutational spectra were also consistent with those expected from the formation of depurinating estrogen-DNA adducts and error-prone repair of the resulting apurinic sites. Taken together, the results of mutagenesis studies support the hypothesis that estrogens initiate mutations by a genotoxic pathway.

NIH-PA Author Manuscript

NIH-PA Author Manuscript

NIH-PA Author Manuscript

If error-prone repair of apurinic sites generates mutations leading to cancer initiation, genetic polymorphisms in BER enzymes could result in greater susceptibility to breast and other cancers. Among the BER genes, the Arg399Gln polymorphic mutation in XRCC1 seems to account for an increased risk of breast cancer (Duell et al., 2001; Kim et al., 2002). XRCC1 binds other BER proteins to participate in initial and late stages of repair (Vidal et al., 2001). One study suggests that following exposure to aflatoxin B_1, the polymorphism at 399 in XRCC1 makes the BER process more error-prone, leading to increased levels of mutations (Lunn et al., 1999; Stark et al., 1988). Thus, XRCC1 could play a significant role in the error-prone BER found in breast cancer. Polymorphisms in other BER genes could also play a role.

14. Imbalance of estrogen metabolism in cancer initiation

The metabolism of estrogens through the catechol estrogen pathway is delineated by a balanced set of activating and protective enzymes (homeostasis), which minimize the oxidation of catechol estrogens to quinones and thus, their reaction with DNA (Fig. 17). Disruption of homeostasis in estrogen metabolism with excessive formation of catechol quinones can lead to cancer initiation. A variety of endogenous and exogenous factors can disrupt estrogen homeostasis. These include diet, environment, lifestyle, aging and genetic factors.

Overexpression of CYP19 (aromatase) in target tissues (Jefcoate et al., 2000; Miller and O'Neill, 1987; Simpson et al., 1994) and/or the presence of unregulated sulfatase that converts an excess of stored E_1-sulfate to E_1(Fig. 17) (Pasqualini et al., 1996; Santner et al., 1984) imbalance the metabolism with excessive synthesis of estrogens.

Another factor that can imbalance estrogen homeostasis is the overexpression of the enzyme CYP1B1, which converts $E_1(E_2)$ predominantly to 4-$OHE_1(E_2)$, the precursors to the major ultimate carcinogenic metabolites $E_1(E_2)$-3,4-Q (Fig. 17) (Hayes et al., 1996; Lu et al., 2007, 2008; Spink et al., 1998). An analogous effect could be obtained by a lack or low level of COMT activity due to polymorphic variation (Mitrunen and Hirvonen, 2003; Yager, 2013). Insufficient activity of COMT would be translated into low levels of methylation of 4-$OHE_1(E_2)$ and subsequent increase of the competitive oxidation of 4-$OHE_1(E_2)$ to $E_1(E_2)$-3,4-Q (Fig. 17). Higher levels of $E_1(E_2)$-3,4-Q can also be obtained by polymorphism in quinone reductase (NQO1) that leads to decreased conversion of quinones to catechols (Fig. 17) (Singh et al., 2009). Similarly, higher levels of $E_1(E_2)$-3,4-Q can be produced when there is a low cellular level of GSH, which is protective because it reacts efficiently with the estrogen quinones.

Imbalances in estrogen metabolism have been observed in animal models for estrogen carcinogenicity: the kidney of male Syrian golden hamsters (Cavalieri et al., 2001), the prostate of Noble rats (Cavalieri et al., 2002a) and the mammary gland of ER-α knockout mice (Devanesan et al., 2001). Imbalance of estrogen homeostasis has also been observed in the breast tissue of women with breast cancer (Rogan et al., 2003; Singh et al., 2005).

a. Imbalance of estrogen homeostasis in the kidney of Syrian golden hamsters

The hamster is an excellent model for studying estrogen homeostasis, because implantation of E_1 or E_2 in male Syrian golden hamsters induces 100% of renal carcinomas, but does not induce liver tumors (Li et al., 1983). Therefore, comparison of the profile of estrogen metabolites, conjugates and DNA adducts in the two organs, after treatment of the hamster with E_2, should provide information on the relative imbalance of estrogen homeostasis in the two organs (Cavalieri et al., 2001). In the liver, more *O*-methylation of 2-$OHE_1(E_2)$ was observed, whereas more formation of $E_1(E_2)$-3,4-Q was detected in the kidney. These results

NIH-PA Author Manuscript

NIH-PA Author Manuscript

NIH-PA Author Manuscript

suggest greater oxidation of catechol estrogens to $E_1(E_2)$-3,4-Q and less protective methylation of 2-$OHE_1(E_2)$ in the kidney. In another experiment, before the hamsters were treated with E_2, normal levels of GSH were depleted with L-buthionine (*S,R*)-sulphoximine, an inhibitor of GSH synthesis. In this case, very low levels of catechol estrogens and methoxy catechol estrogens were observed in the kidney compared with the liver, suggesting little protective reduction of estrogen quinones to catechol estrogens in the kidney by quinone reductase (Fig. 17). More importantly, the 4-$OHE_1(E_2)$-1-N7Gua depurinating adduct, arising from reaction of $E_1(E_2)$-3,4-Q with DNA, was detected in the kidney, but not in the liver (Cavalieri et al., 2001).

These results suggest that cancer initiation in the kidney occurs because of poor methylation of the catechol estrogens, rendering more competitive the oxidation of catechol estrogens to catechol quinones, as well as poor reduction activity to remove the estrogen quinones (Fig. 17). These two effects increase the levels of estrogen quinones that can react with DNA and eventually initiate cancer.

b. Imbalance of estrogen homeostasis in the prostate of Noble rats

The male Noble rat is a good model for the study of prostate cancer. Treatment of these rats with testosterone plus E_2 induces ductal adenocarcinoma of the prostate in 100% of the animals, whereas treatment with testosterone alone causes prostatic cancer in only 40% of the animals (Bosland et al., 1995). The carcinomas arise in the dorsolateral and periurethral regions of the prostate, but not in the ventral or anterior prostate. It is hypothesized that estrogens initiate prostate cancer via formation of $E_1(E_2)$-3,4-Q, while testosterone promotes cancer development (Bosland et al., 1995).

To study the role of estrogens in the initiation of prostate cancer, rats were treated with 6 μmol of 4-OHE_2 or E_2-3,4-Q/100g body weight for 90 min. The rats were then sacrificed and the prostates were excised, separated into the four regions, extracted and analyzed by high pressure liquid chromatography for estrogen metabolites and conjugates (Cavalieri et al., 2002a).

After treatment with 4-OHE_2, the two regions in which tumors do not develop (ventral and anterior prostate) had higher levels of 4-methyoxyCE than the two areas in which carcinomas were induced by treatment with E_2 and testosterone (dorsolateral and periurethral prostate). This finding suggests that the protective enzyme COMT is more effective in the ventral and anterior prostate than in the other two regions. In addition, the level of GSH conjugates was higher in the non-susceptible ventral and anterior prostate than in the susceptible dorsolateral and periurethral prostate.

This could mean that the two non-susceptible regions have better protection at the catechol level with greater COMT activity and also a better conjugative protection at the quinone level with a higher level of GSH. The results verify that less $E_1(E_2)$-3,4-Q can react with DNA.

When the rats were treated with E_2-3,4-Q instead of 4-OHE_2, the levels of GSH conjugates and the 4-methoxyCE were produced in larger abundance in the two non-susceptible regions than in the susceptible regions, suggesting more COMT activity at the catechol level and a better conjugation at the quinone level. In addition, a more effective reduction of E_2-3,4-Q to 4-OHE_2, presumably catalyzed by quinone reductase, could also be observed (Fig. 17) to render the two regions not susceptible.

NIH-PA Author Manuscript

NIH-PA Author Manuscript

NIH-PA Author Manuscript

c. Imbalance of estrogen homeostasis in the mammary gland of ERKO/*Wnt*-1 mice

A novel model for breast cancer was established by crossing mice carrying the *Wnt*-1 transgene (100% of adult females develop spontaneous mammary tumors) with the ERKO mouse line, in which the mice lack ER-α. Mammary tumors develop in these mice despite the lack of functional ER-α (Bocchinfuso et al., 1999). To begin investigating whether estrogen metabolite-mediated genotoxicity plays a critical role in the initiation of mammary tumors, the pattern of estrogen metabolites and conjugates was analyzed in ERKO/*Wnt*-1 mice. Extracts of hyperplastic mammary tissue and mammary tumors were analyzed by HPLC interfaced with an electrochemical detector (Devanesan et al., 2001). Picomole amounts of 4-$OHE_1(E_2)$ were detected, but their methoxy conjugates were not. Neither 2-$OHE_1(E_2)$ nor 2-$OCH_3E_1(E_2)$ was detected. However, the GSH conjugates of $E_1(E_2)$-3,4-Q or their hydrolytic products (conjugates of cysteine and *N*-acetylcysteine) were detected in picomole amounts in both tumors and hyperplastic mammary tissue, demonstrating the formation of $E_1(E_2)$-3,4-Q. These preliminary findings indicate that estrogen homeostasis is imbalanced in the mammary tissue; that is, the 2-$OHE_1(E_2)$, the 2-$OCH_3E_1(E_2)$ and 4-$OCH_3E_1(E_2)$ were not detected, but the GSH conjugates of $E_1(E_2)$-3,4-Q were. These results are consistent with the abundant evidence that the $E_1(E_2)$-3,4-Q play the preponderant role in the reaction with DNA and initiation of cancer.

d. Imbalance of estrogen homeostasis in the breast of women with breast carcinoma

A study of breast tissue from women with and without breast cancer provides key evidence in support of the concept of altered estrogen homeostasis (Rogan, et al., 2003). In fact, relative imbalances in estrogen homeostasis were observed in the analysis of women with breast cancer (Fig. 20). Levels of E_1 and E_2 in women with carcinoma were somewhat higher than those in controls. In women without cancer, a slightly larger amount of 2-$OHE_1(E_2)$ than 4-$OHE_1(E_2)$ was observed. In women with carcinoma, the 4-$OHE_1(E_2)$ were three times more abundant than the 2-$OHE_1(E_2)$. The 4-$OHE_1(E_2)$ were also four times higher than in women without cancer ($p < 0.01$). Furthermore, a slightly lower level of methylation was observed for the catechol estrogens vs the controls. Levels of conjugates were three times those in controls, suggesting a larger probability for the $E_1(E_2)$-2,3-Q and $E_1(E_2)$-3,4-Q to react with DNA in the breast tissue of women with carcinoma. Levels of 4-$OHE_1(E_2)$ ($p < 0.01$) and quinone conjugates ($p < 0.003$) appear to be highly significant predictors of breast cancer (Rogan et al., 2003).

Further evidence of imbalance in estrogen homeostasis derives from preliminary evidence for the greater expression of estrogen-protective enzymes (COMT and NQO1) (Figs. 17, 21) in breast tissue of women without breast cancer and higher expression of estrogen-activating enzymes (CYP19 and CYP1B1) (Figs. 17, 21) in breast tissue of women with breast cancer (Singh et al., 2005).

It is apparent from these animal and human studies that the oxidative stress leading to the excessive formation of semiquinones and quinones from catechol estrogens (Fig. 17) is the result of an imbalance of one or more enzymes involved in the maintenance of estrogen homeostasis.

In addition to endogenous factors that can disrupt estrogen homeostasis, there are environmental factors that can also imbalance estrogen metabolism. These factors include substances we ingest through the nose, mouth and skin. For example, pesticides and herbicides in the soil, pollutants in the air, cigarette smoke and contaminants in food can affect estrogen metabolism with increased formation of catechol estrogen quinones. For example, dioxin induces expression of the activating enzyme CYP1B1 (Fig. 17) (Lu et al.,

NIH-PA Author Manuscript

NIH-PA Author Manuscript

NIH-PA Author Manuscript

2007, 2008). These compounds do not act as direct carcinogens themselves, but can make the estrogens become carcinogenic by disrupting homeostasis.

15. Transformation of human breast epithelial cells lacking ER-α by estrogens

Further evidence for the initiation of cancer by estrogen-DNA adducts has been provided by the use of cultured human breast epithelial MCF-10F cells. These cells are an immortalized, non-transformed ER-α-negative cell line. Treatment of these cells with E_2 or 4-OHE_2 generates the depurinating N3Ade and N7Gua estrogen-DNA adducts (Lu et al., 2007, 2008; Saeed et al., 2007b). At doses of 0.007 nM to 3.5 μM, treatment with E_2 or 4-OHE_2 leads to transformation of the cells as detected by their ability to form colonies in soft agar (Lareef et al., 2005; Russo and Russo, 2004; Russo et al., 2003). These cells are transformed by estrogens even in the presence of the anti-estrogen tamoxifen or ICI-182,780 (Russo and Russo, 2004). The results indicate that transformation occurs through the genotoxic effects of the estrogen metabolites. The 2-OHE_2 metabolite induces these changes to a much smaller extent. Implantation of estrogen-transformed MCF-10F cells, selected by their invasiveness, into severely compromised immune-deficient mice produces tumors (Russo et al., 2006).

These results demonstrate that ER-α-negative human breast epithelial cells are transformed by the genotoxic effects of catechol estrogen quinones, supporting the hypothesis that formation of specific estrogen-DNA adducts is the crucial event in the initiation of estrogen-induced cancer.

16. Carcinogenic activity of estrogens in animal models

The carcinogenicity of estrogens was first demonstrated in laboratory animals. When male Syrian golden hamsters were implanted with E_1, E_2, DES or HES, induction of kidney tumors was obtained (Li et al., 1983). In a similar experiment, it was later discovered that 4-$OHE_1(E_2)$, but not 2-$OHE_1(E_2)$ induced kidney tumors in the hamsters (Li and Li, 1987; Liehr et al., 1986). In CD-1 mice, 4-OHE_2 induced uterine adenocarcinomas after neonatal exposure, while 2-OHE_2 displayed borderline activity (Newbold and Liehr, 2000). The lack or very low level of carcinogenicity of the 2-$OHE_1(E_2)$ is consistent with the much smaller capacity of the 2,3-quinones to react with DNA to produce adducts, compared with that of the 3,4-quinones (Zahid et al., 2006). Nonetheless, the studies in the above animal models did not clarify the questions about the role of ER-α-mediated events in cancer induction by estrogens.

To address these questions, the ERKO/*Wnt*-1 mouse, a strain of transgenic mice with ER-α knocked out was developed by Bocchinfuso et al (Bocchinfuso et al., 1999; Bocchinfuso and Korach, 1997). Despite the presence of the *Wnt*-1 transgene, these mice were not expected to develop mammary tumors because of the lack of ER-α. Instead, female ERKO/*Wnt*-1 mice developed 100% mammary tumors, although at a slower rate than the parent female *Wnt*-1 mice (Bocchinfuso et al., 1999). The catechol estrogens 4-$OHE_1(E_2)$ and the GSH conjugates derived by reaction of $E_1(E_2)$-3,4-Q with GSH were detected in mammary tissue from female ERKO/*Wnt*-1 mice, but no methoxy catechol estrogens were detected (Devanesan et al., 2001), suggesting that these mice have little protection in the oxidation of 4-$OHE_1(E_2)$ to the reactive quinones (Fig. 17).

To further understand the mechanism of cancer initiation by estrogens, female ERKO/*Wnt*-1 mice were ovariectomized at 15 days of age, removing the major source of estrogens, and implanted with one of several doses of E_2. Mammary tumors developed in a dose-dependent

NIH-PA Author Manuscript

NIH-PA Author Manuscript

NIH-PA Author Manuscript

manner (Santen et al., 2003; Yue et al., 2003). Tumors were induced even after implantation of E_2 plus the anti-estrogen ICI-182,780 (Santen et al., 2009). Taken together, these results offer strong evidence that estrogens initiate cancer via a genotoxic mechanism, rather than estrogen receptor-mediated events.

17. Analysis of depurinating estrogen-DNA adducts in human subjects with and without cancer

Development of noninvasive tests of cancer risk has been a major goal for decades. Analysis of depurinating estrogen-DNA adducts, estrogen metabolites and estrogen conjugates provides biomarkers of risk that are related to the first critical step in the initiation of a number of prevalent human cancers.

a. Breast cancer

If estrogens initiate breast cancer by a genotoxic mechanism, formation of depurinating estrogen-DNA adducts should be significantly higher in women at high risk for breast cancer or diagnosed with the disease, compared to women at normal risk. In addition, observation of higher levels of estrogen-DNA adducts in women at high risk for breast cancer would suggest that formation of these adducts is a causative factor in the etiology of breast cancer rather than a consequence of the disease.

To date, three studies have been conducted in women at normal or high risk for breast cancer and those diagnosed with the disease. High risk women were those whose Gail Model score estimated a 5-year risk > 1.66% (Gail et al., 1989). The Gail Model is used to identify women at high risk for breast cancer. It is calculated based on age, age at menarche, age at first birth, prior breast biopsies and atypical hyperplasia, and number of first degree relatives (mother, sister, daughter) diagnosed with breast cancer.

In the first two studies, a spot urine sample (~50 ml) was collected from each subject, partially purified by solid-phase extraction, and analyzed for 38 estrogen metabolites, conjugates and depurinating DNA adducts (Table 4) (Gaikwad et al., 2008). The 38 analytes were identified and quantified, and the ratio of the adducts 4-$OHE_1(E_2)$-1-N3Ade, 4-$OHE_1(E_2)$-1-N7Gua and 2-$OHE_1(E_2)$-6-N3Ade to their respective metabolites and conjugates was calculated for each subject (Fig. 22).

$$\text{ratio}=\frac{4-\text{OHE}_1(\text{E}_2)-1-\text{N3Ade}+4-\text{OHE}_1(\text{E}_2)-1-\text{N7Gua}}{4-\text{catecholestrogens}+4-\text{catecholestrogens conjugates}}+\frac{2-\text{OHE}_1(\text{E}_2)-6-\text{N3Ade}}{2-\text{catecholestrogens}+2-\text{catecholestrogens conjugates}}\times 1000$$

In the first study of 46 normal-risk women, 12 high-risk women and 17 women with breast cancer, the ratio in normal-risk women was significantly lower than the ratios in the high-risk ($p < 0.001$) and breast cancer ($p < 0.001$) groups (Gaikwad et al., 2008). In the second study, similar differences were observed between the 40 normal-risk women, 40-high-risk women and 40 women with breast cancer (both $p < 0.001$, Fig. 22) (Gaikwad et al., 2009b).

A third study was conducted with serum from 74 normal-risk women, 80 high-risk women and 79 women with breast cancer. The larger number of subjects improved the reliability, with $p < 0.001$ in comparing normal-risk women to either high-risk women or women with breast cancer (Fig. 22) (Pruthi et al., 2012). Similar differences were observed when the three categories of women were compared among premenopausal women and peri/

NIH-PA Author Manuscript

NIH-PA Author Manuscript

NIH-PA Author Manuscript

postmenopausal women (Fig. 23) (Pruthi et al., 2012). Highly significant differences were observed between normal-risk women and either high-risk women or women with breast cancer. Menopausal status did not alter this finding.

The results obtained in serum samples were used to compare the sensitivity (women with low risk) and specificity (women with high risk) of the assay and to select a cut-off ratio for low risk (Fig. 24) (Pruthi et al., 2012). The sensitivity and specificity were maximized at an adduct ratio of 77, which was selected as the cut-off point for low risk. For women with an adduct ratio greater than 77, the odds of being at high risk for breast cancer were eight times higher than for those with a ratio less than 77.

In all three studies the high ratios typically resulted from high levels of adducts and low levels of metabolites and conjugates. In some samples, though, a high ratio resulted from an average level of adducts and extremely low levels of metabolites and conjugates. This indicated that a large proportion of the estrogen present had been metabolized into catechol-estrogen quinones that reacted with DNA to form adducts.

In the ratio of depurinating DNA adducts to metabolites and conjugates (see Figure 22), the 4-$OHE_1(E_2)$-1-N3Ade and 4-$OHE_1(E_2)$-1-N7Gua adducts play the preponderant role (> 97%), while the small amounts of 2-$OHE_1(E_2)$-6-N3Ade play a minor role (< 3%). This is due to the poor ability of $E_1(E_2)$-2,3-Q to react with DNA compared to $E_1(E_2)$-3,4-Q (Zahid et al., 2006), and it correlates with the marginal carcinogenic activity of 2-$OHE_1(E_2)$ in animal models (Li and Li, 1987; Liehr et al., 1986; Newbold and Liehr, 2000).

Overall, the high ratios of estrogen-DNA adducts to metabolites and conjugates in women at high risk for breast cancer is consistent with formation of these adducts being a causative factor in the etiology of breast cancer.

b. Prostate cancer

To determine whether men with prostate cancer form high levels of depurinating estrogen-DNA adducts, urine samples from men diagnosed with prostate cancer (n=7) or urological conditions (n=4, erectile dysfunction or benign prostatic hypertrophy), as well as healthy men, were analyzed to determine the presence of 4-$OHE_1(E_2)$-1-N3Ade, one of the major depurinating estrogen-DNA adducts (Fig. 25) (Markushin et al., 2006).

Several detection methods were used to analyze the 20-ml urine samples. Each sample was extracted by using affinity columns equipped with a monoclonal antibody (MAb), which was specifically developed for the 4-$OHE_1(E_2)$-1-N3Ade adduct and highly discriminating against closely related estrogen metabolites (Markushin et al., 2005). The extracts eluted from the affinity column were analyzed by laser-excited low-temperature phosphorescence spectroscopy (LTP) and by ultraperformance liquid chromatography-tandem mass spectrometry (LC/MS/MS). In addition another aliquot of each urine sample was lyophilized, extracted with methanol, pre-concentrated and analyzed by capillary electrophoresis with field amplified sample stacking (CE/FASS) and detected by absorbance-based electropherograms.

In Figure 25, the bars in the back row represent the concentration of 4-$OHE_1(E_2)$-1-N3Ade determined by CE/FASS. Only the samples from the 11 subjects with prostate cancer or a urological condition contain detectable 4-$OHE_1(E_2)$-1-N3Ade, with concentrations ranging from 15–240 pmol adduct per mg of creatinine in the urine. The identity of the adducts was confirmed by low temperature (77K) phosphorescence spectroscopy, as presented by the middle row of bars in Figure 25. Examples of the phosphorescence spectra are shown in the right inset of Figure 25 for subjects #1, #4 and #6, and the spectra are nearly

NIH-PA Author Manuscript

NIH-PA Author Manuscript

NIH-PA Author Manuscript

indistinguishable from that of the standard 4-OHE_1-1-N3Ade (red spectrum). This second method of detection indicated concentrations of adducts in the range of 10–150 pmol per mg creatinine. The five healthy control men had only background levels of the adducts.

LC/MS/MS was also used to validate the identification and quantification of the adducts in the samples eluted from the immunoaffinity columns, as shown in the front row of bars in Figure 25. The LC/MS/MS obtained for subject #11 is shown in the left inset to Figure 25. The major peak of the chromatogram corresponds to the 4-OHE_1-1-N3Ade adduct, with *m/z* 420.1. The upper spectrum corresponds to the daughter ions at *m/z* 296 and *m/z* 135.9 obtained by fragmentation of the parent ion.

Although the amount of adducts for each subject is similar in all three methods, the concentration of adducts in the samples eluted from the immunoaffinity columns (LTP and LC/MS/MS) was less than the concentration detected by CE/FASS. This was expected because recovery of the 4-$OHE_1(E_2)$-1-N3Ade from the columns was 70–80% (Markushin et al., 2005). In summary, detectable levels of 4-$OHE_1(E_2)$-1-N3Ade are excreted in the urine of men with prostate cancer, as well as some other urological conditions, suggesting that the depurinating adducts may be biomarkers for risk of developing prostate cancer.

A larger case-control study of men with and without prostate cancer was conducted, in which urine samples were analyzed for 38 estrogen metabolites, conjugates and depurinating DNA adducts. In this study of 14 men diagnosed with prostate cancer (age 50 or older) and 125 healthy control men (ages 45 to 83), a morning spot urine sample was collected and the ratio of estrogen-DNA adducts to their respective estrogen metabolites and conjugates was analyzed by using UPLC-MS/MS (Yang et al., 2009).

The ratio of depurinating estrogen-DNA adducts to estrogen metabolites and conjugates (Fig. 26) was significantly higher ($p < 0.001$) in the men diagnosed with prostate cancer (median = 57.34) than in the healthy control men (median = 23.39) (Yang et al., 2009). The results of this study suggest that formation of depurinating estrogen-DNA adducts could play a critical role in the etiology of prostate cancer and that the ratio could serve as a potential biomarker for risk of developing prostate cancer.

c. Non-Hodgkin lymphoma

A similar study was conducted in men diagnosed with non-Hodgkin lymphoma (Gaikwad et al., 2009a). The catechol quinones of E_2 and benzene, a known inducer of leukemia and lymphoma (Mehlman, 2006; Miligi et al., 2006; Steinmaus et al., 2008), induce proliferation of human blood mononuclear cells, including those that give rise to leukemia and non-Hodgkin lymphoma (Chakravarti et al., 2006). The 38 estrogen metabolites, conjugates and depurinating DNA adducts were analyzed in urine samples from 15 men diagnosed with non-Hodgkin lymphoma and 30 healthy control men by using UPLC-MS/MS (Fig. 27). Men diagnosed with non-Hodgkin lymphoma had a median ratio of 86.0, whereas the control men had a median ratio of 18.0, and the difference between the two groups was statistically significant ($p < 0.0007$). These results suggest that formation of estrogen-DNA adducts may play a critical role in the etiology of non-Hodgkin lymphoma.

d. Thyroid cancer

Greater exposure to estrogens may be a risk factor for developing thyroid cancer. Well-differentiated thyroid cancer occurs most frequently in premenopausal women (Yu et al., 2010), and women with thyroid cancer appear to be at greater risk of developing breast cancer (Vassilopoulou-Sellin et al, 1999). To investigate the role of estrogen genotoxicity in thyroid cancer, a spot urine sample was collected from 40 women diagnosed with thyroid

NIH-PA Author Manuscript

NIH-PA Author Manuscript

NIH-PA Author Manuscript

cancer and 40 age-matched healthy control women (Zahid et al., 2013b). After partial purification of an aliquot of each urine sample by solid phase extraction, 38 estrogen metabolites, conjugates and depurinating DNA adducts were analyzed by using UPLC-MS/MS, and the ratio of estrogen-DNA adducts to their respective metabolites and conjugates was calculated for each sample (Fig. 28). The ratio differed significantly between cases (M = 102.7) and controls (M = 13.5, $p < 0.0001$), demonstrating high specificity and sensitivity. These results indicate that estrogen metabolism is unbalanced in women with thyroid cancer and suggest that formation of estrogen-DNA adducts could play a role in the etiology of the disease.

e. Ovarian cancer

The high ratio of estrogen-DNA adducts to estrogen metabolites and conjugates observed in women at high risk for breast cancer (Gaikwad et al., 2008, 2009b; Pruthi et al., 2012), led us to hypothesize that formation of estrogen-DNA adducts might play a critical role in the initiation of gynecological cancers such as ovarian cancer. To investigate this hypothesis, a case-control study was conducted with women diagnosed with ovarian cancer and healthy control women who had never been diagnosed with cancer. A spot urine sample was collected from 34 women diagnosed with ovarian cancer and 36 healthy control women. After partial purification by solid phase extraction, an aliquot of each urine sample was analyzed for 38 estrogen metabolites, conjugates and depurinating DNA adducts by using UPLC-MS/MS, and the ratio of DNA adducts to metabolites and conjugates was calculated (Fig. 29) (Zahid et al., 2013a). Almost all of the women diagnosed with ovarian cancer had higher DNA adduct ratios ($M=91.4 \pm 43.1$) than the healthy control women ($M=24.7 \pm 12.7$), and the difference was highly significant ($p < 0.0001$). These results indicate that estrogen metabolism is unbalanced in women with ovarian cancer and suggest that formation of estrogen-DNA adducts could play a role in the etiology of ovarian cancer.

In addition, single nucleotide polymorphisms (SNPs) were measured in DNA purified from saliva collected from the same subjects with and without ovarian cancer. The CYP1B1 (V432L) and COMT (V158M) polymorphisms were related to the adduct ratio and diagnosis with ovarian cancer. The DNA adduct ratio was increasingly higher in women with one and two high activity CYP1B1 alleles, showing a dose response relationship. In women who were homozygous for the low activity COMT allele, the CYP1B1 high activity allele was associated with a significantly increased DNA adduct ratio. The combination of high-risk CYP1B1 and COMT alleles elevated the odds ratio of having ovarian cancer to 5.93 compared to having the low-risk CYP1B1 and COMT alleles. These results indicate that unbalanced estrogen metabolism leading to formation of estrogen-DNA adducts is a causative factor in the initiation of ovarian cancer.

In summary, unbalanced catechol estrogen metabolism is observed in women diagnosed with breast cancer, thyroid cancer or ovarian cancer, as well as in men diagnosed with prostate cancer or non-Hodgkin lymphoma. The observation of high estrogen-DNA adduct ratios in women at high risk of breast cancer, along with a variety of results from other studies of estrogen carcinogenesis, indicate that formation of estrogen-DNA adducts plays a critical role in the etiology of these cancers.

18. Prevention of cancer by *N*-acetylcysteine and resveratrol acting through antioxidant and enzyme-modulating properties

The metabolism of estrogens via the catechol estrogen pathway is characterized by a balanced set of activating and protective enzymes (homeostasis). Homeostasis minimizes the oxidation of catechol estrogens to quinones, which can react with DNA (Fig. 17).

NIH-PA Author Manuscript

NIH-PA Author Manuscript

NIH-PA Author Manuscript

Imbalances in estrogen metabolism with excessive formation of catechol estrogen quinones can lead to cancer initiation. Many factors can disrupt estrogen homeostasis, including diet, environment, lifestyle, aging and genetic factors.

Five key estrogen-metabolizing enzymes participate in the catechol estrogen pathway. There are two activating enzymes. One is CYP19 (aromatase), which converts androgens to estrogens (Fig. 17). The second activating enzyme is CYP1B1, which converts $E_1(E_2)$ almost exclusively to 4-$OHE_1(E_2)$ (Fig. 17). Further oxidation of 4-$OHE_1(E_2)$ leads to $E_1(E_2)$-3,4-Q, the predominant metabolites that can react with DNA and initiate cancer. The protective enzymes are COMT, quinone reductase and glutathione-*S*-transferase (GST). COMT catalyzes the methylation of catechol estrogens, thereby preventing their conversion to semiquinones and quinones (Fig. 17) (Yager, 2013), whereas the quinone reductases NQO1 and NQO2 reduce catechol estrogen quinones back to catechol estrogens (Gaikwad et al., 2007, 2009c; Montano, et al., 2007).

Breast tissue from women who do not have breast cancer tended to have high levels of expression of the protective enzymes COMT and NQO1 and low levels of CYP19 and CYP1B1 (Figs. 17 and 21) (Singh et al., 2005). In contrast, non-tumor breast tissue from women diagnosed with breast cancer tended to have high levels of the activating enzymes CYP19 and CYP1B1, with low levels of the protective COMT and NQO1 (Figs. 17 and 21) (Singh et al., 2005).

GSH reacts non-enzymatically with the catechol estrogen quinones, but the third protective enzyme, GST, renders this reaction more efficient (Fig. 17), thereby preventing reaction of the catechol estrogen quinones with DNA.

The abundance of catechol estrogen quinones available to react with DNA to form adducts rests on the relative levels of activity of these five enzymes in cells. Balanced and unbalanced estrogen homeostasis can be preserved or mitigated, respectively, by the use of specific compounds, such as *N*-acetylcysteine (NAC) and resveratrol (Resv) (Fig. 32).

NAC is the acetyl derivative of the amino acid Cys, which is one component of the antioxidant tripeptide GSH. Resv, 3,5,4′-hydroxystilbene, is a natural antioxidant present in grapes and many other plants.

a. *N*-Acetylcysteine

The paradigm of cancer initiation by estrogens hinges on estrogen metabolism that involves disrupted homeostatic balance between activating and deactivating enzymes (Fig. 17). NAC can prevent damage to DNA by inhibiting formation of the electrophilic catechol estrogen quinones and/or reacting with them. The antimutagenic and anticarcinogenic properties of NAC are attributed to multiple protective mechanisms, including its nucleophilicity, antioxidant activity and inhibition of DNA adduct formation.

Hydrolysis of NAC by acylase in the liver and gut yields Cys, the precursor to intracellular GSH, guaranteeing replenishment of the critical tripeptide. Changes in GSH homeostasis have been implicated in the etiology and progression of a variety of human diseases, including cancer (Townsend et al., 2003). GSH cannot be used as a preventing agent because it does not cross cell membranes. The use of Cys as a preventing agent is limited by its toxicity in humans. In contrast, NAC has very low toxicity in humans and can cross the blood-brain barrier (De Flora et al., 1995).

NAC reacts efficiently with the electrophilic $E_1(E_2)$-3,4-Q (Cao et al., 1998a, 1998b) to prevent their reaction with DNA. When E_2-3,4-Q or lactoperoxidase-activated 4-OHE_2 was

NIH-PA Author Manuscript

NIH-PA Author Manuscript

NIH-PA Author Manuscript

reacted with DNA *in vitro*, NAC inhibited formation of the adducts 4-OHE_2-1-N3Ade and 4-OHE_2-1-N7Gua in a dose-dependent manner (Fig. 33) (Zahid et al., 2007). In the reaction of E_2-3,4-Q with DNA, NAC inhibited adduct formation by reacting with the quinone itself, and the maximum amount of inhibition was 68–70%. When the enzyme-activated 4-OHE_2 was reacted with DNA, NAC inhibited adduct formation not only by reacting itself with the quinone that was formed, but also by reducing E_2-3,4-semiquinone back to 4-OHE_2, limiting the amount of E_2-3,4-Q even further. These combined effects led to 83–84% inhibition of adduct formation (Zahid et al., 2007). The greater level of inhibition observed with lactoperoxidase-activated 4-OHE_2 can be explained by reduction of the estrogen semiquinone back to catechol, as also demonstrated by Samuni, et al. (Samuni et al., 2003).

In the oxidation of 4-$OHE_1(E_2)$ to semiquinones and quinones, formation of the depurinating adducts 4-$OHE_1(E_2)$-1-N3Ade and 4-$OHE_1(E_2)$-1-N7Gua by reaction of $E_1(E_2)$-3,4-Q with DNA, the last reaction can be reduced or prevented by conjugation of the quinone with GSH or with NAC (Fig. 34) (Zahid et al., 2010a). The NAC conjugate is also produced by the mercapturic acid biosynthetic pathway, starting with 4-$OHE_1(E_2)$-2-SG, followed by 4-$OHE_1(E_2)$-2-Cys and subsequent acetylation to 4-$OHE_1(E_2)$-2-NAC (Boyland and Chasseaud, 1969).

Treatment of MCF-10F cells, which are immortalized but not transformed human breast epithelial cells that lack ERα, with E_2-3,4-Q or 4-OHE_2 leads to formation of the depurinating adducts 4-OHE_2-1-N3Ade and 4-OHE_2-1-N7Gua. This process is inhibited when NAC is included in the culture medium (Fig. 35). In a dose response study, NAC inhibited formation of both 4-OHE_2-1-N3Ade and 4-OHE_2-1-N7Gua adducts about 69% in cells treated with E_2-3,4-Q (Fig. 35A) (Boyland and Chasseaud, 1969). Even greater inhibition was observed when the cells were treated with 4-OHE_2, giving a maximum 85% inhibition (Fig. 35B). Once again, the greater inhibition in cells treated with 4-OHE_2 plus NAC occurred because NAC not only reacted with E_2-3,4-Q itself, but also reduced the E_2-3,4-semiquinone back to 4-OHE_2(Samuni et al., 2003; Zahid et al., 2010a). An additional effect of NAC arose from its role in supporting synthesis of GSH, which in turn can lead to more NAC via the mercapturic acid biosynthesis pathway (Boyland and Chasseaud, 1969).

Similar results were observed when E6 immortalized mouse mammary cells were treated with E_2-3,4-Q or 4-OHE_2 plus NAC (Venugopal et al., 2008). These cells contain ERα, but the metabolism of 4-OHE_2 and formation of DNA adducts occurred very similarly to that in MCF-10F cells, which lack ERα. The E6 cells incubated with E_2-3,4-Q or 4-OHE_2 form similar amounts of 4-OHE_2-1-N3Ade and 4-OHE_2-1-N7Gua adducts. Inclusion of equimolar NAC in the medium reduced adduct formation from E_2-3,4-Q about 70% and about 90% when 4-OHE_2 was used instead (Venugopal et al., 2008).

Inclusion of NAC in the medium along with 4-OHE_2 or E_2-3,4-Q also inhibited malignant transformation of the E6 cells, as determined by colony formation in soft agar (Venugopal et al., 2008). Inhibition of transformation with NAC was far more effective when the cells were treated with 4-OHE_2 than with E_2-3,4-Q, once again confirming that the inhibitory properties of NAC include both reacting with E_2-3,4-Q and reducing E_2-3,4-semiquinone back to the catechol estrogen 4-OHE_2(Boyland and Chasseaud, 1969; Samuni et al., 2003).

In summary, in the initiation of cancer by estrogens, NAC acts as an antioxidant by reducing the semiquinone to catechol. NAC also acts as a preventing agent by keeping the cell replenished with GSH and acting as an antimutagenic, anticarcinogenic agent by reacting with E_2-3,4-Q, thereby inhibiting formation of estrogen-DNA adducts.

NIH-PA Author Manuscript

NIH-PA Author Manuscript

NIH-PA Author Manuscript

b. Resveratrol

Resv is found in various plants, including grapes and peanuts, and wine. This compound exerts pleiotropic effects, which include chemoprevention in diverse *in vitro* and *in vivo* systems (Aziz et al., 2003; Jang et al., 1997), modulation of CYP1A1 and CYP1B1 (Chang et al., 2000; Chen et al., 2004; Chun et al., 1999; Guengerich et al., 2003), antimutagenic and anticarcinogenic properties (Jang et al., 1997; Saiko et al., 2008), antioxidant and anti-inflammatory properties (Das and Das, 2007; Leonard et al., 2003; Subbaramaiah et al., 1998), reduction of estrogen semiquinones to catechol estrogens (Lu et al., 2008; Zahid et al., 2007; 2008) and induction of quinone reductase (Floreani et al., 2003; Lu et al., 2008; Montano et al., 2007; Zahid et al., 2008). Some of these properties are attributed to the easy hydrogen abstraction from the 4′-OH bond, with the formation of a 4′-oxyradical (Fig. 32) (Stivala et al., 2001). The easy abstraction is a consequence of the great resonance stabilization energy of the 4′-oxyradical (Stivala et al., 2001).

Although Resv has been found to be safe for human consumption at doses up to 5 g, investigators have shown its bioavailability to be very low. The studies on bioavailability have been conducted using single doses (Boocock et al., 2007; Walle et al., 2004). When oral Resv (0.5, 1, 2.5 or 5 g) was administered and plasma and urine analyzed, Resv plasma concentrations peaked 1.5 h post-administration, and the levels of glucuronide and sulfate conjugates were several-fold higher than that of Resv itself (Boocock et al., 2007). Bioavailability does not appear to have been studied following daily doses of Resv for an extended period of time. Despite the low bioavailability of Resv in humans, the compound has been shown to have significant biological effects.

Resv modulates CYP1A1 and CYP1B1. These are two important enzymes because they catalyze the oxidation of E_1 and E_2 to 2-OHE_1(E_2) (CYP1A1) and, more importantly, 4-OHE_1(E_2) (CYP1B1), as seen in Figure 17. Resv was found to inhibit dioxin-induced expression of CYP1A1 and CYP1B1 in cultured MCF-10A human mammary epithelial cells (Chen et al., 2004). This compound also inhibits the catalytic activity of human CYP1A1 in a dose-dependent manner (Chun et al., 1999). Resv is a noncompetitive inhibitor of CYP1B1 (Guengerich et al., 2003), and inhibits the catalytic activity and gene expression of CYP1B1 in cultured human mammary MCF-7 cells (Chang et al., 2000).

The ability of Resv to inhibit formation of estrogen-DNA adducts was investigated. As expected, when E_2-3,4-Q was reacted with DNA, Resv had no effect on formation of the 4-OHE_2-1-N3Ade and 4-OHE_2-1-N7Gua adducts (Fig. 36) (Zahid et al., 2007). This is because Resv has no ability to react with E_2-3,4-Q to prevent formation of the adducts. In contrast, NAC reduced the amount of adducts formed when E_2-3,4-Q was reacted with DNA (Fig. 33) (Zahid et al., 2007). When lactoperoxidase-activated 4-OHE_2, however, was incubated with DNA in the presence of Resv, formation of the adducts was inhibited, being reduced almost to zero with three-times as much Resv as 4-OHE_2(Fig. 36) (Zahid et al., 2007). Resv inhibited formation of the estrogen-DNA adducts by reducing E_2-3,4-semiquinones back to 4-OHE_2, thus preventing formation of the reactive E_2-3,4-Q. Thus, both NAC and Resv effectively reduce the semiquinone back to catechol in the catechol estrogen pathway (Fig. 17).

Resv was also shown to be an effective inducer of quinone reductase (NQO1) in MCF-10F cells (Fig. 37) (Lu et al., 2008; Zahid et al., 2008). Incubation of the cells with 25 μM Resv for 48 h almost doubled the amount of NQO1 in the cells, and the catalytic activity reducing E_2-3,4-Q to 4-OHE_2 was inhibited by the specific NQO1 inhibitor dicumarol (Fig. 37). These results confirmed previous studies of NQO1 induction by Resv (Floreani et al., 2003; Montano et al., 2007). When MCF-10F cells preincubated with Resv for 48 h were treated for 24 h with different levels of 4-OHE_2, the amounts of 4-OHE_2-1-N3Ade and 4-OHE_2-1-

NIH-PA Author Manuscript

NIH-PA Author Manuscript

NIH-PA Author Manuscript

N7Gua adducts formed were significantly reduced (Fig. 38) (Zahid et al., 2008). This reduction occurred because the preincubation with Resv had induced NQO1 in the cells. When the cells preincubated with Resv were then incubated with 4-OHE_2 plus fresh Resv for 24 h, formation of the adducts was completely eliminated (Fig. 38). In this case, not only was NQO1 induced, but the fresh Resv reduced any E_2-3,4-semiquinone back to 4-OHE_2, preventing formation of the reactive E_2-3,4-Q and, thus, formation of the estrogen-DNA adducts.

When MCF-10F cells were pretreated with dioxin to induce CYP1B1 and then treated with one of three levels of E_2, the 4-OHE_2-1-N3Ade and 4-OHE_2-1-N7Gua adducts were formed (Fig. 39) (Lu et al., 2008). When the cells were pretreated with dioxin and Resv, however, no adducts were detected, indicating that NQO1 was highly induced by the Resv. The same effects were seen when transformation of these cells was studied by culturing the treated cells in soft agar (Fig. 40) (Lu et al., 2008). Incubation of the MCF-10F cells with E_2 led to colonies of transformed cells and pretreatment with dioxin increased the number of colonies. When pretreatment also included Resv, however, the number of colonies of transformed cells was significantly reduced (Fig. 40).

In summary, the studies described above demonstrate that one of the important effects of Resv is reduction of semiquinones to catechol estrogens. Another significant characteristic of Resv is its ability to induce NQO1. Resv also modulates CYP1A1 and CYP1B1, which is more important because its product, 4-OHE_1(E_2), is a precursor to the predominant (97%) estrogen-DNA adducts that initiate cancer. These three characteristics of Resv reduce the effective amount of catechol estrogen quinones available to react with DNA and form the critical adducts for initiating cancer by estrogens.

c. *N*-Acetylcysteine and resveratrol

The combined effects of NAC and Resv on the formation of estrogen-DNA adducts was studied by incubating MCF-10F cells with 4-OHE_2 in the presence of NAC and/or Resv (Fig. 41) (Zahid et al., 2011a). In this experiment, Resv was always present at a molar ratio of 0.6 to 1 NAC. NAC was present at molar ratios of 0.61 to 60-times the 10 μM 4-OHE_2. NAC and Resv each individually reduced the amount of estrogen-DNA adducts formed in 24 h (Fig. 41). When both NAC and Resv were present in the culture medium, the level of adducts formed decreased even more than with the individual compounds. With 15-times more NAC (and 9-times more Resv) than 4-OHE_2, formation of the adducts was 95% inhibited. Higher concentrations of NAC plus Resv completely inhibited adduct formation.

NAC exerts its protective effects chemically, both by directly reacting with the catechol estrogen quinones and as an antioxidant that reduces the estrogen semiquinones back to catechol estrogens. NAC also is hydrolyzed to Cys, which is used in the biosynthesis of the scavenger GSH and, also, new NAC. In contrast, Resv exerts its protective effects both chemically and biologically. It serves the former function by acting as an antioxidant to reduce estrogen semiquinones back to catechol estrogens. Biologically, Resv induces quinone reductase and modulates CYP1A1 and CYP1B1, both inhibiting their gene expression and their catalytic activity. Therefore, these two compounds complement one another to minimize the metabolism of estrogens from catechols to quinones. These combined effects minimize formation of estrogen-DNA adducts, and, thus, the initiation of cancer. The preventive effects of Resv and NAC need to be demonstrated in humans, first by showing that the levels of estrogen-DNA adducts are reduced and, second, by also showing that administration of NAC and Resv reduces the incidence of breast and other human cancers.

NIH-PA Author Manuscript

NIH-PA Author Manuscript

NIH-PA Author Manuscript

19. Conclusions

Studies of PAH carcinogenesis led to fundamental discoveries that laid the groundwork for understanding estrogen carcinogenesis. The first of these discoveries is that chemical carcinogens form two types of DNA adducts, stable ones that remain in DNA unless removed by repair and depurinating adducts that are spontaneously lost from DNA by breaking of the glycosyl bond between the purine base (Ade or Gua) and deoxyribose. The depurinating adducts are the predominant ones formed by strong PAH carcinogens, such as BP, DB[*a,l*]P, DMBA and MC.

The second discovery is that formation of depurinating PAH-DNA adducts correlates with the sites of cancer-initiating mutations. For example, in mouse skin, DB[*a,l*]P and DMBA form primarily Ade depurinating adducts and generate A to T mutations in codon 61 of the H-*ras* oncogene. In contrast, BP forms about 50% adducts at Gua and 25% adducts at Ade and generates about 50% G to T transversions at codon 13 and 25% A to T transversions at codon 61 in the H-*ras* oncogene. This discovery reveals the primary importance of depurinating DNA adducts in carcinogenesis.

Extension of these two discoveries to estrogens enabled rapid understanding of the critical mechanism of estrogen carcinogenesis. Normally, the oxidative metabolism of estrogens via the catechol estrogen pathway is in homeostasis, with deactivating mechanisms protecting cells from excessive oxidation to catechol quinones, which can react with DNA to form predominantly depurinating estrogen-DNA adducts. When homeostasis is disrupted, more catechol estrogen quinones are formed, consequently leading to larger amounts of depurinating estrogen-DNA adducts. These adducts can generate mutations in cultured mammalian cells and in laboratory animals, thus demonstrating the genotoxicity of estrogens.

Furthermore, treatment of ER-negative human mammary cells with E_2 or 4-OHE_2 transforms the cells to malignancy. These cells can then induce tumors when injected into severely compromised immunodeficient mice.

Formation of depurinating estrogen-DNA adducts correlates with risk of developing cancer. Analysis of estrogen metabolites, conjugates and DNA adducts in urine or serum shows that women at high risk for breast cancer have significantly higher levels of estrogen-DNA adducts than women at normal risk for breast cancer. These results suggest that formation of depurinating estrogen-DNA adducts is a critical step in the initiation of breast cancer. Higher levels of estrogen-DNA adducts are also detected in women diagnosed with breast cancer, ovarian cancer or thyroid cancer. Similarly, men with prostate cancer or non-Hodgkin lymphoma have higher levels of estrogen-DNA adducts than healthy men without cancer. Therefore, depurinating estrogen-DNA adducts appear to be biomarkers for risk of developing a number of cancers.

Finally, understanding the mechanism of estrogen carcinogenesis has provided a basis for developing an approach to preventing prevalent types of cancer. The dietary supplements NAC and Resv can prevent formation of estrogen-DNA adducts by inhibiting formation of the catechol estrogen quinones or their reaction with DNA. If the initiation of cancer is blocked, promotion, progression and development of the disease would be prevented. This approach does not require knowledge of the genes involved or the series of events that follow initiation. Thus, use of NAC and Resv could prove to be a widely applicable strategy for cancer prevention.

Following Ockham’s Razor, the mechanism of cancer initiation by estrogens has been elucidated for some of the prevalent cancers. This knowledge has provided an approach to

NIH-PA Author Manuscript

NIH-PA Author Manuscript

NIH-PA Author Manuscript

cancer prevention that does not require the study of the complex series of steps occurring after cancer initiation and leading to cancer development.

Acknowledgments

We wish to acknowledge the contributions the following people have made to this research. Without their input, these discoveries could not have been made.

David Longfellow, Ph.D., Chief of the Chemical and Physical Carcinogenesis Branch, National Cancer Institute, for many years, had the intuition early on that our research in PAH and, later, estrogen carcinogenesis followed the right track, and he steadily supported this research.

Joachim Liehr, Ph.D., was one of the pioneers in realizing that estrogens could become chemical carcinogens in our body.

Ryszard Jankowiak, Ph.D., contributed structure elucidation of PAH-DNA adducts and identified them in animals for the first time; he also was the first to identify estrogen-DNA adducts in people.

Cheryl Beseler, Ph.D., has contributed her invaluable expertise in biochemistry, molecular biology, epidemiology and biostatistics to our studies of estrogen carcinogenesis in people.

Robert Roth, Ph.D., a superb organic chemist, contributed immensely to the chemistry of PAH radical cations.

Paula Mailander contributed her technical skills, first, in *in vitro* and *in vivo* animal studies and, later, to the molecular biology conducted in our research group.

Paolo Cremonesi, Ph.D., contributed to our understanding of the chemistry and physical chemistry of PAH radical cations, as well as the synthesis and structure elucidation of PAH-DNA adducts.

Prabu Devanesan, Ph.D., was a pioneer in identifying and quantifying PAH-DNA adducts *in vitro* and *in vivo*, as well as elucidating the oxidative metabolism of estrogens to form DNA adducts *in vitro* and *in vivo*.

Sheila Higginbotham was excellent in conducting animal studies with both PAH and estrogens.

N.V.S. RamaKrishna, Ph.D., was superb and highly productive in the synthesis and structure elucidation of PAH-DNA adducts formed *in vitro* and *in vivo*.

Rosa Todorovic, Ph.D., a productive biochemist, distinguished herself in identifying both stable and depurinating DNA adducts formed by PAH and estrogens.

Kai-Ming Li, Ph.D., an organic and analytical chemist, was outstanding in the synthesis and structure elucidation of DNA adducts formed by PAH and estrogens, as well as their identification in *in vitro* and *in vivo* studies.

Dhrubajyoti Chakravarti, Ph.D., an outstanding biochemist and molecular biologist, discovered the correlation between depurinating DNA adducts and cancer-initiating mutations.

Douglas Stack, Ph.D., a superb organic chemist, was the first to synthesize stable and depurinating estrogen-DNA adducts.

Patrick Mulder, Ph.D., elucidated the mechanism of activation of 1,2,3,4-tetrahydro-7,12-dimethylbenz[*a*]anthracene and synthesized fluorinated benzo[*a*]pyrenes, which were used to elucidate the mechanism of oxygen transfer by cytochrome P450.

Liang Chen, Ph.D., conducted a definitive study of stable and depurinating DNA adducts formed in the target organ mouse skin treated with benzo[*a*]pyrene.

Muhammad Saeed, Ph.D., an outstanding organic chemist, elucidated the mechanism of activation of diethylstilbestrol and hexestrol to form DNA adducts, as well as the mechanism of tumor initiation by naphthalene *in vitro* and in mouse skin.

Muhammad Zahid, Ph.D., synthesized the depurinating N3Ade adduct formed by 2-OHE_1(E_2), demonstrated that E_2-3,4-Q forms depurinating DNA adducts much more effectively than E_2-2,3-Q, showed how *N*-acetylcysteine and resveratrol inhibit formation of estrogen-DNA adducts in cultured human mammary cells, demonstrated the

NIH-PA Author Manuscript

NIH-PA Author Manuscript

NIH-PA Author Manuscript

formation of depurinating dopamine-DNA adducts in relation to the potential initiation of Parkinson's disease, and became an expert at analyzing estrogen metabolites, conjugates and depurinating DNA adducts in urine and serum.

Nilesh Gaikwad, Ph.D., established the method for analyzing estrogen metabolites, conjugates and depurinating DNA adducts in urine or serum by using ultraperformance liquid chromatography/tandem mass spectrometry (UPLC-MS/MS), as well as demonstrating that the quinone reductases NQO1 and NQO2 reduce catechol estrogen quinones to catechol estrogens.

Seema Singh, Ph.D., demonstrated that estrogen activating enzymes are expressed at higher levels in non-tumor breast tissue from women with breast cancer and protective enzymes are expressed at higher levels in breast tissue from women without breast cancer.

Fang Lu, Ph.D., a graduate student in our research group, demonstrated that induction of activating enzymes in cultured human mammary cells treated with 4-OHE_2 led to increased formation of estrogen-DNA adducts. He also demonstrated that the dietary supplement resveratrol can reduce formation of estrogen-DNA adducts and eliminate cell transformation by 4-OHE_2.

Li Yang, Ph.D., a graduate student in our research group, analyzed estrogen metabolites, conjugates and depurinating DNA adducts by UPLC-MS/MS. She demonstrated that men with prostate cancer have higher levels of adducts compared to healthy men without cancer and that serum samples can be analyzed to show that women diagnosed with breast cancer or at high risk of the disease have higher levels of adducts than healthy normal-risk women.

We give a special thanks to Ms Sherry Cherek, who has been our coordinator for over a decade. She is an assistant who represents perfect competency, effectiveness, high productivity and reliability.

Core support at the Eppley Institute is provided by grant P30 36727 from the National Cancer Institute.

References

Alpert AJ, Cavalieri EL. Metabolism of 6-substituted benzo[*a*]pyrene derivatives:*O*-Dealkylation and regiospecificity in aromatic hydroxylations. J. Med. Chem. 1980; 23:919–927. [PubMed: 7401117]

Amin S, Huie K, Balanikas G, Hecht SS, Pataki J, Harvey RG. High stereoselectivity in mouse skin metabolic activation of methylchrysenes to tumorigenic dihydrodiols. Cancer Res. 1987; 47:3613–3617. [PubMed: 3594428]

Amin S, Huie K, Melikian AA, Leszczynska JM, Hecht SS. Comparative metabolic activation in mouse skin of the weak carcinogen 6-methylchrysene and the strong carcinogen 5-methylchrysene. Cancer Res. 1985; 45:6406–6442. [PubMed: 4063989]

Arcos, JC.; Argus, MF. Chemical induction of cancer. Vol. VolIIA. New York: Academic Press; 1974.

Atkinson JK, Hollenberg PF, Ingold KU, Johnson CC, Le Tadic MH, Newcomb M, Putt DA. Cytochrome P450-catalyzed hydroxylation of hydrocarbons: Kinetic deuterium isotope effects for the hydroxylation of an ultrafast radical clock. Biochemistry. 1994; 33:10630–10637. [PubMed: 8075063]

Aziz MH, Kumar R, Ahmad N. Cancer chemoprevention by resveratrol: In vitro and in vivo studies and the underlying mechanisms (review). Int. J. Oncol. 2003; 23:17–28. [PubMed: 12792772]

Baird WM, Dipple A, Grover PL, Sims P, Brookes P. Studies on the formation of hydrocarbon-deoxyribonucleoside products by the binding of derivatives of 7-methylbenz(a)anthracene to DNA in aqueous solution and in mouse embryo cells in culture. Cancer Res. 1973; 33:2386–2392. [PubMed: 4795391]

Bernelot-Moens C, Glickman BW, Gordon AJ. Induction of specific frameshift and base substitution events by benzo[*a*]pyrene diol epoxide in excision repair-deficient *Escherichia coli*. Carcinogenesis. 1990; 11:781–785. [PubMed: 2110513]

Bigger CA, Tomaszewski JE, Dipple A. Differences between products of binding of 7,12-dimethylbenz[*a*]anthracene to DNA in mouse skin and in a rat liver microsomal system. Biochem. Biophys. Res. Commun. 1978; 80:229–235. [PubMed: 414751]

Blackburn GM, Taussig PE, Will JP. Binding of benzo[*a*]pyrene to DNA investigated by tritium displacement. J. Chem. Soc. Chem. Commun. 1974:907–908.

NIH-PA Author Manuscript

NIH-PA Author Manuscript

NIH-PA Author Manuscript

Blaich G, Göttlicher M, Cikryt P, Metzler M. Effects of various inducers on diethylstilbestrol metabolism, drug-metabolizing enzyme activities and the aromatic hydrocarbon (Ah) receptor in male Syrian golden hamster liver. J. Steroid Biochem. 1990; 35:201–204. [PubMed: 2155352]

Bocchinfuso WP, Hively WP, Couse JF, Varmus HE, Korach KS. A mouse mammary tumor virus-*Wnt*-1 transgene induces mammary gland hyperplasia and tumorigenesis in mice lacking estrogen receptor-α. Cancer Res. 1999; 59:1869–1876. [PubMed: 10213494]

Bocchinfuso WP, Korach KS. Mammary gland development and tumorigenesis in estrogen receptor knockout mice. J. Mammary Gland Biol. Neoplasia. 1997; 2:323–334. [PubMed: 10935020]

Bolton JL, Shen L. p-Quinone methides are the major decomposition products of catechol estrogen o-quinones. Carcinogenesis. 1998; 17:925–929. [PubMed: 8640939]

Boocock DJ, Faust GE, Patel KR, Schinas AM, Brown VA, Ducharme MP, Booth TD, Crowell JA, Perloff M, Gescher AJ, Steward WP, Brenner DE. Phase I dose escalation pharmacokinetic study in health volunteers of resveratrol, a potential cancer chemopreventive agent. Cancer Epidemiol. Biomarkers Prev. 2007; 16:1246–1252. [PubMed: 17548692]

Borgen A, Darvey H, Castagnoli N, Crocker TT, Rasmussen RE, Wang IY. Metabolic conversion of benzo(a)pyrene by Syrian hamster liver microsomes and binding of metabolites to deoxyribonucleic acid. J. Med. Chem. 1973; 16:502–506. [PubMed: 4718466]

Bosland MC, Ford H, Horton L. Induction at high incidence of ductal prostate adenocarcinomas in NBL/Cr and Sprague-Dawley Hsd:SD rats treated with a combination of testosterone and estradiol-17β or diethylstilbestrol. Carcinogenesis. 1995; 16:1311–1317. [PubMed: 7788848]

Boyland E, Chasseaud LF. The role of glutathione and glutathione S-transferases in mercapturic acid biosynthesis. Adv. Enzymol. Relat. Areas Mol. Biol. 1969; 32:173–219. [PubMed: 4892500]

Brown K, Buchmann A, Balmain A. Carcinogen-induced mutations in the mouse c-Ha-*ras* gene provide evidence of multiple pathways for tumor progression. Proc. Natl. Acad. Sci. USA. 1990; 87:538–542. [PubMed: 2105486]

Buhler DR, Unlü F, Thakker DR, Slaga TJ, Conney AH, Wood AW, Chang RL, Levin W, Jerina DM. Effect of a 6-fluoro substituent on the metabolism and biological activity of benzo[*a*]pyrene. Cancer Res. 1983; 43:1541–1549. [PubMed: 6299523]

Cai H, Bloom LB, Eritja R, Goodman MF. Kinetics of deoxyribonucleotide insertion and extension at abasic template lesions in different sequence contexts using HIV-1 reverse transcriptase. J. Biol. Chem. 1993; 268:23567–23572. [PubMed: 7693691]

Cao K, Devanesan PD, Ramanathan R, Gross ML, Rogan EG, Cavalieri EL. Covalent binding of catechol estrogens to glutathione catalyzed by horseradish peroxidase, lactoperoxidase, or rat liver microsomes. Chem. Res. Toxicol. 1998a; 11:917–924. [PubMed: 9705754]

Cao K, Stack DE, Ramanathan R, Gross ML, Rogan EG, Cavalieri EL. Synthesis and structure elucidation of estrogen quinones conjugated with cysteine, *N*-acetylcysteine, and glutathione. Chem. Res. Toxicol. 1998b; 11:909–916. [PubMed: 9705753]

Carmichael PL, Platt KL, Shé MN, Lecoq S, Oesch F, Phillips DH, Grover PL. Evidence for the involvement of a bis-diol-epoxide in the metabolic activation of dibenz[*a*,*h*]anthracene to DNA-binding species in mouse skin. Cancer Res. 1993; 53:944–948. [PubMed: 8439967]

Caspary W, Cohen B, Lesko S, Ts'o PO. Electron paramagnetic resonance study of iodine-induced radicals of benzo[*a*]pyrene and other polycyclic hydrocarbons. Biochemistry. 1973; 12:2649–2656. [PubMed: 4351206]

Cavalieri E. Minisymposium on endogenous carcinogens: The catechol estrogen pathway. An introduction. Polycyclic Aromat. Compd. 1994; 6:223–228.

Cavalieri E, Auerbach R. Reactions between activated benzo[*a*]pyrene and nucleophilic compounds, with possible implications on the mechanism of tumor initiation. J. Natl. Cancer Inst. 1974; 53:393–397. [PubMed: 4843270]

Cavalieri E, Calvin M. Molecular characteristics of some carcinogenic hydrocarbons. Proc. Natl. Acad. Sci. USA. 1971; 68:1251–1253. [PubMed: 5288372]

Cavalieri E, Calvin M. 220 MHz nuclear magnetic resonance analysis and the selective protonation of benzo[*a*]pyrene and 6-methylbenzo[*a*]pyrene. J. Chem. Soc. Perkin Trans I. 1972:1253–1256.

Cavalieri E, Chakravarti D, Guttenplan J, Hart E, Ingle J, Jankowiak R, Muti P, Rogan E, Russo J, Santen R, Sutter T. Catechol estrogen quinones as initiators of breast and other human cancers.

NIH-PA Author Manuscript

NIH-PA Author Manuscript

NIH-PA Author Manuscript

Implications for biomarkers of susceptibility and cancer prevention. BBA-Reviews on Cancer. 2006; 1766:63–78. [PubMed: 16675129]

Cavalieri E, Devanesan P, Rogan E. Radical cations in the horseradish peroxidase and prostaglandin H synthase mediated metabolism and binding of benzo[*a*]pyrene to deoxyribonucleic acid. Biochem. Pharmacol. 1988a; 37:2183–2187. [PubMed: 3132173]

Cavalieri, E.; Frenkel, K.; Liehr, JG.; Rogan, E.; Roy, D. Estrogens as endogenous genotoxic agents: DNA adducts and mutations. In: Cavalieri, E.; Rogan, E., editors. JNCI Monograph: Estrogens as Endogenous Carcinogens in the Breast and Prostate, No. 27. Maryland: Oxford University Press; 2000. p. 75-93.

Cavalieri E, Higginbotham S, Rogan E. Dibenzo[*a*,*l*]pyrene: the most potent carcinogenic aromatic hydrocarbon. Polycyclic Aromat. Compd. 1994; 6:177–183.

Cavalieri E, Rogan E. Role of radical cations in aromatic hydrocarbon carcinogenesis. Environ. Health Perspectives. 1985; 64:69–84.

Cavalieri, E.; Rogan, E. Mechanisms of tumor initiation by polycyclic aromatic hydrocarbons in mammals. In: Neilson, AH., editor. The Handbook of Environmental Chemistry, Vol. 3J: PAHs and Related Compounds. Heidelberg: Springer-Verlag; 1998. p. 81-117.

Cavalieri E, Rogan E. Unbalanced metabolism of endogenous estrogens in the etiology and prevention of human cancer. J. Steroid Biochem. Mol. Biol. 2011; 125:169–180. [PubMed: 21397019]

Cavalieri E, Rogan E, Cremonesi P, Devanesan P. Radical cations as precursors in the metabolic formation of quinones from benzo[*a*]pyrene and 6-fluorobenzo[*a*]pyrene: Fluoro substitution as a probe for one-electron oxidation in aromatic substrates. Biochem. Pharmacol. 1988b; 37:2173–2182. [PubMed: 2837229]

Cavalieri E, Rogan E, Higginbotham S, Cremonesi P, Salmasi S. Tumor-initiating activity in mouse skin and carcinogenicity in rat mammary gland of fluorinated derivatives of benzo[*a*]pyrene and 3-methylcholanthrene. J. Cancer Res. Clin. Oncol. 1988c; 114:16–22. [PubMed: 3350838]

Cavalieri E, Rogan E, Roth RW, Saugier RK, Hakam A. The relationship between ionization potential and horseradish peroxidase/hydrogen peroxide-catalyzed binding of aromatic hydrocarbons to DNA. Chem.-Biol. Interact. 1983; 47:87–109. [PubMed: 6640787]

Cavalieri E, Rogan E, Sinha D. Carcinogenicity of aromatic hydrocarbons directly applied to rat mammary gland. J. Cancer Res. Clin. Oncol. 1988d; 114:3–9. [PubMed: 3350839]

Cavalieri, E.; Rogan, E.; Warner, C.; Bobst, A. Synthesis and characterization of benzo[*a*]pyrene and 6-methylbenzo[*a*]pyrene radical cations. In: Cooke, WM.; Dennis, AJ., editors. Polynuclear Aromatic Hydrocarbons: Mechanisms, Methods and Metabolism. Columbus: Battelle Press; 1985. p. 227-236.

Cavalieri E, Roth R. Reaction of methylbenzanthracenes and pyridine by one-electron oxidation: A model for metabolic activation and binding of carcinogenic aromatic hydrocarbons. J. Org. Chem. 1976; 41:2679–2684. [PubMed: 950580]

Cavalieri E, Roth R, Althoff J, Grandjean C, Patil K, Marsh S, McLaughlin D. Carcinogenicity and metabolic profiles of 3-methylcholanthrene oxygenated derivatives at the 1 and 2 positions. Chem.-Biol. Interact. 1978; 22:69–81. [PubMed: 688526]

Cavalieri, E.; Roth, R.; Rogan, EG. Metabolic activation of aromatic hydrocarbons by one-electron oxidation in relation to the mechanism of tumor initiation. In: Freudenthal, RI.; Jones, PW., editors. Polynuclear Aromatic Hydrocarbons: Chemistry, Metabolism and Carcinogenesis. Vol. Vol. 1. New York: Raven Press; 1976. p. 181-190.

Cavalieri, E.; Sinha, D.; Rogan, E. Rat mammary gland vs mouse skin: different mechanisms of activation of aromatic hydrocarbons. In: Bjorseth, A.; Dennis, AJ., editors. Polynuclear aromatic hydrocarbons: chemistry and biological effects. Columbus: Battelle Press; 1980. p. 215-231.

Cavalieri EL, Devanesan P, Bosland MC, Badawi AF, Rogan EG. Catechol estrogen metabolites and conjugates in different regions of the prostate of Noble rats treated with 4-hydroxyestradiol: Implications for estrogen-induced initiation of prostate cancer. Carcinogenesis. 2002a; 23:329–333. [PubMed: 11872641]

Cavalieri EL, Higginbotham S, RamaKrishna NVS, Devanesan PD, Todorovic R, Rogan EG, Salmasi S. Comparative dose-response tumorigenicity studies of dibenzo[*a*,*l*]pyrene vs 7,12-

NIH-PA Author Manuscript

NIH-PA Author Manuscript

NIH-PA Author Manuscript

dimethylbenz[*a*]anthracene, benzo[*a*]pyrene and two dibenzo[*a,l*]pyrene dihydrodiols in mouse skin and rat mammary gland. Carcinogenesis. 1991; 12:1939–1944. [PubMed: 1934274]

Cavalieri EL, Kumar S, Todorovic R, Higginbotham S, Badawi AF, Rogan EG. Imbalance of estrogen homeostasis in kidney and liver of hamsters treated with estradiol: Implications for estrogen-induced initiation of renal tumors. Chem. Res. Toxicol. 2001; 14:1041–1050. [PubMed: 11511178]

Cavalieri EL, Li K-M, Balu N, Saeed M, Devanesan P, Higginbotham S, Zhao J, Gross ML, Rogan E. Catechol *ortho*-quinones: The electrophilic compounds that form depurinating DNA adducts and could initiate cancer and other diseases. Carcinogenesis. 2002b; 23:1071–1077. [PubMed: 12082031]

Cavalieri EL, Rogan EG. The approach to understanding aromatic hydrocarbon carcinogenesis. The central role of radical cations in metabolic activation. Pharmac. Ther. 1992; 55:183–199.

Cavalieri EL, Rogan EG. Depurinating estrogen-DNA adducts in the etiology and prevention of breast and other human cancers. Future Oncology. 2010; 6:75–91. [PubMed: 20021210]

Cavalieri EL, Rogan EG, Devanesan PD, Cremonesi P, Cerny RL, Gross ML, Bodell WJ. Binding of benzo[*a*]pyrene to DNA by cytochrome P450-catalyzed one-electron oxidation in rat liver microsomes and nuclei. Biochemistry. 1990a; 29:4820–4827. [PubMed: 2364062]

Cavalieri EL, Rogan EG, Higginbotham S, Cremonesi P, Salmasi S. Tumor-initiating activity in mouse skin and carcinogenicity in rat mammary gland of dibenzo[*a*]pyrenes: the very potent activity of dibenzo[*a,l*]pyrene. J. Cancer Res. Clin. Oncol. 1989; 115:67–72. [PubMed: 2921274]

Cavalieri EL, Rogan EG, Higginbotham S, Cremonesi P, Salmasi S. Tumorigenicity of 7,12-dimethylbenz[*a*]anthracene, some of its fluorinated derivatives and 1,2,3,4-tetrahydro-7,12-dimethylbenz[*a*]anthracene in mouse skin and rat mammary gland. Polycyclic Aromatic Compounds. 1990b; 1:59–70.

Cavalieri EL, Rogan EG, Li K-M, Todorovic R, Ariese F, Jankowiak R, Grubor N, Small GJ. Identification and quantification of the depurinating DNA adducts formed in mouse skin treated with dibenzo[*a,l*]pyrene (DB[*a,l*]P), or its metabolites and in rat mammary gland treated with DB[*a,l*]P. Chem. Res. Toxicol. 2005; 18:976–983. [PubMed: 15962932]

Cavalieri, EL.; Rogan, EG.; Murray, WJ.; RamaKrishna, NVS. Mechanistic aspects of benzo[*a*]pyrene metabolism. In: Garrigues, P.; Lamotte, M., editors. Polycyclic Aromatic Compounds. Langhorne, PA: Gordon and Breach; 1993. p. 1047-1054.

Cavalieri EL, Stack DE, Devanesan PD, Todorovic R, Dwivedy I, Higginbotham S, Johansson SL, Patil KD, Gross ML, Gooden JK, Ramanathan R, Cerny RL, Rogan EG. Molecular origin of cancer: Catechol estrogen-3,4-quinones as endogenous tumor initiators. Proc. Natl. Acad. Sci. USA. 1997; 94:10937–10942. [PubMed: 9380738]

Chakravarti D, Mailander P, Cavalieri EL, Rogan EG. Evidence that error-prone DNA repair converts dibenzo[*a,l*]pyrene-induced depurinating lesions into mutations: formation, clonal proliferation and regression of initiated cells carrying H-*ras* oncogene mutations in early preneoplasia. Mutat. Res. 2000; 456:17–32. [PubMed: 11087892]

Chakravarti D, Mailander P, Li K-M, Higginbotham S, Zhang H, Gross ML, Cavalieri E, Rogan E. Evidence that a burst of DNA depurination in SENCAR mouse skin induces error-prone repair and form mutations in the H-*ras* gene. Oncogene. 2001; 20:7945–7953. [PubMed: 11753677]

Chakravarti D, Pelling JC, Cavalieri EL, Rogan EG. Relating aromatic hydrocarbon-induced DNA adducts and c-Harvey-*ras* mutations in mouse skin papillomas: the role of apurinic sites. Proc. Natl. Acad. Sci. USA. 1995; 92:10422–10426. [PubMed: 7479797]

Chakravarti D, Zahid M, Backora M, Myers EM, Gaikwad N, Weisenburger DD, Cavalieri EL, Rogan EG, Joshi SS. Ortho-quinones of benzene and estrogen induce hyperproliferation of human peripheral blood mononuclear cells. Leuk Lymp. 2006; 47:2635–2644.

Chang TK, Lee WB, Ko HH. Trans-resveratrol modulates the catalytic activity and mRNA expression of the procarcinogen-activating human cytochrome P450 1B1. Can. J. Physiol. Pharmacol. 2000; 78:874–881. [PubMed: 11100935]

Chary P, Latham GJ, Robberson DL, Kim SJ, Han S, Harris CM, Harris TM, Lloyd RS. In vivo and in vitro replication consequences of stereoisomeric benzo[*a,l*]pyrene-7,8-dihydrodiol 9,10-epoxide

NIH-PA Author Manuscript

NIH-PA Author Manuscript

NIH-PA Author Manuscript

adducts on adenine N6 at the second position of N-ras codon 61. J. Biol. Chem. 1995; 270:4990–5000. [PubMed: 7890605]

Chen L, Devanesan PD, Higginbotham S, Ariese F, Jankowiak R, Small GJ, Rogan EG, Cavalieri EL. Expanded analysis of benzo[*a*]pyrene-DNA adducts formed in vitro and in mouse skin: their significance in tumor initiation. Chem. Res. Toxicol. 1996; 9:897–903. [PubMed: 8828927]

Chen ZH, Hurh YJ, Na HK, Kim JH, Chun YJ, Kim DH, Kang KS, Cho MH, Surh YJ. Resveratrol inhibits TCDD-induced expression of CYP1A1 and CYP1B1 and catechol estrogen-mediated oxidative DNA damage in cultured human mammary epithelial cells. Carcinogenesis. 2004; 25:2005–2013. [PubMed: 15142886]

Cheng SC, Prakash AS, Pigott MA, Hilton BD, Lee H, Harvey RG, Dipple A. A metabolite of the carcinogen 7,12-dimethylbenz[*a*]anthracene that reacts predominantly with adenine residues in DNA. Carcinogenesis. 1988a; 9:1721–1723. [PubMed: 3136949]

Cheng SC, Prakash AS, Pigott MA, Hilton BD, Roman JM, Lee HM, Harvey RG, Dipple A. Characterization of the 7,12-dimethylbenz[*a*]anthracene-adenine nucleoside adducts. Chem. Res. Toxicol. 1988b; 1:216–221. [PubMed: 2979734]

Chou MW, Fu PP. Sterioselective metabolism of 8- and 9-fluorobenzo[*a*]pyrene by rat liver microsomes: absolute configurations of *trans*-dihydrodiol metabolites. J. Toxic. Environ. Health. 1984; 14:221–223.

Chou MW, Yang SK, Sydor W, Yang CS. Metabolism of 7,12-dimethylbenz *(a)*anthracene and 7-hydroxymethyl-12-methylbenz(*a*)anthracene by rat liver and microsomes. Cancer Res. 1981; 41:1559–1564. [PubMed: 6783297]

Chouroulinkov I, Gentil A, Grover PL, Sims P. Tumor-initiating activities on mouse skin of dihydrodiols derived from benzo[*a*]pyrene. Br. J. Cancer. 1976; 34:523–532. [PubMed: 999784]

Chouroulinkov I, Gentil A, Tierney B, Grover PL, Sims P. The initiation of tumours on mouse skin by dihydrodiols derived from 7,12-dimethylbenz(*a*)anthracene and 3-methylcholanthrene. Int. J. Cancer. 1979; 24:455–460. [PubMed: 118940]

Chun YJ, Kim MY, Guengerich FP. Resveratrol is a selective human cytochrome P45 1A1 inhibitor. Biochem. Biophys. Res. Commun. 1999; 262:20–24. [PubMed: 10448061]

Colapietro AM, Goodell AL, Smart RC. Characterization of benzo[*a*]pyrene-initiated mouse skin papillomas for Ha-*ras* mutations and protein kinase C levels. Carcinogenesis. 1993; 14:2289–2295. [PubMed: 8242857]

Conney AH. Induction of microsomal enzymes by foreign chemicals and carcinogenesis by polycyclic aromatic hydrocarbons. G.H. A. Clowes Memorial Lecture. Cancer Res. 1982; 42:4875–4917. [PubMed: 6814745]

Cook JW, Hewett CL, Hieger I. The isolation of a cancer-producing hydrocarbon from coal tar, I, II and III. J. Chem. Soc. 1933:395–405.

Cooper CS, Ribeiro O, Hewer A, Walsh C, Pal K, Grover PL, Sims P. The involvement of a ‘bay-region’ and a non-‘bay-region’ diol-epoxide in the metabolic activation of benza[*a*]anthracene in mouse skin and hamster embryo cells. Carcinogenesis. 1980; 1:233–243. [PubMed: 22283004]

Cremonesi P, Cavalieri E, Rogan E. One-electron oxidation of 6-substituted benzo[*a*]pyrenes by manganic acetate. J. Org. Chem. 1989; 54:3561–3570.

Cremonesi P, Hietbrink B, Rogan EG, Cavalieri EL. One-electron oxidation of dibenzo[*a*]pyrenes by manganic acetate. J. Org. Chem. 1992a; 57:3309–3312.

Cremonesi P, Rogan E, Cavalieri E. Correlation studies of anodic peak potentials and ionization potentials for polycyclic aromatic hydrocarbons. Chem. Res. Toxicol. 1992b; 5:346–355. [PubMed: 1504257]

Cremonesi P, Stack DE, Rogan EG, Cavalieri EL. Radical cations of benzo[*a*]pyrene and 6-substituted derivatives: synthesis and reaction with nucleophiles. J. Org. Chem. 1994; 59:7683–7687.

Croy RG, Selkirk JK, Harvey RG, Engel JF, Gelboin HV. Separation of ten benzo(*a*)pyrene phenols by recycle high pressure liquid chromatography and identification of four phenols as metabolites. Biochem. Pharmacol. 1976; 25:227–230. [PubMed: 1259790]

Das S, Das DK. Anti-inflammatory responses of resveratrol. Inflammation & Allergy - Drug Targets. 2007; 6:168–173. [PubMed: 17897053]

NIH-PA Author Manuscript

NIH-PA Author Manuscript

NIH-PA Author Manuscript

Dawson JH. Probing structure-function relations in heme-containing oxygenases and peroxidases. Science. 1988; 240:433–439. [PubMed: 3358128]

De Flora S, Cesarone CF, Balansky RM, Albini A, D'Agostini F, Bennicelli C, Bagnasco M, Camoirano A, Scatolini L, Rovida A, Izzotti A. Chemopreventive properties and mechanisms of *N*-acetylcysteine. The experimental background. J. Cell. Biochem. 1995; 22(Suppl.):33–41.

Devanesan P, Rogan E, Cavalieri E. The relationship between ionization potential and prostaglandin H synthase-catalyzed binding of aromatic hydrocarbons to DNA. Chem.-Biol. Interact. 1987; 61:89–95. [PubMed: 3102084]

Devanesan P, Santen RJ, Bocchinfuso WP, Korach KS, Rogan EG, Cavalieri EL. Catechol estrogen metabolites and conjugates in mammary tumors and hyperplastic tissue from estrogen receptor alpha knock out (ERKO)/*Wnt* 1 mice; implications for initiation of mammary tumors. Carcinogenesis. 2001; 22:1573–1576. [PubMed: 11532882]

Devanesan PD, Cremonesi P, Nunnally JE, Rogan EG, Cavalieri EL. Metabolism and mutagenicity of dibenzo[*a*,*e*]pyrene and the very potent environmental carcinogen dibenzo[*a*,*l*]pyrene. Chem. Res. Toxicol. 1990; 3:580–586. [PubMed: 2103330]

Devanesan PD, Higginbotham S, Ariese F, Jankowiak R, Suh M, Small GJ, Cavalieri EL, Rogan EG. Depurinating and stable benzo[*a*]pyrene-DNA adducts formed in isolated rat liver nuclei. Chem. Res. Toxicol. 1996; 8:1113–1116. [PubMed: 8902265]

Devanesan PD, RamaKrishna NVS, Padmavathi NS, Higginbotham S, Rogan EG, Cavalieri EL, Marsch GA, Jankowiak R, Small GJ. Identification and quantitation of 7,12-dimethylbenz[*a*]anthracene-DNA adducts formed in mouse skin. Chem. Res. Toxicol. 1993; 6:364–371. [PubMed: 7686409]

Devanesan PD, RamaKrishna NVS, Todorovic R, Rogan EG, Cavalieri EL, Jeong H, Jankowiak R, Small GJ. Identification and quantitation of benzo[*a*]pyrene-DNA adducts formed by rat liver microsomes in vitro. Chem. Res. Toxicol. 1992; 5:302–309. [PubMed: 1643262]

Dickson RB, Stancel GM. Estrogen receptor-mediated processes in normal and cancer cells. J. Natl. Cancer Inst. Monogr. 2000; 27:135–145. [PubMed: 10963625]

DiGiovanni J, Diamond L, Singer JM, Daniel FB, Witiak DT, Slaga TJ. Tumor-initiating activity of 4-fluoro-7,12-dimethylbenz[*a*]anthracene and 1,2,3,4-tetrahydro-7,12-dimethylbenz[*a*]anthracene in female SENCAR mice. Carcinogenesis. 1982; 3:651–655. [PubMed: 6811143]

Dipple, A. Polycyclic aromatic carcinogens. In: Searle, CE., editor. Chemical carcinogens. Washington: American Chemical Society; 1976. p. 345-314.

Dipple, A.; Moschel, RC.; Bigger, CAH. Polynuclear aromatic carcinogens. In: Searle, CE., editor. Chemical Carcinogens. 2nd ed. Vol. Vol. 1. Washington: American Chemical Society; 1984. p. 41-163.

Dix TA, Marnett LJ. Metabolism of polycyclic aromatic hydrocarbon derivatives to ultimate carcinogens during lipid-peroxidation. Science. 1983; 221:77–79. [PubMed: 6304879]

Drevon C, Piccoli C, Montesano R. Mutagenicity assays of estrogenic hormones in mammalian cells. Mutat. Res. 1981; 89:83–90. [PubMed: 7242549]

Duell EJ, Millikan RC, Pittman GS, Winkel S, Lunn RM, Tse CK, Eaton A, Mohrenweiser HW, Newman B, Bell DA. Polymorphisms in the DNA repair gene XRCC1 and breast cancer. Cancer Epidemiol. Biomarkers Prev. 2001; 10:217–222. [PubMed: 11303590]

Dunning WF, Curtis MP. Relative carcinogenic activity of monomethyl derivatives of benzo[*a*]anthracene in Fisher line 344 rats. J. Natl. Cancer Inst. 1960; 25:387–391.

Dwivedy I, Devanesan P, Cremonesi P, Rogan E, Cavalieri E. Synthesis and characterization of estrogens 2,3- and 2,3-quinones. Comparison of DNA adducts formed by the quinones *versus* horseradish peroxidase-activated catechol estrogens. Chem. Res. Toxicol. 1992; 5:828–833. [PubMed: 1336990]

Eisenstadt E, Warren AJ, Porter J, Atkins D, Miller JH. Carcinogenic epoxides of benzo[*a*]pyrene and cyclopental[*cd*]pyrene induce base substitutions via specific transversions. Proc. Natl. Acad. Sci. USA. 1982; 79:1945–1949. [PubMed: 7043469]

Feigelson HS, Henderson BE. Estrogens and breast cancer. Carcinogenesis. 1996; 17:2279–2284. [PubMed: 8968038]

NIH-PA Author Manuscript

NIH-PA Author Manuscript

NIH-PA Author Manuscript

Floreani M, Napoli E, Quintieri L, Palatini P. Oral administration of *trans*-resveratrol to guinea pigs increases cardiac DT-diaphorase and catalase activities, and protects isolated atria from menadione toxicity. Life Sciences. 2003; 72:2741–2750. [PubMed: 12679191]

Fried, J. One-electron oxidation of polycyclic aromatics as a model for the metabolic activation of carcinogenic hydrocarbons. In: Ts'o, POP.; DiPaolo, J., editors. Chemical Carcinogens, Part A. New York: Marcel Dekker; 1974. p. 197-215.

Fried J, Schumm DE. One electron transfer oxidation of 7,12-dimethylbenz[*a*]anthracene, a model for the metabolic activation of carcinogenic hydrocarbons. J. Am. Chem. Soc. 1967; 89:5508–5509. [PubMed: 6073144]

Fuchs J, Mlcoch J, Oesch F, Platt KL. Characterization of highly polar DNA adducts derived from dibenz[*a*,*h*]anthracene (DBA), 3,4-dihydroxy-3,4-dihydro-DBA, and 3,4,10,11-tetrahydroxy-3,4,10,11-tetrahydro-DBA. Toxicol. Ind. Health. 1993a; 9:503–509. [PubMed: 8367889]

Fuchs J, Mlcoch J, Platt KL, Oesch F. Characterization of highly polar bis-dihydrodiol epoxide–DNA adducts formed after metabolic activation of dibenz[*a*,*h*]anthracene. Carcinogenesis. 1993b; 14:863–867. [PubMed: 8504478]

Furth, J. Hormones as etiological agents in neoplasia. In: Becker, FF., editor. Cancer. A Comprehensive Treatise, 1. Etiology: Chemical and Physical Carcinogenesis. Vol. 4. NY, USA: Cancer Plenum Press; 1982. p. 89-134.

Gaikwad N, Yang L, Weisenburger DD, Vose J, Beseler C, Rogan E, Cavalieri E. Urinary biomarkers suggest that estrogen-DNA adducts may play a role in the aetiology of non-Hodgkin lymphoma. Biomarkers. 2009a; 14:502–512. [PubMed: 19863189]

Gaikwad NW, Rogan EG, Cavalieri EL. Evidence from ESI-MS for NQO1-catalyzed reduction of estrogen ortho-quinones. Free Radic. Biol. Med. 2007; 43:1289–1298. [PubMed: 17893042]

Gaikwad NW, Yang L, Muti P, Meza JL, Pruthi S, Ingle JN, Rogan EG, Cavalieri EL. The molecular etiology of breast cancer: evidence from biomarkers of risk. Int. J. Cancer. 2008; 122:1949–1957. [PubMed: 18098283]

Gaikwad NW, Yang L, Pruthi S, Ingle JN, Sandhu N, Rogan E, Cavalieri E. Urine biomarkers of risk in the molecular etiology of breast cancer. Breast Cancer: Basic & Clinical Research. 2009b; 3:1–8. [PubMed: 21556245]

Gaikwad NW, Yang L, Rogan EG, Cavalieri EL. Evidence from ESI-MS for NQO2-catalyzed reduction of estrogen *ortho*-quinones. Free Radic. Biol. Med. 2009c; 46:253–262. [PubMed: 18996184]

Gail MH, Brinton LA, Byar DP, Corle DK, Green SB, Schairer C, Mulvhill JJ. Projecting individualized probabilities of developing breast cancer for white females who are being examined annually. J. Natl. Cancer Inst. 1989; 81:1879–1886. [PubMed: 2593165]

Gelboin HV. Benzo[*a*]pyrene metabolism, activation and carcinogenesis: role and regulation of mixed-function oxidases and related enzymes. Physiol. Rev. 1980; 60:1107–1166. [PubMed: 7001511]

Gill HS, Kole PL, Wiley JC, Li KM, Higginbotham S, Rogan EG, Cavalieri EL. Synthesis and tumor-initiating activity in mouse skin of dibenzo[*a*,*l*]pyrene *syn*- and *anti*-fjord-region diol epoxides. Carcinogenesis. 1994; 15:2455–2460. [PubMed: 7955091]

Gill RD, Butterworth BE, Nettikumara AN, DiGiovanni J. Relationship between DNA adduct formation and unscheduled DNA synthesis (UDS) in cultured mouse epidermal keratinocytes. Environ. Mol. Mutagen. 1991; 18:200–206. [PubMed: 1915314]

Greenlee WF, Gross EA, Irons RD. Relationship between benzene toxicity and the disposition of 14C-labelled benzene metabolites in the rat. Chem. Biol. Interact. 1981; 33:285–299. [PubMed: 7460069]

Groves JT, Haushalter RC, Nakamura M, Nemo TE, Evans BJ. High-valent iron-porphyrin complexes related to peroxidase and cytochrome P-450. J. Amer. Chem. Soc. 1981; 103:2884–2886.

Groves JT, McClusky GA. Aliphatic hydroxylation by highly purified liver microsomal cytochrome P-450: Evidence for a carbon radical intermediate. Biochem. Biophys. Res. Commun. 1978; 81:154–160. [PubMed: 656092]

Guengerich FP, Chunb YJ, Kima D, Gillam EMJ, Shimada T. Cytochrome P450 1B1: a target for inhibition in anticarcinogenesis strategies. Mutation Research. 2003:523–524. 173–182.

NIH-PA Author Manuscript

NIH-PA Author Manuscript

NIH-PA Author Manuscript

Haaf H, Metzler M. In vitro metabolism of diethylstilbestrol by hepatic, renal and uterine microsomes of rats and hamsters. Effects of different inducers. Biochem. Pharmacol. 1985; 34:3107–3115. [PubMed: 4038324]

Hahn WC, Weinberg RA. Rules for making human tumor cells. N. Engl. J. Med. 2002; 347:1593–1603. [PubMed: 12432047]

Hanson AA, Rogan EG, Cavalieri EL. Synthesis of adducts formed by iodine oxidation of aromatic hydrocarbons in the presence of deoxyribonucleosides and nucleobases. Chem. Res. Toxicol. 1998; 11:1201–1208. [PubMed: 9778317]

Harvey RG, Dunne FB. Multiple regions of metabolic activation of carcinogenic hydrocarbons. Nature (Lond). 1978; 274:566–568. [PubMed: 96349]

Hayes CL, Spink DC, Spink BC, Cao JQ, Walker NJ, Sutter TR. 17β-Estradiol hydroxylation catalyzed by human cytochrome P450 1B1. Proc. Natl. Acad. Sci. USA. 1996; 93:9776–9781. [PubMed: 8790407]

Hecht SS, Bondinell WE, Hoffmann D. Chrysene and methylchrysenes: presence in tobacco smoke and carcinogenicity. J. Natl. Cancer Inst. 1974; 53:1121–1133. [PubMed: 4427391]

Hecht SS, Hirota N, Loy M, Hoffmann D. Tumor-initiating activity of fluorinated 5-methylchrysenes. Cancer Res. 1978a; 38:1694–1698. [PubMed: 647679]

Hecht SS, LaVoie E, Mazzarese R, Amin S, Bedenko V, Hoffmann D. 1,2-Dihydro-1,2-dihydroxy-5-methylchrysene, a major activated metabolite of the environmental carcinogen 5-methylchrysene. Cancer Res. 1978b; 38:2191–2194. [PubMed: 350385]

Hecht SS, LaVoie E, Mazzarese R, Hirota N, Ohmori T, Hoffmann D. Comparative mutagenicity, tumor-initiating activity, carcinogenicity and in vitro metabolism of fluorinated 5-methylchrysenes. J. Natl. Cancer Inst. 1979a; 63:855–861. [PubMed: 288940]

Hecht, SS.; Mazzarese, R.; Amin, S.; La Voie, E.; Hoffmann, D. On the metabolic activation of 5-methylchrysene. In: Jones, PW.; Leber, P., editors. Polynuclear aromatic hydrocarbons. Ann Arbor: Ann Arbor Science; 1979b. p. 733-752.

Herbst AL, Ulfelder H, Poskanzer DC. Adenocarcinoma of the vagina. Association of maternal stilbestrol therapy with tumor appearance in young women. N. Engl. J. Med. 1971; 284:878–881. [PubMed: 5549830]

Hieger I. The spectra of cancer-producing tars and oils and of related substances. Biochem. J. 1930; 24:505–511. [PubMed: 16744389]

Higginbotham S, RamaKrishna NVS, Johansson SL, Rogan EG, Cavalieri EL. Tumor-initiating activity and carcinogenicity of dibenzo[*a*,*l*]pyrene versus 7,12-dimethylbenz[*a*]anthracene and benzo[*a*]pyrene at low doses in mouse skin. Carcinogenesis. 1993; 14:875–878. [PubMed: 8504480]

Hinrichs B, Zahid M, Saeed M, Ali MF, Cavalieri EL, Rogan EG. Formation of diethylstilbestrol-DNA adducts in human breast epithelial cells and inhibition by resveratrol. J. Steroid Biochem. Mol. Biol. 2011; 127:276–281. [PubMed: 21896331]

Hoffman D, Bondinell WE, Wynder EL. Carcinogenecity of methylchrysenes. Science. 1974; 183:215–216. [PubMed: 4808861]

Holder G, Yagi H, Dansette P, Jerina DM, Levin W, Lu AY, Conney AH. Effects of inducers and epoxide hydrase on the metabolism of benzo[*a*]pyrene by liver microsomes and a reconstituted system: analysis by high pressure liquid chromatography. Proc. Natl. Acad. Sci. USA. 1974; 71:4356–4360. [PubMed: 4530987]

Ide H, Murayama H, Murakami A, Morii T, Makino K. Effects of base damages on DNA replication-mechanism of preferential purine nucleotide insertion opposite abasic site in template DNA. Nucl. Acids Res. Symp. Ser. 1992; 27:167–168.

International Agency for Research on Cancer. IARC monographs on the evaluation of carcinogenic risk of chemicals to humans. Vol. Vol. 3. Lyon: IARC; 1973.

International Agency for Research on Cancer. IARC monographs on the evaluation of the carcinogenic risk of chemicals to humans. Vol. Vol. 32. Lyon: IARC; 1983.

Jan S-T, Devanesan P, Stack D, Ramanathan R, Byun J, Gross ML, Rogan E, Cavalieri E. Metabolic activation and formation of DNA adducts of hexestrol, a synthetic non-steroidal carcinogenic estrogen. Chem. Res. Toxicol. 1998; 11:412–419. [PubMed: 9585471]

NIH-PA Author Manuscript

NIH-PA Author Manuscript

NIH-PA Author Manuscript

Jang M, Cai L, Udeani GO, Slowing KV, Thomas CF, Beecher CW, Fong HH, Farnsworth NR, Kinghorn AD, Mehta RG, Moon RC, Pezzuto JM. Cancer chemopreventive activity of resveratrol, a natural product derived from grapes. Science. 1997; 275:218–220. [PubMed: 8985016]

Jefcoate, CR.; Liehr, JG.; Santen, RJ.; Sutter, TR.; Yager, JD.; Yue, W.; Santner, SJ.; Tekmal, R.; Demers, L.; Pauley, R.; Naftolin, F.; Mor, G.; Berstein, L. Tissue-specific synthesis and oxidative metabolism of estrogens. In: Cavalieri, E.; Rogan, E., editors. JNCI Monograph 27: Estrogens as Endogenous Carcinogens in the Breast and Prostate. Oxford Press; 2000. p. 95-112.

Jeftic L, Adams RN. Electrochemical oxidation pathways of benzo[*a*]pyrene. J. Am. Chem. Soc. 1970; 92:1332–1337. [PubMed: 5414746]

Jerina DM, Daly JW. Arene oxides: a new aspect of drug metabolism. Science. 1974; 185:573–582. [PubMed: 4841570]

Jerina, DM.; Daly, JW. Oxidation at carbon. In: Parke, DV.; Smith, RL., editors. Drug Metabolism-From Microbe to Man. London: Taylor and Francis; 1977. p. 13-32.

Johnson MD, Calvin M. Induced nucleophilic substitution in benzo[*a*]pyrene. Nature (London). 1973; 241:271–272. [PubMed: 4701885]

Kappus, H. Lipid peroxidation: Mechanisms, analysis, enzymology and biological relevance. In: Sies, H., editor. Oxidative Stress. New York: Academic Press; 1985. p. 273-310.

Kasper CB. Biochemical distinctions between the nuclear and microsomal membranes from rat hepatocytes. J. Biol. Chem. 1971; 246:577–581. [PubMed: 5542672]

Khandwala AS, Kasper CB. Preferential induction of aryl hydroxylase activity in rat liver nuclear envelope by 3-methylcholanthrene. Biochem. Biophys. Res. Commun. 1973; 54:1241–1246. [PubMed: 4754707]

Kim SU, Park SK, Yoo KY, Yoon KS, Choi JY, Seo JS, Park WY, Kim JH, Noh DY, Ahn SH, Choe KJ, Strickland PT, Hirvonen A, Kang D. XRCC1 genetic polymorphism and breast cancer risk. Pharmacogenetics. 2002; 12:335–338. [PubMed: 12042672]

Klinedinst DK, Drinkwater NR. Mutagenesis by apurinic sites in normal and ataxia telangiectasia human lymphoblastoid cells. Mol. Carcinogenesis. 1992; 6:32–42.

Koreeda M, Moore PD, Wislocki PG, Levin W, Yagi H, Jerina DM. Binding of benzo[*a*]pyrene 7,8-diol-9,10-epoxides to DNA, RNA and protein of mouse skin occurs with high stereoselectivity. Science. 1978; 199:778–781. [PubMed: 622566]

Lang R, Redmann U. Non-mutagenicity of some sex hormones in the Ames salmonella/microsome mutagenicity test. Mutat. Res. 1979; 67:361–365. [PubMed: 384238]

Lang R, Reimann R. Studies for a genotoxic potential of some endogenous and exogenous sex steroidsICommunication: examination for the induction of gene mutations using the Ames Salmonella/microsome test and the HGPRT test in V79 cells. Environ. Mol. Mutagen. 1993; 21:272–304. [PubMed: 8462531]

Lareef MH, Garber J, Russo PA, Russo IH, Heulings R, Russo J. The estrogen antagonist ICI-182-780 does not inhibit the transformation phenotypes induced by 17-beta-estradiol and 4-OH estradiol in human breast epithelial cells. Int. J. Oncol. 2005; 26:423–429. [PubMed: 15645127]

Lecoq S, Pfau W, Grover PL, Phillips DH. HPLC separation of ^{32}P-postlabelled DNA adducts formed from dibenz[*a*,*h*]anthracene in skin. Chem.-biol. Interact. 1992; 85:173–185. [PubMed: 1493608]

Lecoq S, She MN, Hewer A, Grover PL, Platt KL, Oesch F, Phillips DH. The metabolic activation of dibenz[*a*,*h*]anthracene in mouse skin examined by 32Ppostlabelling: Minor contribution of the 3,4-diol 1,2-oxides to DNA binding. Carcinogenesis. 1991; 12:1079–1083. [PubMed: 2044188]

Leonard SS, Xia C, Jiang BH, Stinefelt B, Klandorf H, Harris GK, Shi X. Resveratrol scavenges reactive oxygen species and effects radical-induced cellular responses. Biochem. Biophys. Res. Commun. 2003; 309:1017–1026. [PubMed: 13679076]

Lesko S, Caspary W, Lorentzen R, Ts'o POP. Enzymic formation of 6-oxobenzo[*a*]pyrene radical in rat liver homogenates for carcinogenic benzo[*a*]pyrene. Biochemistry. 1975; 14:3978–3984.

Lesko SA Jr, Smith A, Ts'o PO, Umans RS. Interaction of nucleic acids IV. The physical binding of 3,4-benzpyrene to nucleosides, nucleotides, nucleic acids and nucleoprotein. Biochemistry. 1968; 7:434–447. [PubMed: 5758559]

NIH-PA Author Manuscript

NIH-PA Author Manuscript

NIH-PA Author Manuscript

Levin W, Buening MK, Wood AW, Chang RL, Thakker DR, Jerina DM, Conney AH. Tumorigenic activity of 3-methylcholanthrene metabolites on mouse skin and in newborn mice. Cancer Res. 1979; 39:3549–3553. [PubMed: 476681]

Levin W, Thakker DR, Wood AW, Chang RL, Lehr RE, Jerina DM, Conney AH. Evidence that benzo(*a*)anthracene 3,4-diol-1,2-epoxide is an ultimate carcinogen on mouse skin. Cancer Res. 1978; 38:1705–1710. [PubMed: 647681]

Levin W, Wood AW, Chang RL, Slaga TJ, Yagi H, Jerina DM, Conney AH. Marked differences in the tumor-initiating activity of optically pure (+)- and (-)-trans-7,8-dihydrodroxy-7,8-dihydrobenzo[*a*]pyrene on mouse skin. Cancer Res. 1977a; 37:2721–2725. [PubMed: 872099]

Levin W, Wood AW, Wislocki PG, Kapitulnik J, Yagi H, Jerina DM, Conney AH. Carcinogeneicity of benzo-ring derivatives of benzo[*a*]pyrene on mouse skin. Cancer Res. 1977b; 37:3356–3361. [PubMed: 884679]

Levin W, Wood AW, Yagi H, Dansette PM, Jerina DM, Conney AH. Carcinogenicity of benzo[*a*]pyrene 4,5-, 7,8- and 9,10-oxides on mouse skin. Proc. Natl. Acad. Sci. USA. 1976a; 73:243–247. [PubMed: 1061121]

Levin W, Wood AW, Yagi H, Jerina DM, Conney AH. (±) *trans*-7,8-Dihydroxy-7,8-dihydrobenzo[*a*]pyrene: a potent skin carcinogen when applied topically to mice. Proc. Natl. Acad. Sci. USA. 1976b; 73:3867–3871. [PubMed: 1069271]

Lewis DF, Ioannides C, Parke DV. Molecular orbital studies of oxygen activation and mechanism of cytochromes P-450-mediated oxidative metabolism of xenobiotics. Chem-Biol. Interact. 1989; 70:263–280. [PubMed: 2743473]

Li JJ. Estrogen carcinogenesis in hamster tissues: update. Endocr. Rev. 1993; 14:94–95. [PubMed: 8491157]

Li JJ, Li SA. Estrogen carcinogenesis in Syrian hamster tissues: Role of metabolism. Fed. Proc. 1987; 46:1858–1863. [PubMed: 3030825]

Li JJ, Li SA. Estrogen carcinogenesis in hamster tissues: a critical review. Endocr. Rev. 1990; 11:524–531. [PubMed: 2292241]

Li JJ, Li SA, Klicka JK, Parsons JA, Lam LK. Relative carcinogenic activity of various synthetic and natural estrogens in the Syrian hamster kidney. Cancer Res. 1983; 43:5200–5204. [PubMed: 6616455]

Li K-M, Todorovic R, Devanesan P, Higginbotham S, Köfeler H, Ramanathan R, Gross ML, Rogan EG, Cavalieri EL. Metabolism and DNA binding studies of 4-hydroxyestradiol and estradiol-3,4-quinone in vitro and in female ACI rat mammary gland in vivo. Carcinogenesis. 2004; 25:289–297. [PubMed: 14578156]

Li K-M, Todorovic R, Devanesan P, Rogan EG, Cavalieri EL. Detection of 3-methylcholanthrene-DNA adducts formed *in vitro*. Proc. Amer. Acad. Cancer Res. 1996; 37:119.

Li K-M, Todorovic R, Rogan EG, Cavalieri EL, Ariese F, Suh M, Jankowiak R, Small GJ. Identification and quantitation of dibenzo[*a,l*]pyrene-DNA adducts formed by rat liver microsomes *in vitro* : Preponderance of depurinating adducts. Biochemistry. 1995; 34:8043–8049. [PubMed: 7794917]

Liehr JG. Is estradiol a genotoxic mutagenic carcinogen? Endocr. Rev. 2000; 21:40–54. [PubMed: 10696569]

Liehr JG, Ballatore AM, Dague BB, Ulubelen AA. Carcinogenicity and metabolic activation of hexestrol. Chem. Biol. Interact. 1985; 55:157–176. [PubMed: 2998630]

Liehr JG, Fang WF, Sirbasku DA, Ari-Ulubelen A. Carcinogenicity of catechol estrogens in Syrian hamsters. J. Steroid Biochem. 1986; 24:353–356. [PubMed: 3009986]

Lindahl T, Nyberg B. Rate of depurination of native deoxyribonucleic acid. Biochemistry. 1972; 11:3610–3618. [PubMed: 4626532]

Loeb LA, Preston BD. Mutagenesis by apurinic/apyrimidine sites. Ann. Rev. Genet. 1986; 20:201–230. [PubMed: 3545059]

Loew GH, Wong J, Phillips J, Hjelmeland L, Pack G. Quantum chemical studies of the metabolism of benzo(a)pyrene. Cancer Biochem. Biophys. 1978; 2:123–130.

NIH-PA Author Manuscript

NIH-PA Author Manuscript

NIH-PA Author Manuscript

Lorentzen RJ, Caspary WJ, Lesko SA, Ts'o POP. The autoxidation of 6-hydroxybenzo[*a*]pyrene and 6-oxobenzo[*a*]pyrene radical, reactive metabolites of benzo[*a*]pyrene. Biochemistry. 1975; 14:3970–3977.

Lu F, Zahid M, Saeed M, Cavalieri EL, Rogan EG. Estrogen metabolism and formation of estrogen-DNA adducts in estradiol-treated MCF-10F cells. The effects of 2,3,7,8-tetrachlorodibenzo-p-dioxin induction and catechol-O-methyltransferase inhibition. J. Steroid Biochem. Mol. Biol. 2007; 105:150–158. [PubMed: 17582757]

Lu F, Zahid M, Saeed M, Cavalieri EL, Rogan EG. Resveratrol prevents estrogen-DNA adduct formation and neoplastic transformation in MCF-10F cells. Cancer Prev. Res. 2008; 1:135–145.

Lunn RM, Langlois RG, Hsieh LL, Thompson CL, Bell DA. XRCC1 polymorphisms: Effects on aflatoxin B1-DNA adducts and glycophorin A variant frequency. Cancer Res. 1999; 59:2557–2561. [PubMed: 10363972]

MacNicoll AD, Grover PL, Sims P. The metabolism of a series of polycyclic hydrocarbons by mouse skin maintained in short-term organ culture. Chem.-biol. Interact. 1980; 29:169–188. [PubMed: 6766358]

Mailander PC, Meza JL, Higginbotham S, Chakravarti D. Induction of A.T to G.C mutations by erroneous repair of depurinated DNA following estrogen treatment of the mammary gland of ACI rats. J. Steroid Biochem. Mol. Biol. 2006; 101:204–215. [PubMed: 16982187]

Männistö PT, Kaakkola S. Catechol-*O*-methyltransferase (COMT): Biochemistry, molecular biology, pharmacology, and clinical efficacy of the new selective COMT inhibitors. Pharmacol. Rev. 1999; 51:593–628. [PubMed: 10581325]

Markushin Y, Gaikwad N, Zhang H, Kapke P, Rogan EG, Cavalieri EL, Trock BJ, Pavlovich C, Jankowiak R. Potential biomarker for early risk assessment of prostate cancer. Prostate. 2006; 66:1565–1571. [PubMed: 16894534]

Markushin Y, Kapke P, Saeed M, Zhang H, Dawoud A, Rogan EG, Cavalieri EL, Jankowiak R. Development of monoclonal antibodies to 4-hydroxyestrogen-2-*N*-acetylcysteine conjugates: Immunoaffinity and spectroscopic studies. Chem. Res. Toxicol. 2005; 18:1520–1527. [PubMed: 16533015]

Marnett LJ. Prostaglandin synthase-mediated metabolism of carcinogens and a potential role of peroxyl radicals as reactive intermediates. Environ. Health Perspect. 1990; 88:5–12. [PubMed: 2125560]

Marnett, LJ.; Weller, P.; Battista, JR. Comparison of the peroxidase activity of heme-proteins and cytochrome P-450. In: Ortiz de Montellano, PR., editor. Cytochrome P-450. New York: Plenum Press; 1986. p. 29-74.

Mehlman MA. Causal relationship between non-Hodgkin's lymphoma and exposure to benzene and benzene-containing solvents. Ann NY Acad Sci. 2006; 1076:120–128. [PubMed: 17119197]

Melikian AA, LaVoie EJ, Hecht SS, Hoffmann D. Influence of bay-region methyl group on formation of 5-methylchrysene dihydrodiol epoxide: DNA adducts in mouse skin. Cancer Res. 1982; 42:1239–1242. [PubMed: 7060000]

Melikian AA, LaVoie EJ, Hecht SS, Hoffmann D. 5-Methylchrysene metabolism in mouse epidermis in vivo, diol epoxide–DNA adduct persistence, and diol epoxide reactivity with DNA as potential factors influencing the predominance of 5-methylchrysene-1,2-diol-3,4-epoxide–DNA adducts in mouse epidermis. Carcinogenesis. 1983; 4:843–849. [PubMed: 6872139]

Menger EM, Spokane RB, Sullivan PD. Free radicals derived from benzo[*a*]pyrene. Biochem. Biophys. Res. Commun. 1976; 71:610–616. [PubMed: 183774]

Metzler M, McLachlan JA. Oxidative metabolism of the synthetic estrogens hexestrol and dienestrol indicates reactive intermediates. Adv. Exp. Med. Biol. 1981; 136(Pt A):829–837. [PubMed: 6283819]

Miligi L, Costantini AS, Benvenuti A, Kriebel D, Bolejack V, Tumino R, Ramazzotti V, Rodella S, Stagnaro E, Crosignani P, Amadori D, Mirabelli D, et al. Occupational exposure to solvents and the risk of lymphomas. Epidemiology. 2006; 17:552–561. [PubMed: 16878041]

Miller EC, Miller JA. Mechanisms of chemical carcinogenesis: Nature of proximate carcinogens and interactions with macromolecules. Pharmacological Reviews. 1966; 18:805–838. [PubMed: 5325210]

NIH-PA Author Manuscript

NIH-PA Author Manuscript

NIH-PA Author Manuscript

Miller EC, Miller JA. Mechanisms of chemical carcinogenesis. Cancer. 1981a; 47:1055–1064. [PubMed: 7016297]

Miller EC, Miller JA. Searches for ultimate chemical carcinogens and their reactions with cellular macromolecules. Cancer. 1981b; 47:2327–2345. [PubMed: 7272889]

Miller JH. Mutational specificity in bacteria. Ann. Rev. Genet. 1983; 17:215–238. [PubMed: 6364961]

Miller WR, O'Neill J. The importance of local synthesis of estrogen within the breast. Steroids. 1987; 50:537–548. [PubMed: 3504615]

Mitrunen K, Hirvonen A. Molecular epidemiology of sporadic breast cancer. The role of polymorphic genes involved in oestrogen biosynthesis and metabolism. Mutat. Res. 2003; 544:9–41. [PubMed: 12888106]

Mobley JA, Bhat AS, Brueggemeier RW. Measurement of oxidative DNA damage by catechol estrogens and analogues *in vitro*. Chem. Res. Toxicol. 1999; 12:270–277. [PubMed: 10077490]

Montano MM, Chaplin LJ, Deng H, Mesia-Vela S, Gaikwad N, Zahid M, Rogan E. Protective roles of quinone reductase and tamoxifen against estrogen-induced mammary tumorigenesis. Oncogene. 2007; 26:3587–3590. [PubMed: 17160017]

Mulder PPJ, Chen L, Sekhar BC, George M, Gross ML, Rogan EG, Cavalieri EL. Synthesis and structure determination of the adducts formed by electrochemical oxidation of 1,2,3,4-tetrahydro-7,12-dimethylbenz[*a*]anthracene in the presence of deoxyribonucleosides or adenine. Chem. Res. Toxicol. 1996; 9:1264–1277. [PubMed: 8951228]

Mulder PPJ, Devanesan P, van Alem K, Lodder G, Rogan EG, Cavalieri EL. Fluorobenzo[*a*]pyrenes as probes of the mechanism of cytochrome P450-catalyzed oxygen transfer in aromatic oxygenations. Free Rad. Biol. & Med. 2003; 34:734–745. [PubMed: 12633750]

Nagata, C.; Tagashira, Y.; Kodama, M. Metabolic activations of benzo(*a*)pyrene: Significance of the free radical. In: Ts'o, POP.; DiPaolo, JA., editors. Chemical Carcinogenesis, Part A. Marcel Dekker; 1974. p. 87-111.

Nandi S. Role of hormones in mammary neoplasia. Cancer Res. 1978; 38:4046–4049. [PubMed: 698952]

Nandi S, Guzman RC, Yang J. Hormones and mammary carcinogenesis in mice, rats, and humans: a unifying hypothesis. Proc. Natl. Acad. Sci. USA. 1995; 92:3650–3657. [PubMed: 7731959]

National Toxicology Program. Toxicology and Carcinogenesis Studies of Naphthalene (CAS No. 91-20-3) in F344/N Rats (Inhalation Studies) (NTP Technical Report No. 500; NIH Publ. No. 01-4434). Research Triangle Park, NC: 2000.

Newbold RR, Liehr JG. Induction of uterine adenocarcinoma in CD-1 mice by catechol estrogens. Cancer Res. 2000; 60:235–237. [PubMed: 10667565]

Nivard MJ, Pastink A, Vogel EW. Molecular analysis of mutations induced in the vermilion gene of *Drosophila melanogaster* by methyl methanesulfonate. Genetics. 1992; 131:673–682. [PubMed: 1628810]

Ortiz de Montellano PR, Stearns RA. Timing of the radical recombination step in cytochrome P-450 catalysis with ring-stained probes. J. Am. Chem. Soc. 1987; 109:3415–3420.

Pasqualini JR, Chetrite G, Blacker C, Feinstein MC, Delalonde L, Talbi M, Maloche C. Concentrations of estrone, estradiol, and estrone sulfate and evaluation of sulfatase and aromatase activities in pre- and postmenopausal breast cancer patients. J. Clin. Endocrinol. Metab. 1996; 81:1460–1464. [PubMed: 8636351]

Pataki J, Balic R. Relative carcinogenicity of some diethylbenz(*a*)anthracenes. J. Med. Chem. 1972; 15:905–909. [PubMed: 5051006]

Paxton MB. Leukemia risk associated with benzene exposure in the Pliofilm cohort. Environ. Health Perspect. 1996; 104(Suppl 6):1431–1436. [PubMed: 9118929]

Peltonen K, Hilton BD, Pataki J, Lee H, Harvey RG, Dipple A. Spectroscopic characterization of syn-5-methylchrysene 1,2-dihydrodiol 3,4-epoxide-deoxyribonucleoside adducts. Chem. Res. Toxicol. 1991; 4:305–310. [PubMed: 1912313]

Platt KL, Schollmeier M, Frank H, Oesch F. Stereoselective metabolism of dibenz(*a*,*h*)anthracene to trans-dihydrodiols and their activation to bacterial mutagens. Environ. Health Perspect. 1990; 88:37–41. [PubMed: 2272331]

NIH-PA Author Manuscript

NIH-PA Author Manuscript

NIH-PA Author Manuscript

Preston-Martin S, Pike MC, Ross RK, Jones PA, Henderson BE. Increased cell division as a cause of human cancer. Cancer Res. 1990; 50:7415–7421. [PubMed: 2174724]

Pruthi S, Yang L, Sandhu NP, Ingle JN, Beseler CL, Suman VJ, Cavalieri EL, Rogan EG. Evaluation of serum estrogen-DNA adducts as potential biomarkers for breast cancer risk. J. Steroid Biochem. Mol. Biol. 2012; 132:73–79. [PubMed: 22386952]

Pullman, A.; Pullman, B. Cancérisation par les Substances Chimiques et Structure Moléculaire. et Cie, Paris: Maisson; 1955.

Pullman A, Pullman B. Molecular electrostatic potential of the nucleic acids. Q. Rev. Biophys. 1981; 14:289–380. [PubMed: 7027300]

Quintanilla M, Brown K, Ramsden M, Balmain A. Carcinogen-specific mutation and amplification of Ha-ras during mouse skin carcinogenesis. Nature. 1986; 322:78–80. [PubMed: 3014349]

RamaKrishna NVS, Cavalieri EL, Rogan EG, Dolnikowski GG, Cerny RL, Gross ML, Jeong H, Jankowiak R, Small GJ. Synthesis and structure determination of the adducts of the potent carcinogen 7,12-dimethylbenz[*a*]anthracene and deoxyribonucleosides formed by electrochemical oxidation: Models for metabolic activation by one-electron oxidation. J. Am. Chem. Soc. 1992a; 114:1863–1874.

RamaKrishna NVS, Devanesan PD, Rogan EG, Cavalieri EL, Jeong H, Jankowiak R, Small GJ. Mechanism of metabolic activation of the potent carcinogen 7,12-dimethylbenz[*a*]anthracene. Chem. Res. Toxicol. 1992b; 5:220–226. [PubMed: 1643251]

RamaKrishna NVS, Gao F, Padmavathi NS, Cavalieri EL, Rogan EG, Cerny RL, Gross ML. Model adducts of benzo[*a*]pyrene and nucleosides formed from its radical cation and diol epoxide. Chem. Res. Toxicol. 1992c; 5:293–302. [PubMed: 1643261]

RamaKrishna NVS, Li K-M, Rogan EG, Cavalieri EL, George M, Cerny RL, Gross ML. Adducts of 6-methylbenzo[*a*]pyrene and 6-fluorobenzo[*a*]pyrene formed by electrochemical oxidation in the presence of deoxyribonucleosides. Chem. Res. Toxicol. 1993a; 6:837–845. [PubMed: 8117923]

RamaKrishna NVS, Padmavathi NS, Cavalieri EL, Rogan EG, Cerny RL, Gross ML. Synthesis and structure determination of the adducts formed by electrochemical oxidation of the potent carcinogen dibenzo[*a,l*]pyrene in the presence of nucleosides. Chem. Res. Toxicol. 1993b; 6:554–560. [PubMed: 8374056]

Reardon DB, Prakash AS, Hilton BD, Roman JM, Pataki J, Harvey RG, Dipple A. Characterization of 5-methylchrysene-1,2-dihydrodiol-3,4-epoxide-DNA adducts. Carcinogenesis. 1987; 8:1317–1322. [PubMed: 3621468]

Reddy MV, Randerath K. Nuclease P_1-mediated enhancement of sensitivity of ^{32}P-postlabeling test for structurally diverse DNA adducts. Carcinogenesis. 1986; 7:1543–1551. [PubMed: 3017601]

Rickert DE, Baker TS, Bus JS, Barrow CS, Irons RD. Benzene disposition in the rat after exposure by inhalation. Toxicol. Appl. Pharmacol. 1979; 49:417–423. [PubMed: 473208]

Rinsky RA, Smith AB, Hornung R, Filloon TG, Young RJ, Okun AH, Landrigan PJ. Benzene and leukemia. An epidemiologic risk assessment. N. Engl. J. Med. 1987; 316:1044–1050. [PubMed: 3561457]

Rochlitz J. Neue Reaktionen der carcinogenen Kohlenwasserstoffe-II. Tetrahedron. 1967; 23:3043–3048. [PubMed: 6045955]

Rodriguez H, Loechler EL. Mutagenesis by (+)antidioepoxide a of benzo[*a*]pyrene: what controls mutagenic specificity? Biochemistry. 1993; 32:1759–1769. [PubMed: 8439538]

Rogan E, Cavalieri E, Tibbels S, Cremonesi P, Warner C, Nagel D, Tomer K, Cerny R, Gross M. Synthesis and identification of benzo[*a*]pyrene-guanine nucleoside adducts formed by electrochemical oxidation and horseradish peroxidase-catalyzed reaction of benzo[*a*]pyrene with DNA. J. Am. Chem. Soc. 1988; 110:4023–4029.

Rogan, E.; Roth, R.; Cavalieri, E. Manganic acetate and horseradish peroxidase/hydrogen peroxide. *In vitro* models of activation or aromatic hydrocarbons by one-electron oxidation. In: Bjorseth, A.; Dennis, AJ., editors. Polynuclear Aromatic Hydrocarbons: Chemistry and Biological Effects. Columbus, OH: Battelle Press; 1980. p. 259-266.

Rogan EG, Badawi AF, Devanesan PD, Meza JL, Edney JA, West WW, Higginbotham SM, Cavalieri EL. Relative imbalances in estrogen metabolism and conjugation in breast tissue of women with

NIH-PA Author Manuscript

NIH-PA Author Manuscript

NIH-PA Author Manuscript

carcinoma: Potential biomarkers of susceptibility to cancer. Carcinogenesis. 2003; 24:697–702. [PubMed: 12727798]

Rogan EG, Cavalieri EL. 3-Methylcholanthrene-inducible binding of aromatic hydrocarbons to DNA in purified rat liver nuclei. Biochem. Biophys. Res. Commun. 1974; 58:1119–1126. [PubMed: 4151893]

Rogan EG, Devanesan PD, RamaKrishna NVS, Higginbotham S, Padmavathi NS, Chapman K, Cavalieri EL, Jeong H, Jankowiak R, Small GJ. Identification and quantitation of benzo[*a*]pyrene-DNA adducts formed in mouse skin. Chem. Res. Toxicol. 1993; 6:356–363. [PubMed: 7686408]

Rogan EG, Mailander P, Cavalieri E. Metabolic activation of aromatic hydrocarbons in purified rat liver nuclei: induction of enzyme activities and binding to DNA with and without monooxygenase-catalyzed formation of active oxygen. Proc. Natl. Acad. Sci. USA. 1976; 73:457–461. [PubMed: 813227]

Rogan EG, RamaKrishna NVS, Higginbotham S, Cavalieri EL, Jankowiak R, Small GJ. Identification and quantitation of 7-(benzo[*a*]pyren-6-yl)guanine in the urine and feces of rats treated with benzo[*a*]pyrene. Chem. Res. Toxicol. 1990; 3:441–444. [PubMed: 2133095]

Russo J, Fernandez SV, Russo PA, Fernbaugh R, Sheriff FS, Lareef HM, Garber J, Russo IH. 17β-Estradiol induces transformations and tumorigenesis in human breast epithelial cells. FASEB J. 2006; 20:1622–1634. [PubMed: 16873885]

Russo J, Hasan Lareef M, Balogh G, Guo S, Russo IH. Estrogen and its metabolites are carcinogenic agents in human breast epithelial cells. J. Steroid Biochem. Mol. Biol. 2003; 87:1–25. [PubMed: 14630087]

Russo J, Russo IH. Genotoxicity of steroidal estrogens. Trends Endocrinol. Metab. 2004; 15:211–214. [PubMed: 15223050]

Sabourin PJ, Bechtold WE, Griffith WC, Birnbaum LS, Lucier G, Henderson RF. Effect of exposure concentration, exposure rate, and route of administration on metabolism of benzene by F344 rats and B6C3F1 mice. Toxicol. Appl. Pharmacol. 1989; 99:421–444. [PubMed: 2749731]

Sadler A, Subrahmanyam VV, Ross D. Oxidation of catechol by horseradish peroxidase and human leukocyte peroxidase: reactions of o-benzoquinone and o-benzosemiquinone. Toxicol. Appl. Pharmacol. 1988; 93:62–71. [PubMed: 2832975]

Saeed M, Gunselman SJ, Higginbotham S, Rogan E, Cavalieri E. Formation of the depurinating N3adenine and N7guanine adducts by reaction of DNA with hexestrol-3′-4′-quinone or enzyme-activated 3′-hydroxyhexestrol. Implications for a unifying mechanism of tumor initiation by natural and synthetic estrogens. Steroids. 2005a; 70:37–45. [PubMed: 15610895]

Saeed M, Higginbotham S, Gaikwad N, Chakravarti D, Rogan E, Cavalieri E. Depurinating naphthalene-DNA adducts in mouse skin related to cancer initiation. Free Radic. Biol. Med. 2009a; 47:1075–1081. [PubMed: 19619639]

Saeed M, Higginbotham S, Rogan E, Cavalieri E. Formation of depurinating N3adenine and N7guanine adducts after reaction of 1,2-naphthoquinone or enzyme-activated 1,2-dihydroxynaphthalene with DNA. Implications for the mechanism of tumor initiation by naphthalene. Chem. Biol. Interact. 2007a; 165:175–188. [PubMed: 17224140]

Saeed M, Rogan E, Cavalieri E. Mechanism of metabolic activation and DNA adduct formation by the human carcinogen diethylstilbestrol: The defining link to natural estrogens. Int. J. Cancer. 2009b; 124:1276–1284. [PubMed: 19089919]

Saeed M, Rogan E, Fernandez SV, Sheriff F, Russo J, Cavalieri E. Formation of depurinating N3Adenine and N7Guanine adducts by MCF-10F cells cultured in the presence of 4-hydroxyestradiol. Int. J. Cancer. 2007b; 120:1821–1824. [PubMed: 17230531]

Saeed M, Zahid M, Gunselman SJ, Rogan E, Cavalieri E. Slow loss of deoxyribose from the N7deoxyguanosine adducts of estradiol-3,4-quinone and hexestrol-3′,4′-quinone. Implications for mutagenic activity. Steroids. 2005b; 70:29–35. [PubMed: 15610894]

Sagher D, Strauss B. Insertion of nucleotides opposite apurinic/apyrimidinic sites in deoxyribonucleic acid during in vitro synthesis: uniqueness of adenine nucleotides. Biochemistry. 1983; 22:4518–4526. [PubMed: 6354260]

NIH-PA Author Manuscript

NIH-PA Author Manuscript

NIH-PA Author Manuscript

Saiko P, Szakmary A, Jaeger W, Szekeres T. Resveratrol and its analogs: defense against cancer, coronary disease and neurodegenerative maladies or just a fad? Mutat. Res. 2008; 658:68–94. [PubMed: 17890139]

Samuni AM, Chuang EY, Krishna MC, Stein W, DeGraff W, Russo A, Mitchell JB. Semiquinone radical intermediate in catecholic estrogen-mediated cytotoxicity and mutagenesis: Chemoprevention strategies with antioxidants. Proc. Natl. Acad. Sci. U.SA. 2003; 100:5390–5395.

Santen R, Cavalieri E, Rogan E, Russo J, Guttenplan J, Ingle J, Yue W. Estrogen mediation of breast tumor formation involves estrogen receptor-dependent, as well as independent, genotoxic effects. Ann. NY Acad. Sci. 2009; 1155:132–140. [PubMed: 19250200]

Santen, RJ.; Yue, W.; Bocchinfusco, W.; Korach, K.; Wang, JP.; Rogan, EG.; Yang, L.; Cavalieri, E.; Russo, J.; Devanesan, P.; Verderame, M. Estradiol-induced carcinogenesis via formation of genotoxic metabolites. In: Ingle, JN.; Dowsett, M., editors. Advances in Endocrine Therapy of Breast Cancer. NY, USA: Marcel Dekker; 2003. p. 163-177.

Santner SJ, Feil PD, Santen RJ. In situ estrogen production via the estrone sulfatase pathway in breast tumors: Relative importance versus the aromatase pathway. J. Clin. Endocrinol. Metab. 1984; 59:29–33. [PubMed: 6725522]

Sawyer TW, Gill RD, Smith-Oliver T, Butterworth BE, DiGiovanni J. Measurement of unscheduled DNA synthesis in primary cultures of adult mouse epidermal keratinocytes. Carcinogenesis. 1988; 9:1197–1202. [PubMed: 3383338]

Schaaper RM, Kunkel TA, Loeb LA. Infidelity of DNA synthesis associated with bypass of apurinic sites. Proc. Natl. Acad. Sci. USA. 1983; 80:487–491. [PubMed: 6300848]

Selkirk JK, Croy RG, Roller PP, Gelboin HV. High-pressure liquid chromatographic analysis of benzo(*a*)pyrene metabolism and covalent binding and the mechanism of activation of 7,8-benzoflavone and 1,2-epoxy-3,3,3-trichloropropane. Cancer Res. 1974; 34:3474–3480. [PubMed: 4429963]

Shibutani S, Margulis LA, Geacintov NE, Grollman AP. Translesional synthesis on a DNA template containing a single stereoisomer of dG(+) or dG(-) anti-BPDE (7,8-dihydroxy anti-9,10-epoxy 7,8,9,10-tetrahydrobenzo[*a*]pyrene). Biochemistry. 1993; 32:7531–7541. [PubMed: 8338850]

Shipman, LL. Ab initio quantum mechanical characterization of the ground electronic state of benzo[*a*]pyrene. Implications for the mechanism of polynuclear aromatic hydrocarbon oxidation to epoxides by cytochrome P-450. In: Jones, PW.; Freudenthal, RI., editors. Carcinogenesis. Vol. Vol. 3. Raven Press; 1978. p. 139-144.

Shou MG, Yang SK. Metabolism of 2S-hydroxy-3-methylcholanthrene by rat liver microsomes. Carcinogenesis. 1990; 11:2037–2045. [PubMed: 2225338]

Simpson ER, Mahendroo MS, Means GD, Kilgore MW, Hinshelwood MM, Graham-Lorence S, Amarneh B, Ito Y, Fisher CR, Michael MD, Mendelson CR, Bulun SE. Aromatase cytochrome P450, the enzyme responsible for estrogen biosynthesis. Endocr. Rev. 1994; 15:342–355. [PubMed: 8076586]

Sims P. The carcinogenic activities in mice of compounds related to 3-methylcholanthrene. Int. J. Cancer. 1967; 2:505–508. [PubMed: 6081593]

Sims, P.; Grover, PL. Involvement of dihydrodiols and diol epoxides in the metabolic activation of polycyclic hydrocarbons other than benzo[*a*]pyrene. In: Gelboin, HV.; Ts'o, POP., editors. Polycyclic Hydrocarbons and Cancer. Vol. Vol. 3. New York: Academic Press; 1981. p. 117-181.

Sims P, Grover PL, Swaisland A, Pal K, Hewer A. Metabolic activation of benzo[*a*]pyrene proceeds by a diol epoxide. Nature. 1974; 252:326–328. [PubMed: 4473724]

Singh S, Chakravarti D, Edney JA, Hollins RR, Johnson PJ, West WW, Higginbotham SM, Cavalieri EL, Rogan EG. Relative imbalances in the expression of estrogen-metabolizing enzymes in the breast tissue of women with breast carcinoma. Oncol. Rep. 2005; 14:1091–1096. [PubMed: 16142378]

Singh S, Zahid M, Saeed M, Gaikwad NW, Meza JL, Cavalieri EL, Rogan EG, Chakravarti D. NAD(P)H:quinone oxidoreductase 1 Arg139Trp and Pro187Ser polymorphism imbalance

NIH-PA Author Manuscript

NIH-PA Author Manuscript

NIH-PA Author Manuscript

estrogen metabolism towards DNA adduct formation in human mammary epithelial cells. J. Steroid Biochem. Mol. Biol. 2009; 117:56–66. [PubMed: 19628038]

Slaga TJ, Bracken WM, Viaje A, Levin W, Yagi H, Jerina DM, Conney AH. Comparison of the tumor-initiating activities of benzo[*a*]pyrene arene oxides and diol-epoxides. Cancer Res. 1977; 37:4130–4133. [PubMed: 908047]

Slaga TJ, Gleason GL, DiGiovanni J, Sukumaran KB, Harvey RG. Potent tumor-initiating activity of the 3,4-dihydrodiol of 7,12-dimethylbenz(*a*)anthracene in mouse skin. Cancer Res. 1979; 39:1934–1936. [PubMed: 109189]

Slaga TJ, Viaje A, Betty DL, Brachen W, Buty SG, Scribner JD. Skin tumor initiating ability of benzo[*a*]pyrene 4,5-, 7,8- and 7,8-diol-9,10-epoxides and 7,8-diol. Cancer Lett. 1976; 2:115–122. [PubMed: 1016959]

Snyder R, Kalf GF. A perspective on benzene leukemogenesis. Crit. Rev. Toxicol. 1994; 24:177–209. [PubMed: 7945890]

Spink DC, Hayes CL, Young NR, Christou M, Sutter TR, Jefcoate CR, Gierthy JF. The effects of 2,3,7,8-tetrachlorodibenzo-p-dioxin on estrogen metabolism in MCF-7 breast cancer cells: Evidence for induction of a novel 17 beta-estradiol 4-hydroxylase. J. Steroid Biochem. Mol. Biol. 1994; 51:251–258. [PubMed: 7826886]

Spink DC, Spink BC, Cao JQ, DePasquale JA, Pentecost BT, Fasco MJ, Li Y, Sutter TR. Differential expression of CYP1A1 and CYP1B1 in human breast epithelial cells and breast tumor cells. Carcinogenesis. 1998; 19:291–298. [PubMed: 9498279]

Stack D, Byun J, Gross ML, Rogan EG, Cavalieri E. Molecular characteristics of catechol estrogen quinones in reactions with deoxyribonucleosides. Chem. Res. Toxicol. 1996; 9:851–859. [PubMed: 8828920]

Stack DE, Cremonesi P, Hanson A, Rogan EG, Cavalieri EL. Radical cations of benzo[*a*]pyrene and 6-substituted derivatives: reaction with nucleophiles and DNA. Xenobiotica. 1995; 25:755–760. [PubMed: 7483671]

Stack DE, Li G, Hill A, Hoffman N. Mechanistic insights into the Michael addition of deoxyguanosine to catechol estrogen-3,4-quinones. Chem. Res. Toxicol. 2008; 21:1415–1425. [PubMed: 18547067]

Stark AA, Malca-Mor L, Herman Y, Liberman DF. DNA strand scission and apurinic sites induced by photoactivated aflatoxins. Cancer Res. 1988; 48:3070–3076. [PubMed: 3130184]

Steinmaus C, Smith AH, Jones RM, Smith MT. Meta-analysis of benzene exposure and non-Hodgkin lymphoma: biases could mask an important association. Occup Environ Med. 2008; 65:371–378. [PubMed: 18417556]

Stevenson JL, Von Haam E. Carcinogenicity of benz[*a*]anthracene and benzo[*c*]phenanthrene derivatives. Am. Inst. Hyg. Ass. J. 1965; 26:475–478.

Stivala LA, Savio M, Carafoli F, Perucca P, Bianchi L, Maga G, Forti L, Pagnoni UM, Albini A, Prosperi E, Vannini V. Specific structural determinants are responsible for the antioxidant activity and the cell cycle effects of resveratrol. J. Biol. Chem. 2001; 276:22586–22594. [PubMed: 11316812]

Strauss BS. Cellular aspects of DNA repair. Adv. Cancer Res. 1985; 45:45–105. [PubMed: 3911748]

Subbaramaiah K, Chung WJ, Michaluart P, Telang N, Tanabe T, Inoue H, Jang M, Pezzuto JM, Dannenberg AJ. Resveratrol inhibits cyclooxygenase-2 transcription and activity in phorbol ester-treated human mammary epithelial cells. J. Biol. Chem. 1998; 273:21875–21882. [PubMed: 9705326]

Sullivan PD, Bannoura F, Daub GH. ^{13}C and ^{1}H EPR analysis of the benzo[*a*]pyrene cation radical. J. Am. Chem. Soc. 1985; 107:32–35.

Talalay P, Dinkova-Kostova AT, Holtzclaw WD. Importance of phase 2 gene regulation in protection against electrophile and reactive oxygen toxicity and carcinogenesis. Adv. Enzyme Regul. 2003; 43:121–134. [PubMed: 12791387]

Thakker DR, Levin W, Stoming TA, Conney AH, Jerina DM. Metabolism of 3-methylcholanthrene by rat liver microsomes and a highly purified monooxygenase system with and without epoxide hydrase. Carcinog.-Compr. Surv. 1978a; 3:253–264.

NIH-PA Author Manuscript

NIH-PA Author Manuscript

NIH-PA Author Manuscript

Thakker DR, Levin W, Wood AW, Conney AH, Stoming TA, Jerina DM. Metabolic formation of 1,9,10-trihydroxy-9,12-dihydro-3-methylcholanthrene. J. Am. Chem. Soc. 1978b; 100:645–647. [PubMed: 624805]

Thakker DR, Levin W, Yagi H, Ryan D, Thomas PE, Karle JM, Lehr RE, Jerina DM, Conney AH. Metabolism of benzo[*a*]anthracene to its tumorigenic 3,4-dihydrodiol. Mol. Pharmacol. 1979a; 15:138–153. [PubMed: 423885]

Thakker DR, Levin W, Yagi H, Turujman S, Kapadia D, Conney AH, Jerina DM. Absolute stereochemistry of the trans-dihydrodiols formed from benzo[*a*]anthracene by liver microsomes. Chem.-biol. Interact. 1979b; 27:145–161. [PubMed: 498352]

Todorovic R, Devanesan P, Rogan E, Cavalieri E. Identification and quantification of stable DNA adducts of dibenzo[*a,l*]pyrene or its metabolites *in vitro* and in mouse skin and rat mammary gland. Chem. Res. Toxicol. 2005; 18:984–990. [PubMed: 15962933]

Tolbert LM, Khanna RK, Popp AE, Gelbaum L, Bottomley LA. Sterioelectronic effects in the deprotonation of arylalkylradical cations: meso-ethylanthracenes. J. Am. Chem. Soc. 1990; 112:2373–2378.

Townsend DM, Tew KD, Tapiero H. The importance of glutathione in human disease. Biomed. Pharmacother. 2003; 57:145–155. [PubMed: 12818476]

Vassilopoulou-Sellin R, Palmer L, Taylor S, Cooksley CS. Incidence of breast carcinoma in women with thyroid carcinoma. Cancer. 1999; 85:696–705. [PubMed: 10091743]

Vaught J, Bresnick E. Binding of polycyclic hydrocarbons to nuclear components in vitro. Biochem. Biophys. Res. Commun. 1976; 69:587–591. [PubMed: 1267804]

Venugopal D, Zahid M, Mailander PC, Meza JL, Rogan EG, Cavalieri EL, Chakravarti D. Reduction of estrogen-induced transformation of mouse mammary epithelial cells by *N*-acetylcysteine. J. Steroid Biochem. Mol. Biol. 2008; 109:22–30. [PubMed: 18226522]

Vericat JA, Cheng SC, Dipple A. Absolute configuration of 7,12-dimethylbenz[*a*]anthracene-DNA adducts in mouse skin epidermis. Cancer Lett. 1991; 57:237–242. [PubMed: 1903326]

Vidal AE, Boiteux S, Hickson ID, Radicella JP. XRCC1 coordinates the initial and late stages of DNA abasic site repair through protein-protein interactions. EMBO J. 2001; 20:6530–6539. [PubMed: 11707423]

Walle T, Hsieh F, DeLegge MH, Oatis JE Jr, Walle UK. High absorption but very low bioavailability of oral resveratrol in humans. Drug Metab. Dispo. 2004; 32:1377–1382.

Wilk M, Bez W, Rochlitz J. Neue Reaktionen der carcinogenen Kohlenwasserstoffe 3,4-Benzpyren, 9,10-Dimethyl-1,2-Benzanthracen und 20-Methylcholanthren. Tetrahedron. 1966; 22:2599–2608.

Wilk M, Girke W. Reactions between benzo[*a*]pyrene and nucleobases by one-electron oxidation. J. Natl. Cancer Inst. 1972; 49:1585–1597. [PubMed: 4647844]

Wislocki PG, Buening MK, Levin W, Lehr RE, Thakker DR, Jerina DM, Conney AH. Tumorigenicity of the diastereomeric benz[*a*]anthracene 3,4-diol-1,2-epoxides and the (+)- and (−)-enantiomers of benz[*a*]anthracene 3,4-dihydrodiol in newborn mice. J. Natl Cancer Inst. 1979; 63:201–204. [PubMed: 286829]

Wislocki PG, Fiorentini KM, Fu PP, Yang SK, Lu AY. Tumor-initiating ability of the twelve monomethylbenz[*a*]anthracenes. Carcinogenesis. 1982; 3:215–217. [PubMed: 7067048]

Yager J. Catechol-*O*-methyltransferase: Characteristics, polymorphisms and role in breast cancer. Drug Discov. Today: Disease Mechanisms. Hormonal and non hormonal mechanisms underlying breast cancer. 2013; 9:e41–e46.

Yang L, Gaikwad N, Meza J, Cavalieri E, Muti P, Trock B, Rogan E. Novel biomarkers for risk of prostate cancer. Results from a case-control study. Prostate. 2009; 69:41–48. [PubMed: 18816637]

Yang SK, Roller PP, Gelboin HV. Enzymatic mechanism of benzo[*a*]pyrene conversion to phenols and diols and an improved high-pressure liquid chromatographic separation of benzo[*a*]pyrene derivatives. Biochemistry. 1977; 16:3680–3687. [PubMed: 889815]

Yu GP, Li JC, Branovan D, McCormick S, Schantz SP. Thyroid cancer incidence and survival in the national cancer institute surveillance, epidemiology, and end results race/ethnicity groups. Thyroid. 2010; 20:465–473. [PubMed: 20384488]

NIH-PA Author Manuscript

NIH-PA Author Manuscript

NIH-PA Author Manuscript

Yue W, Santen RJ, Wang JP, Li Y, Verderame MF, Bocchinfuso WP, Korach KS, Devanesan P, Todorovic R, Rogan EG, Cavalieri EL. Genotoxic metabolites of estradiol in breast: potential mechanism of estradiol induced carcinogenesis. J. Steroid Biochem. Mol. Biol. 2003; 86:477–486. [PubMed: 14623547]

Zahid M, Beseler CL, Hall JB, LeVan T, Cavalieri EL, Rogan EG. Unbalanced estrogen metabolism in ovarian cancer. Unpublished results. 2013a

Zahid M, Gaikwad N, Rogan EG, Cavalieri EL. Inhibition of depurinating estrogen-DNA adduct formation by natural compounds. Chem. Res. Toxicol. 2007; 20:1947–1953. [PubMed: 18039013]

Zahid M, Gaikwad NW, Ali MF, Lu F, Saeed M, Yang L, Rogan EG, Cavalieri EL. Prevention of estrogen-DNA adduct formation in MCF-10F cells by resveratrol. Free Radic. Biol. Med. 2008; 45:136–145. [PubMed: 18423413]

Zahid M, Goldner W, Beseler C, Rogan E, Cavalieri E. Unbalanced estrogen metabolism in thyroid cancer. Int. J. Cancer. 2013b in press.

Zahid M, Kohli E, Saeed M, Rogan E, Cavalieri E. The greater reactivity of estradiol-3,4-quinone versus estradiol-2,3-quinone with DNA in the formation of depurinating adducts. Implications for tumor-initiating activity. Chem. Res. Toxicol. 2006; 19:164–172. [PubMed: 16411670]

Zahid M, Saeed M, Ali MF, Rogan EG, Cavalieri EL. N-acetylcysteine blocks formation of cancer-initiating estrogen-DNA adducts in cells. Free Radic. Biol. Med. 2010a; 49:392–400. [PubMed: 20472053]

Zahid M, Saeed M, Beseler C, Rogan EG, Cavalieri EL. Resveratrol and *N*-acetylcysteine block the cancer-initiating step in MCF-10F cells. Free Radic. Biol. Med. 2011a; 50:78–85. [PubMed: 20934508]

Zahid M, Saeed M, Rogan EG, Cavalieri EL. Benzene and dopamine catechol quinones could initiate cancer or neurogenic disease. Free Radic. Biol. Med. 2010b; 48:318–324. [PubMed: 19909805]

Zahid M, Saeed M, Yang L, Beseler C, Rogan E, Cavalieri E. Formation of dopamine quinone-DNA adducts and their potential role in the etiology of Parkinson's disease. IUBMB Life. 2011b; 63:1087–1093. [PubMed: 22045657]

Zhao Z, Kosinska W, Khmelnitsky M, Cavalieri EL, Rogan EG, Chakravarti D, Sacks PG, Guttenplan JB. Mutagenic activity of 4-hydroxyestradiol, but not 2-hydroxyestradiol, in BB2 rat embryonic cells, and the mutational spectrum of 4-hydroxyestradiol. Chem. Res. Toxicol. 2006; 19:475–479. [PubMed: 16544955]

Zhu BT, Conney AH. Functional role of estrogen metabolism in target cells: review and perspectives. Carcinogenesis. 1998; 9:1–27. [PubMed: 9472688]

NIH-PA Author Manuscript

NIH-PA Author Manuscript

NIH-PA Author Manuscript

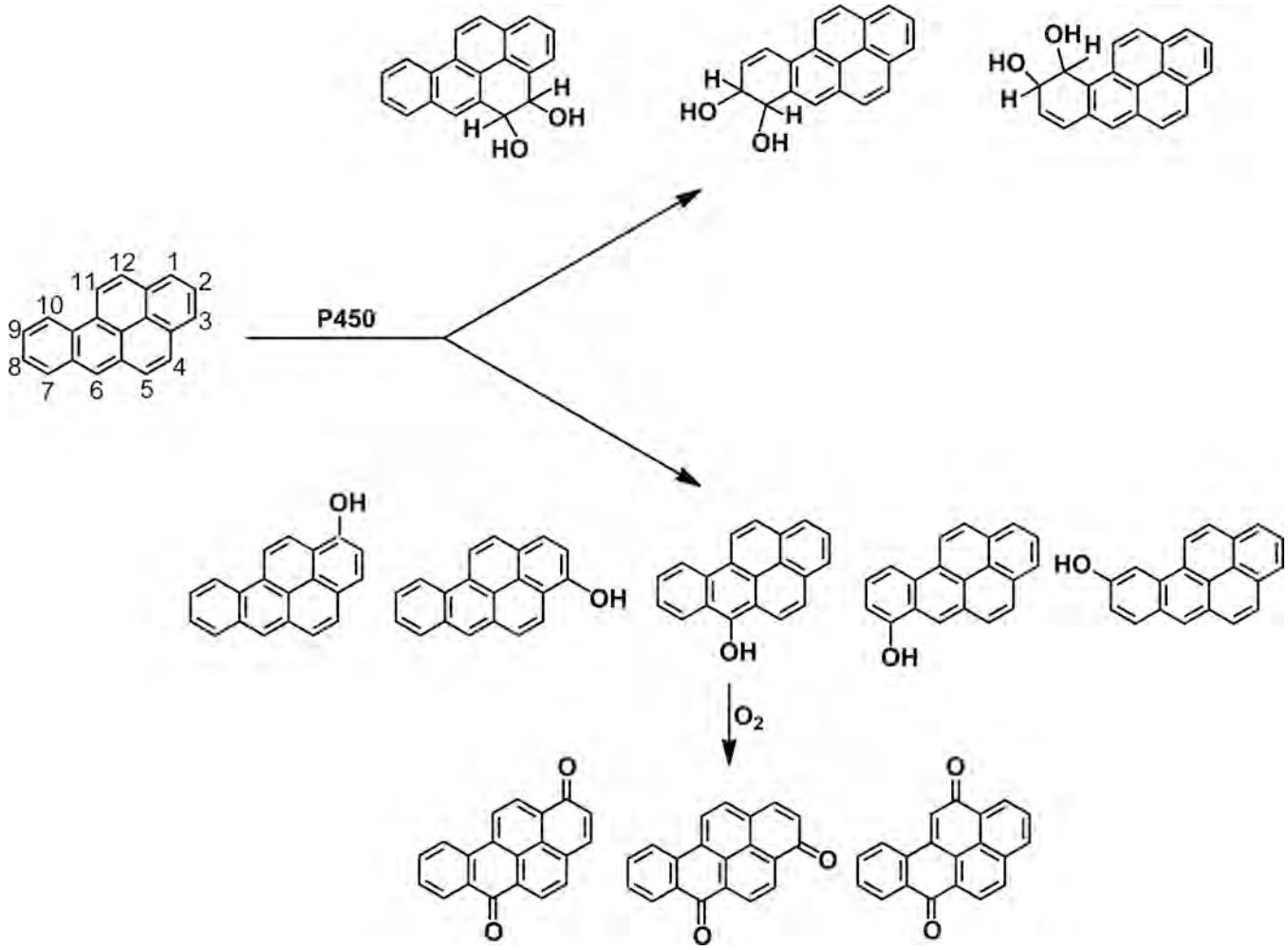

Figure 1.
Metabolism of BP catalyzed by cytochrome P450.

NIH-PA Author Manuscript

NIH-PA Author Manuscript

NIH-PA Author Manuscript

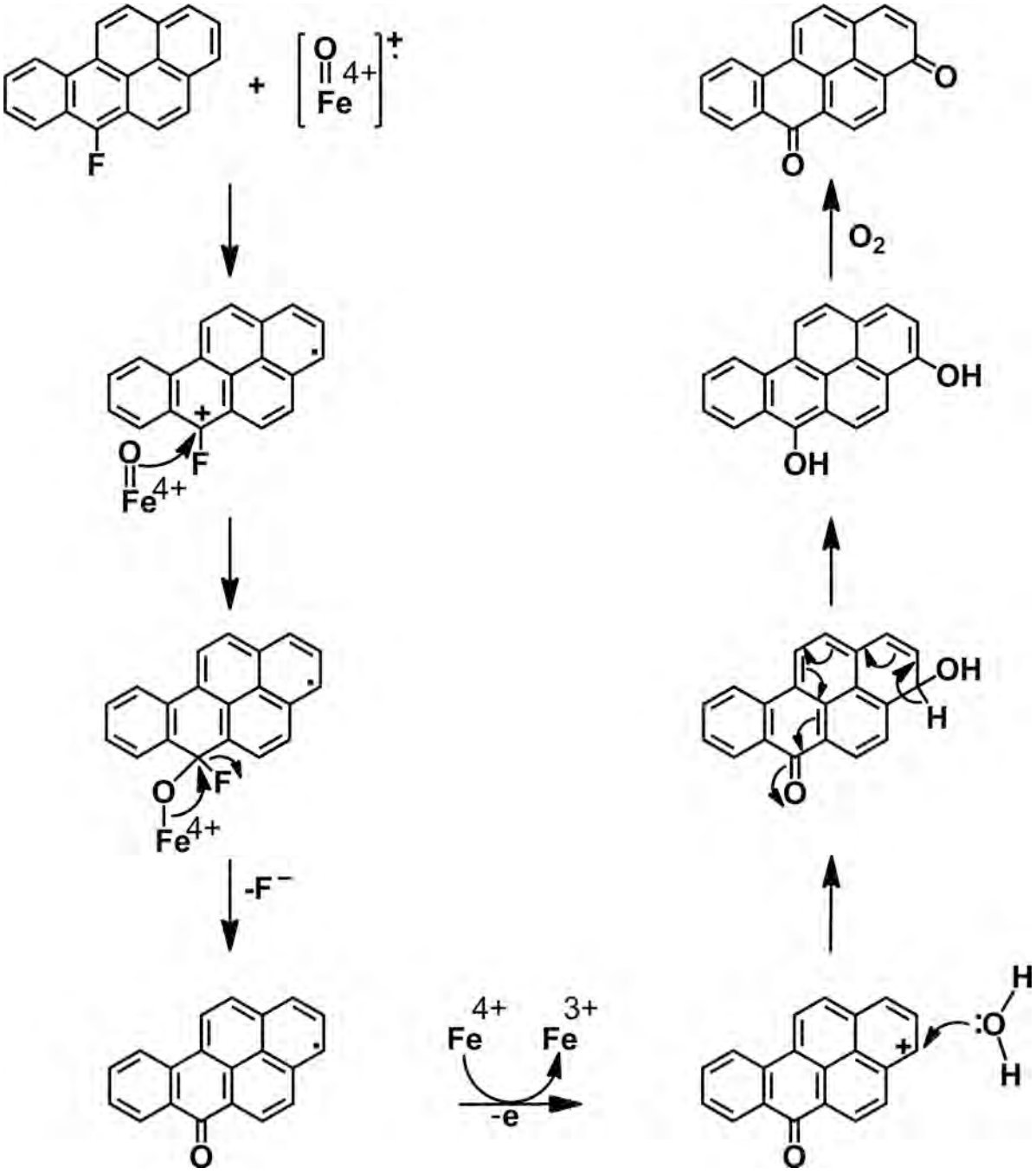

Figure 2.
Mechanism of oxygen transfer from cytochrome P450 to 6-FBP to form BP-3,6-quinone; the similar formation of BP-1,6- and 6,12-quinone is not shown.

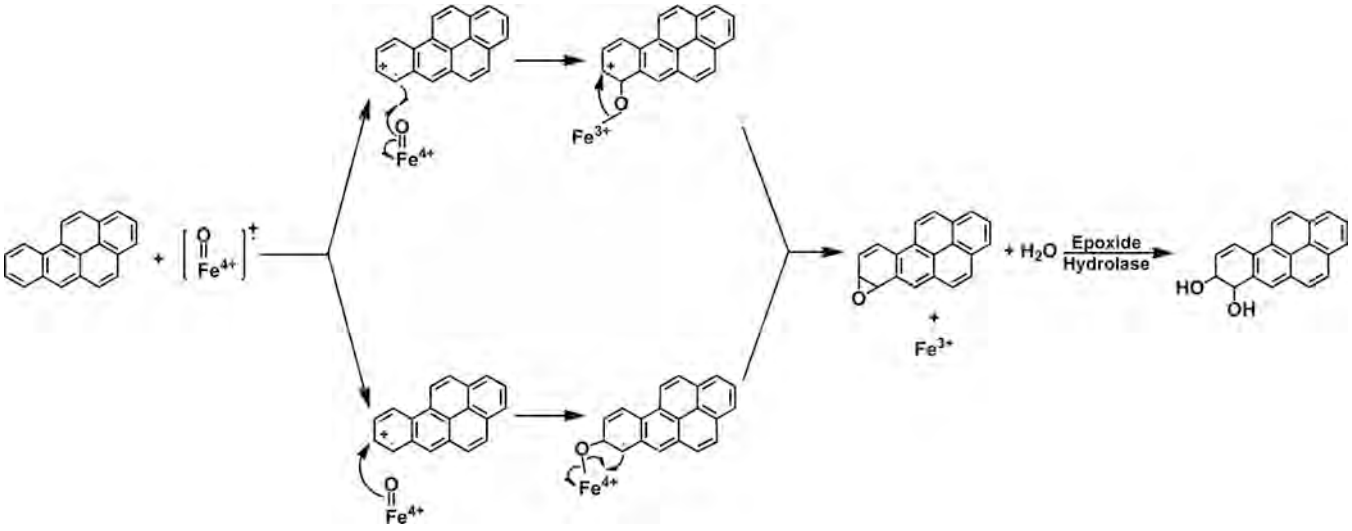

Figure 3.
Proposed mechanism for the formation of BP-7,8-dihydrodiol.

NIH-PA Author Manuscript
NIH-PA Author Manuscript
NIH-PA Author Manuscript

NIH-PA Author Manuscript
NIH-PA Author Manuscript
NIH-PA Author Manuscript

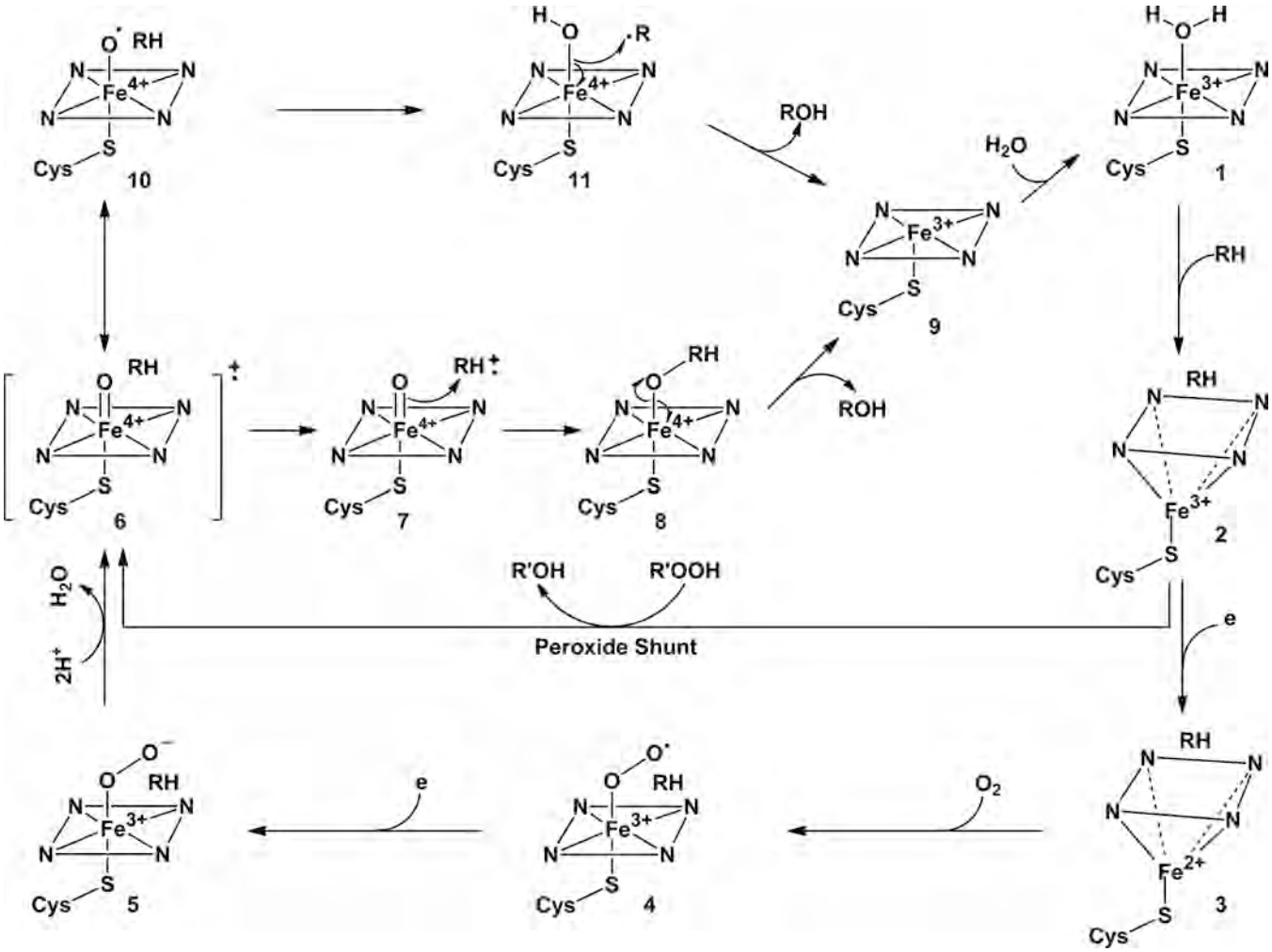

Figure 4.
Catalytic cycle of cytochrome P450 illustrating the postulated structures of the intermediates involved in activation of molecular oxygen and in oxygenation of substrates.

NIH-PA Author Manuscript

NIH-PA Author Manuscript

NIH-PA Author Manuscript

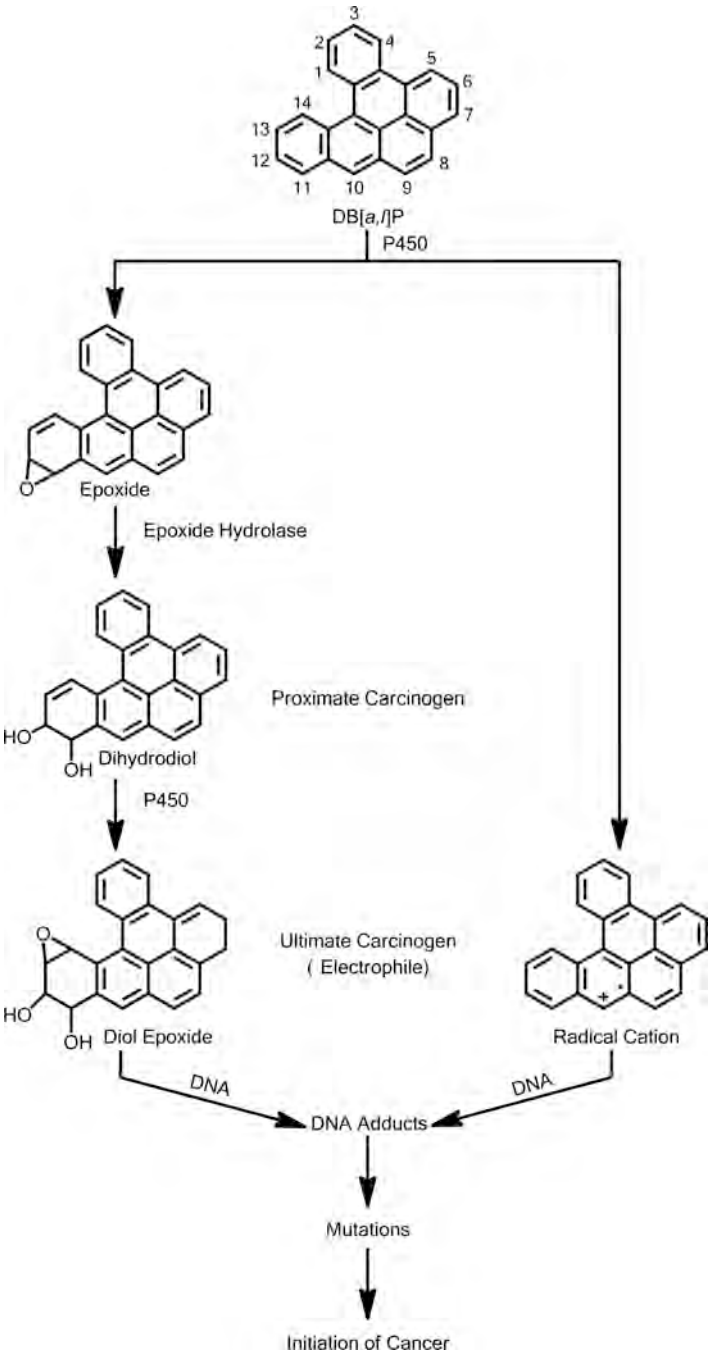

Figure 5.
Metabolic activation of DB[*a*,*l*]P by the diol epoxide and radical cation pathways.

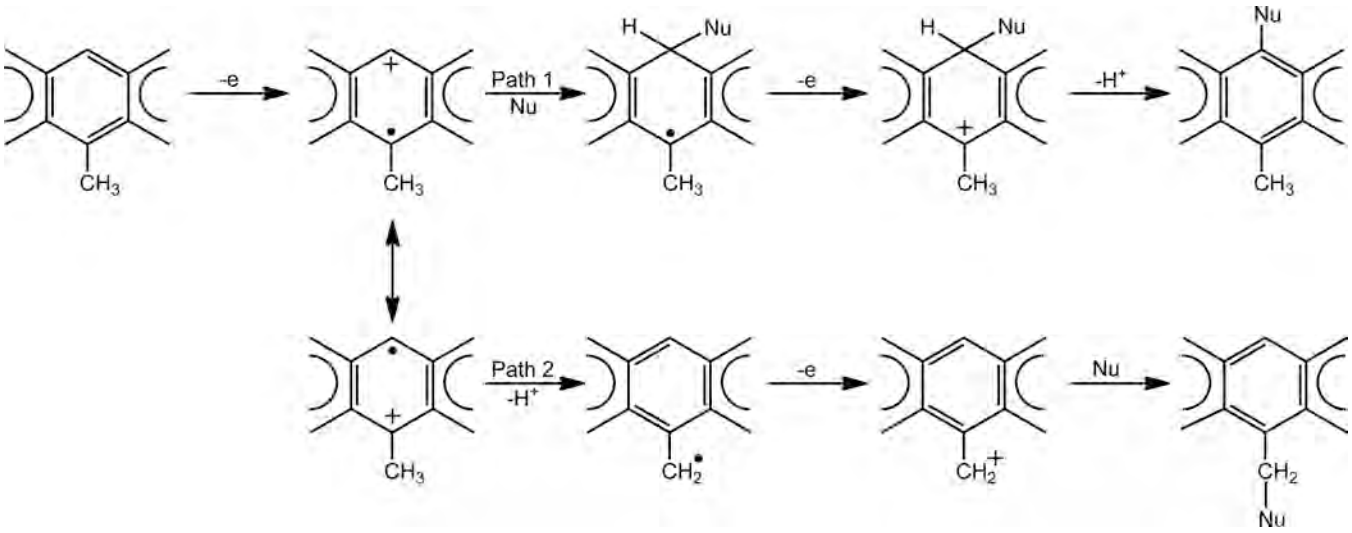

Figure 6.
Nucleophilic trapping of radical cations at unsubstituted and methyl-substituted positions in PAH.

NIH-PA Author Manuscript
NIH-PA Author Manuscript
NIH-PA Author Manuscript

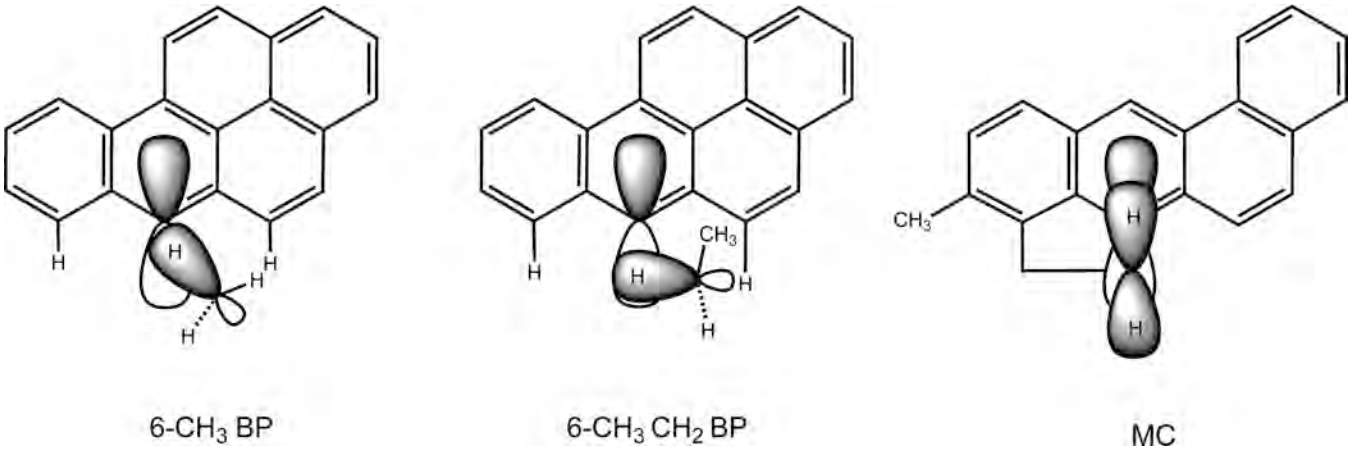

Figure 7.

Favorable partial alignment of the C-H bond of the methyl group with the π-system in 6-CH_3BP to cause deprotonation in 6-CH_3BP (*left*), compared to the less favorable alignment of the C-H bond of the benzylic methylene group in 6-C_2H_5BP that prevents deprotonation (*center*). Complete alignment of the C-H bond of the methylene group in MC that causes deprotonation.

NIH-PA Author Manuscript NIH-PA Author Manuscript NIH-PA Author Manuscript

Figure 8.
Structures of 5-methylchrysene, benz[*a*]anthracene and dibenz[*a*,*h*]anthracene.

NIH-PA Author Manuscript
NIH-PA Author Manuscript
NIH-PA Author Manuscript

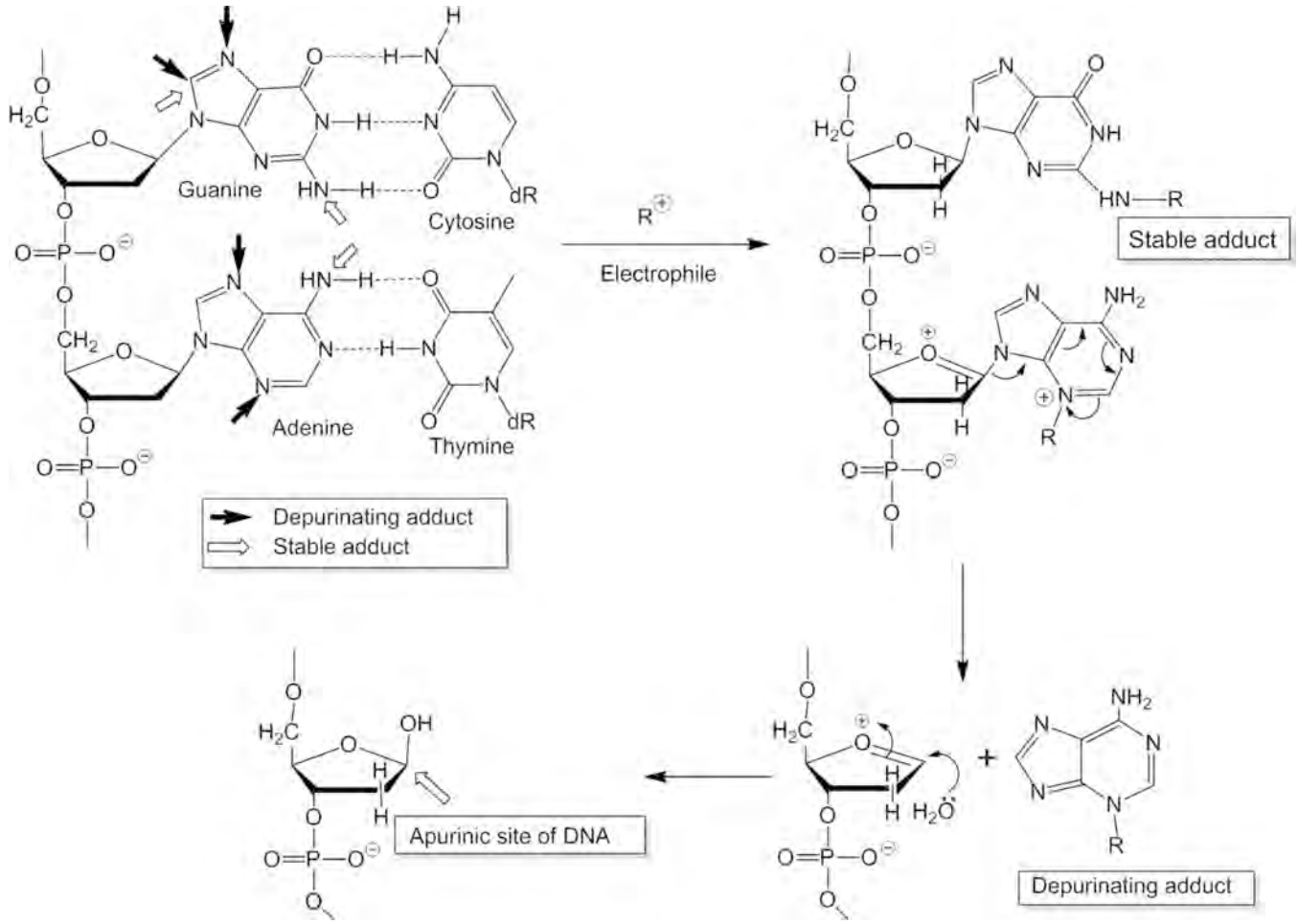

Figure 9.
Formation of stable and depurinating adducts with generation of apurinic sites in DNA.

NIH-PA Author Manuscript NIH-PA Author Manuscript NIH-PA Author Manuscript

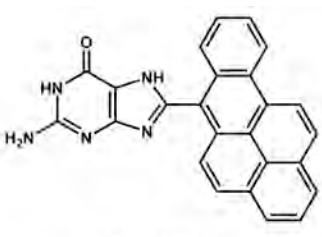

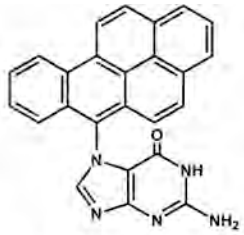

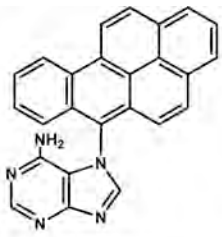

	BP-6-C8Gua	BP-6-N7Gua	BP-6-N7Ade
Microsomes			
BP	1.5 (14%)	1.2 (12%)	4.0 (38%)
Mouse skin			
BP	0.70 (34%)	0.20 (10%)	0.45 (22%)

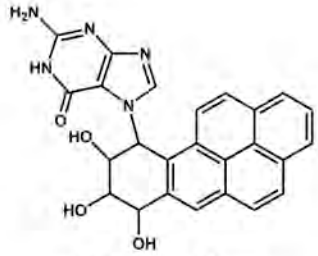

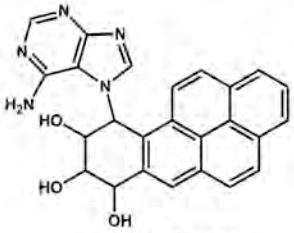

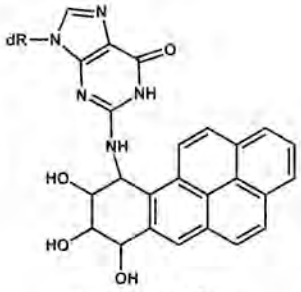

	BPDE-10-N7Gua	BPDE-10-N7Ade	BPDE-10-N^{2}dG stable adduct	Unidentified stable adducts
Microsomes				
BP	0.2 (2%)	0.2 (2%)	2.7 (26%)	0.6 (6%)
BP-7,8-dihydrodiol	1.8 (2%)	5.3 (5%)	90 (90%)	2.5 (3%)
(±)-*anti*-BPDE	1.9 (1%)	1.2 (1%)	191 (96%)	4.8 (2%)
Mouse skin				
BP	0.05 (2%)	0.07 (3%)	0.49 (23%)	0.13 (6%)
BP-7,8-dihydrodiol	0.37 (12%)	0.80 (25%)	1.9 (61%)	0.07 (2%)
(±)-*anti*-BPDE	0.07 (0.1%)	0.55 (1.2%)	46.6 (98.1%)	0.30 (0.6%)

Figure 10.

Depurinating and stable DNA adducts formed by rat liver microsomes or in mouse skin treated with BP, BP-7,8-dihydrodiol or *anti*-BPDE. The upper row is depurinating adducts formed by BP radical cations, whereas the lower row of depurinating and stable adducts is formed by the diol epoxide. The level of adducts is expressed as μmol/mol DNA-P (% of total adducts).

NIH-PA Author Manuscript NIH-PA Author Manuscript NIH-PA Author Manuscript

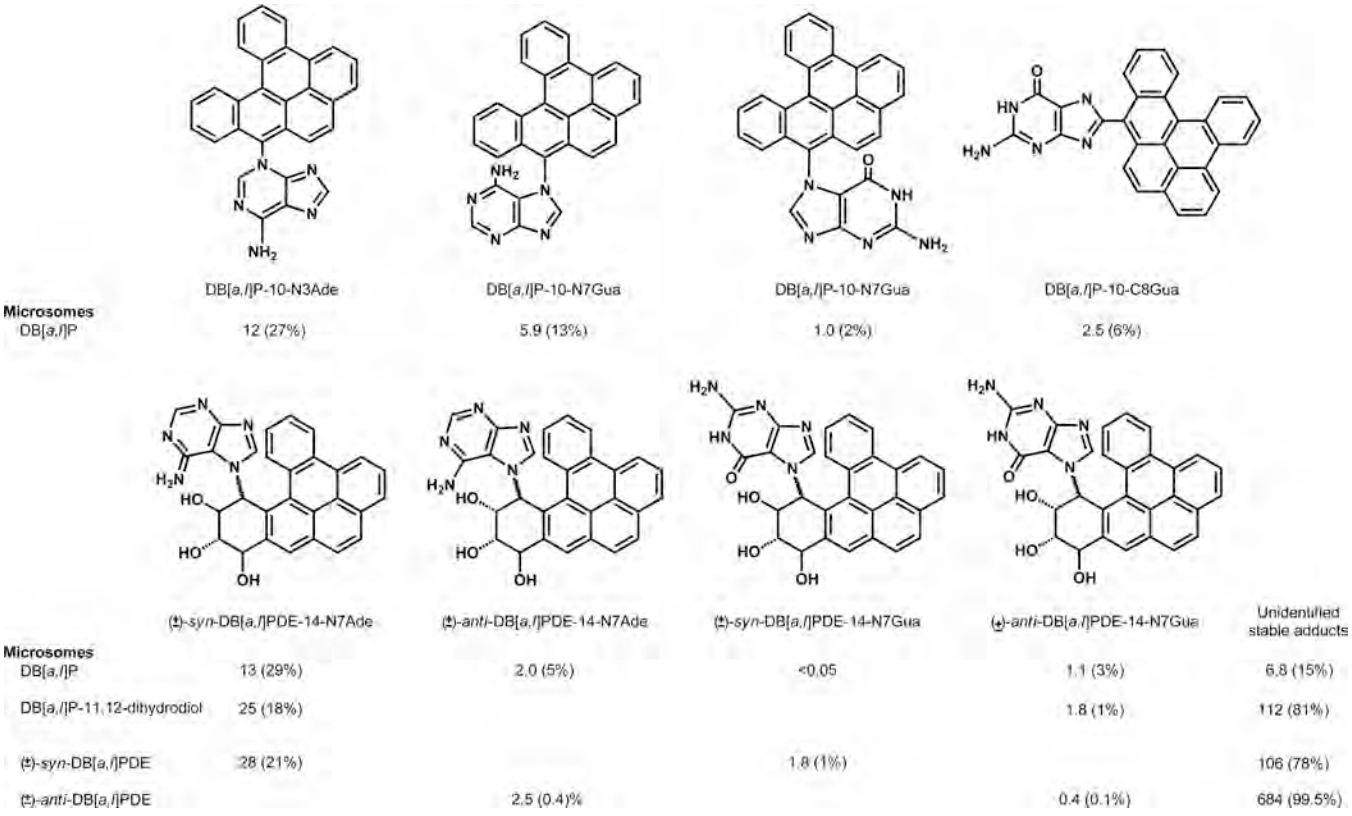

Figure 11.

Depurinating and stable adducts formed after activation of DB[*a,l*]P or DB[*a,l*]P-11,12-dihydrodiol by rat liver microsomes or reaction of *syn*-DB[*a,l*]PDE or *anti*-DB[*a,l*]PDE with DNA. The upper row is depurinating adducts form by DB[*a,l*]P radical cations, whereas the lower row of depurinating and stable adducts is formed by the diol epoxide. The level of adducts is expressed as μmol/mol DNA-P (% of total adducts).

NIH-PA Author Manuscript NIH-PA Author Manuscript NIH-PA Author Manuscript

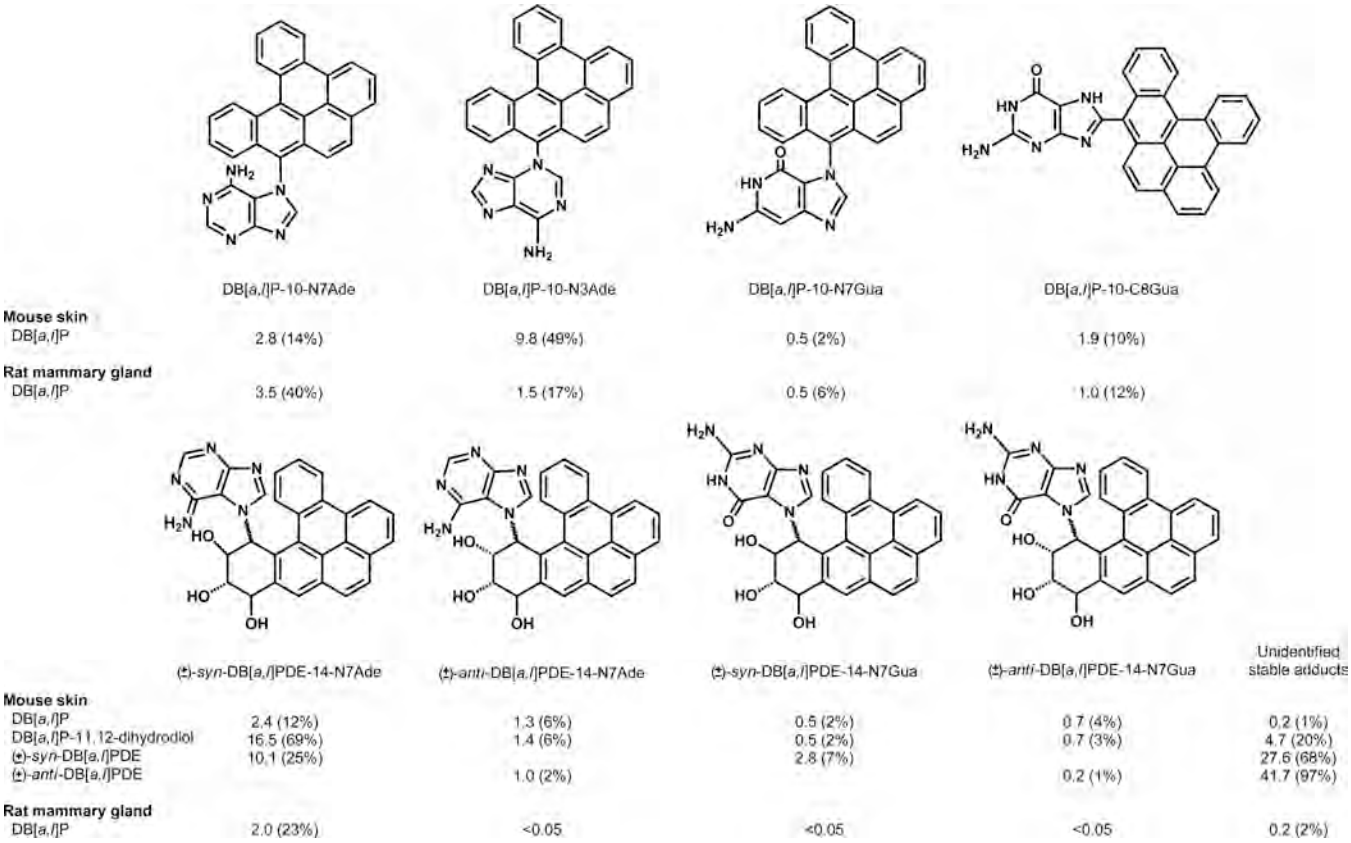

Mouse skin					
DB[*a,l*]P	2.8 (14%)	9.8 (49%)	0.5 (2%)	1.9 (10%)	
Rat mammary gland					
DB[*a,l*]P	3.5 (40%)	1.5 (17%)	0.5 (6%)	1.0 (12%)	
Mouse skin					
DB[*a,l*]P	2.4 (12%)	1.3 (6%)	0.5 (2%)	0.7 (4%)	0.2 (1%)
DB[*a,l*]P-11,12-dihydrodiol	16.5 (69%)	1.4 (6%)	0.5 (2%)	0.7 (3%)	4.7 (20%)
(±)-*syn*-DB[*a,l*]PDE	10.1 (25%)		2.8 (7%)		27.6 (68%)
(±)-*anti*-DB[*a,l*]PDE		1.0 (2%)		0.2 (1%)	41.7 (97%)
Rat mammary gland					
DB[*a,l*]P	2.0 (23%)	<0.05	<0.05	<0.05	0.2 (2%)

Figure 12.

Stable and depurinating adducts formed in mouse skin treated with DB[*a,l*]P, DB[*a,l*]P-11,12-dihydrodiol, *syn*-DB[*a,l*]PDE or *anti*-DB[*a,l*]PDE, and in rat mammary gland treated with DB[*a,l*]P. The upper row is depurinating adducts form by DB[*a,l*]P radical cations, whereas the lower row of depurinating and stable adducts is formed by the diol epoxide. The level of adducts is expressed as μmol/mol DNA-P (% of total adducts).

NIH-PA Author Manuscript NIH-PA Author Manuscript NIH-PA Author Manuscript

NIH-PA Author Manuscript

NIH-PA Author Manuscript

NIH-PA Author Manuscript

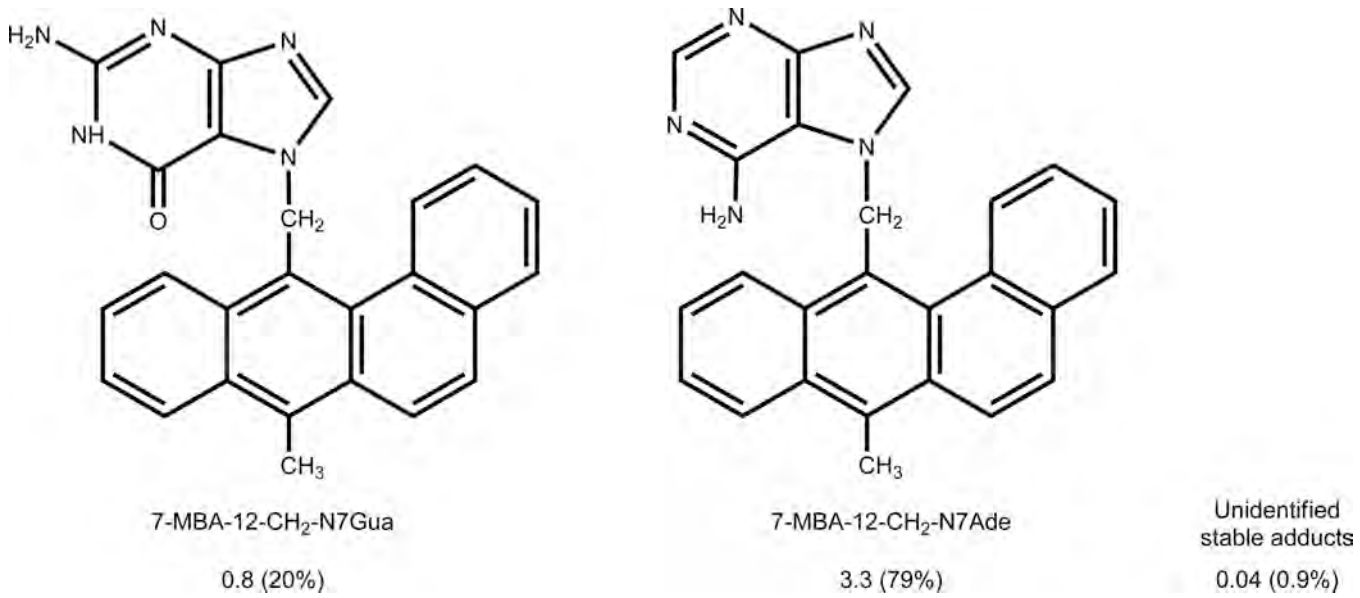

Figure 13.
Stable and depurinating adducts formed in mouse skin treated with DMBA. The level of adducts is expressed as μmol/mol DNA-P (% of total adducts).

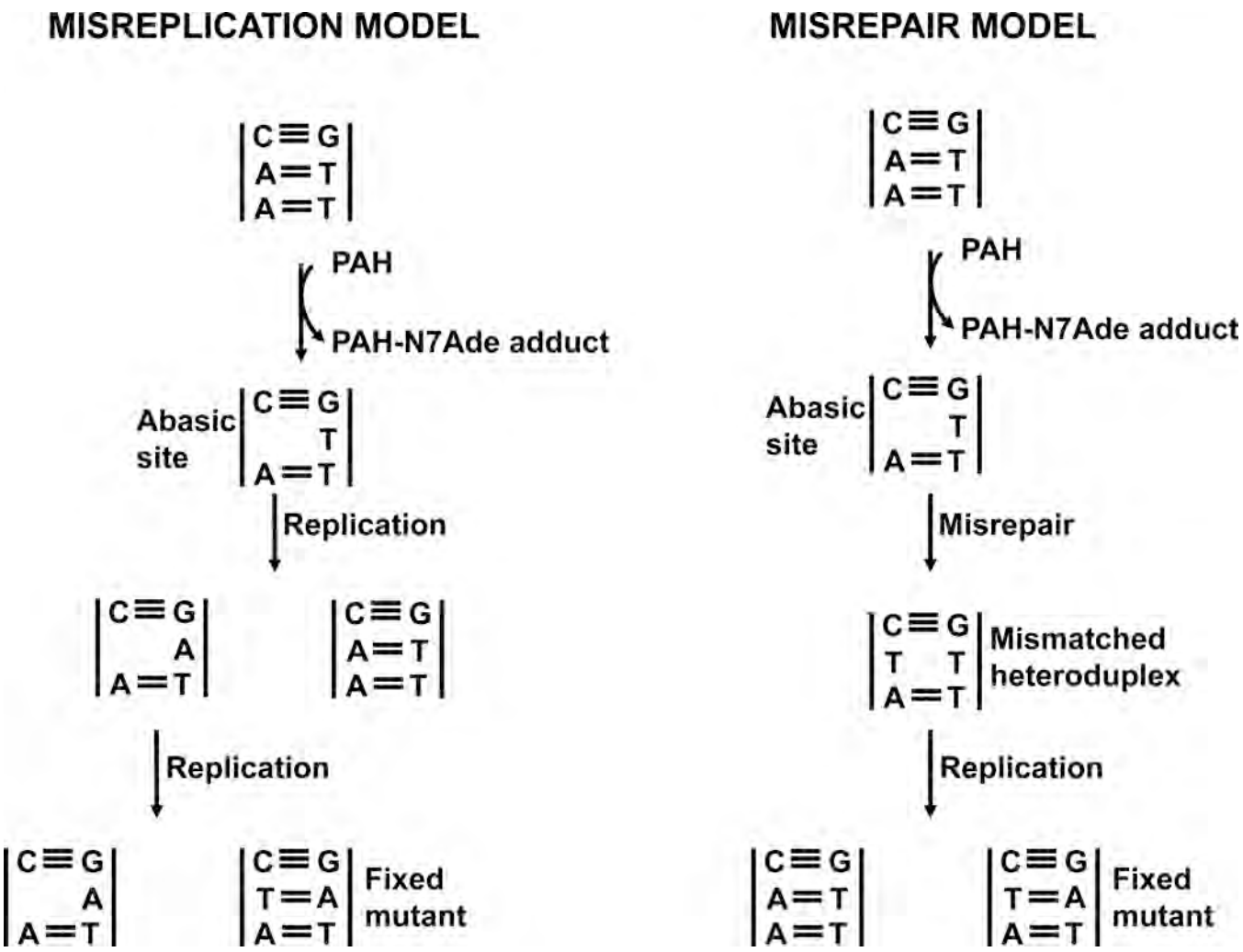

Figure 14.
Generation of a mutation by misreplication or misrepair of an apurinic site.

NIH-PA Author Manuscript
NIH-PA Author Manuscript
NIH-PA Author Manuscript

NIH-PA Author Manuscript

NIH-PA Author Manuscript

NIH-PA Author Manuscript

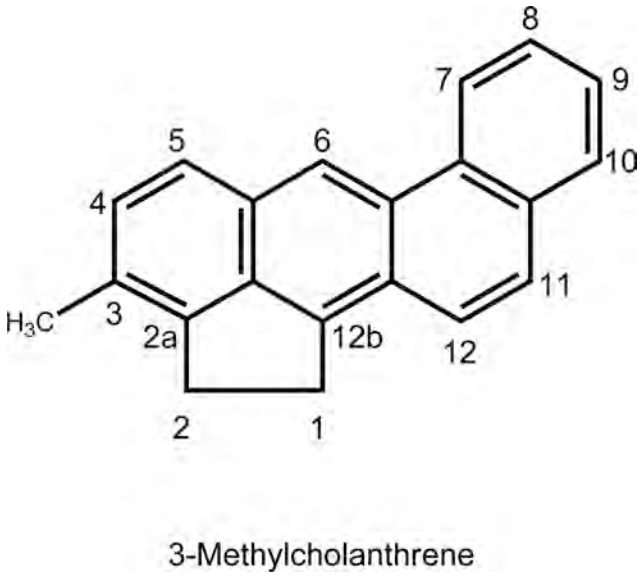

Figure 15.
Structure of 3-methylcholanthrene.

NIH-PA Author Manuscript
NIH-PA Author Manuscript
NIH-PA Author Manuscript

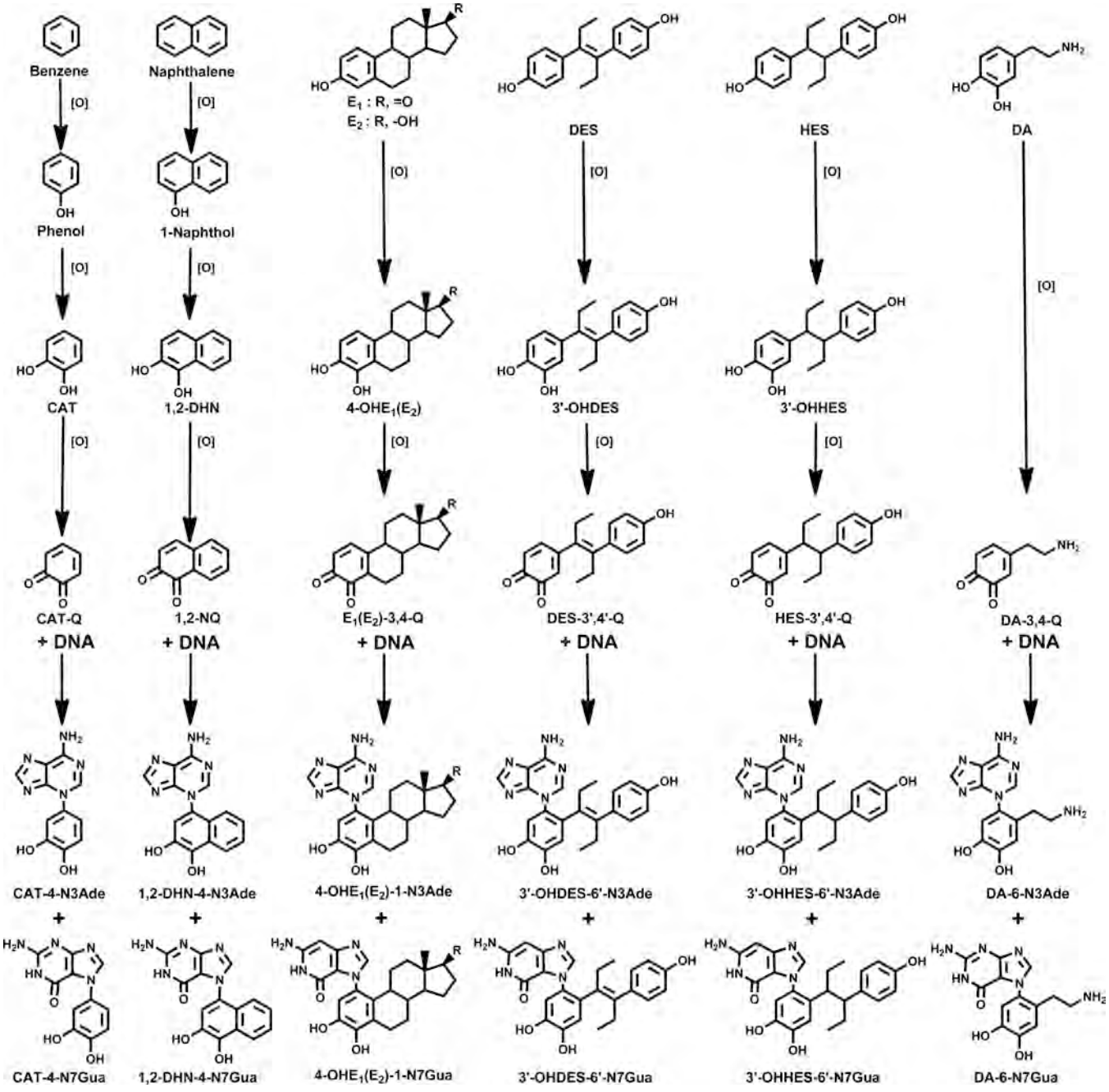

Figure 16.

Unified mechanism of metabolic activation and reaction with DNA to form depurinating DNA adducts for benzene, naphthalene, estrone (E_1)/estradiol (E_2), diethylstilbestrol (DES), hexestrol (HES) and dopamine (DA).

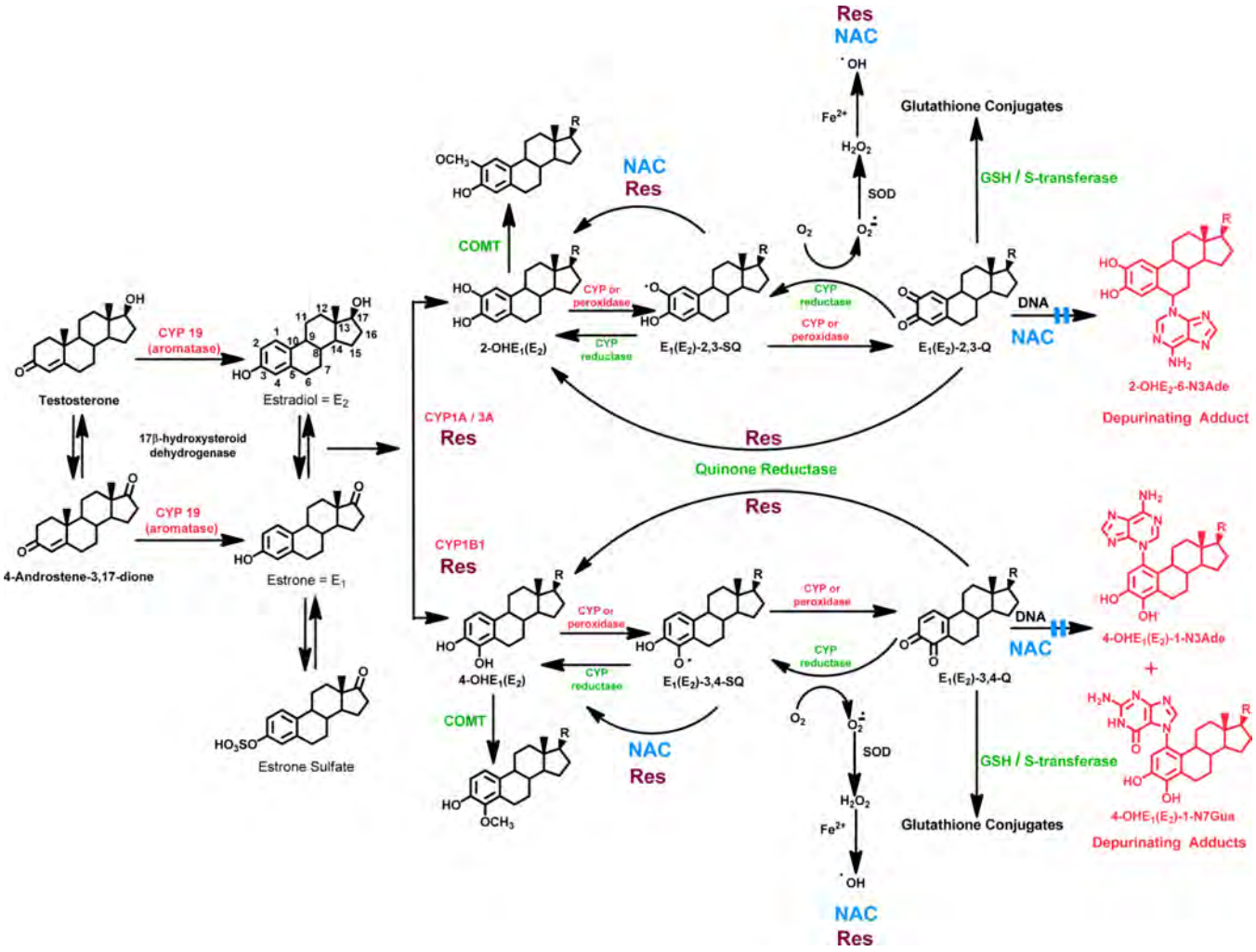

Figure 17.

Formation, metabolism and DNA adducts of estrogens. Activating enzymes and depurinating DNA adducts are in red and protective enzymes are in green. *N*-Acetylcysteine (NAC, shown in blue) and resveratrol (Res, shown in burgundy) indicate various steps where NAC and Res could ameliorate unbalanced estrogen metabolism and reduce formation of depurinating estrogen-DNA adducts.

NIH-PA Author Manuscript NIH-PA Author Manuscript NIH-PA Author Manuscript

NIH-PA Author Manuscript

NIH-PA Author Manuscript

NIH-PA Author Manuscript

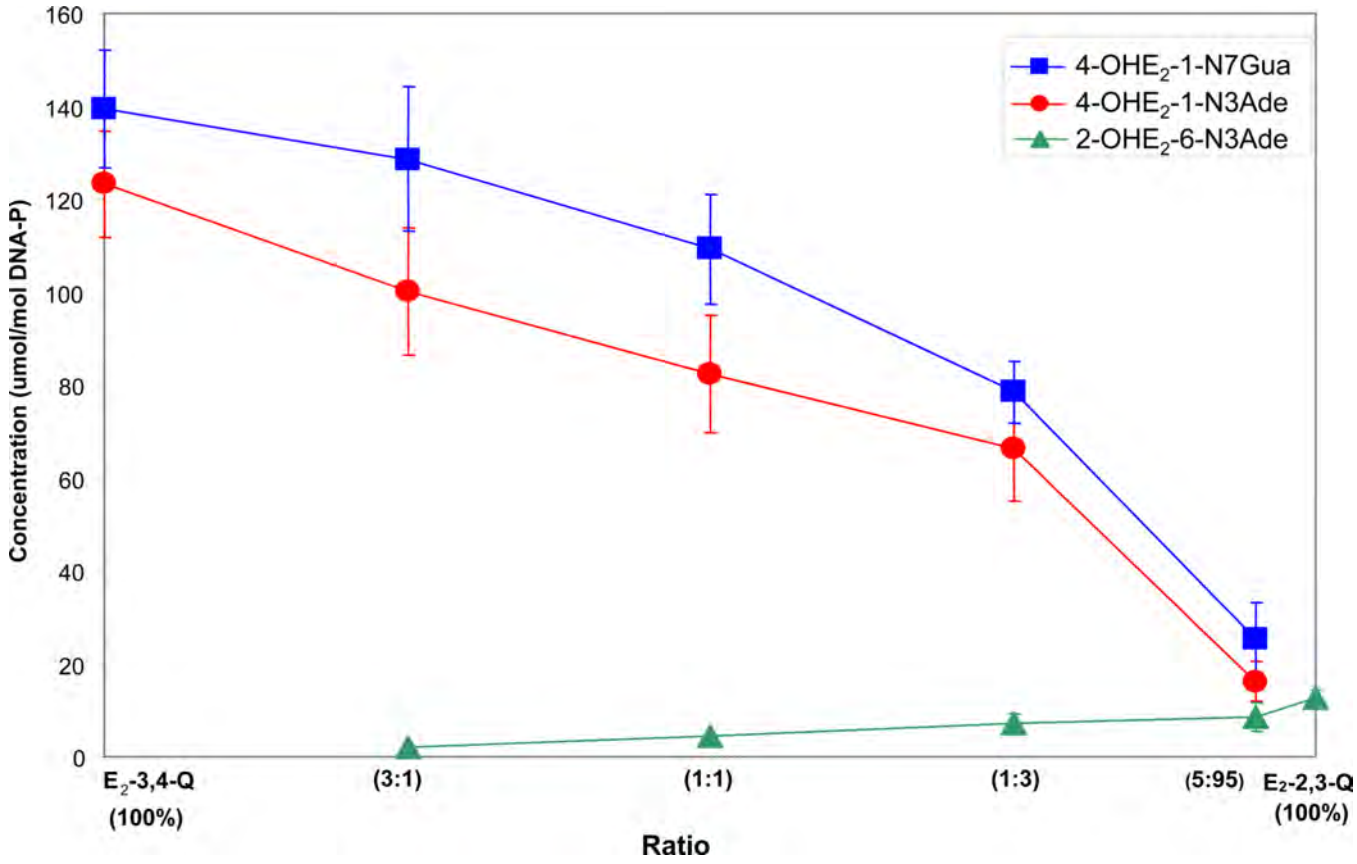

Figure 18.

Depurinating adducts formed after 10 h (to allow complete depurination of 4-OHE_2-1-N7Gua) by mixtures of E_2-3,4-Q and E_2-2,3-Q reacted with DNA at different ratios. The levels of stable adducts formed in the mixtures ranged from 0.1% to 1% of the total adducts (Zahid et al., 2006).

NIH-PA Author Manuscript
NIH-PA Author Manuscript
NIH-PA Author Manuscript

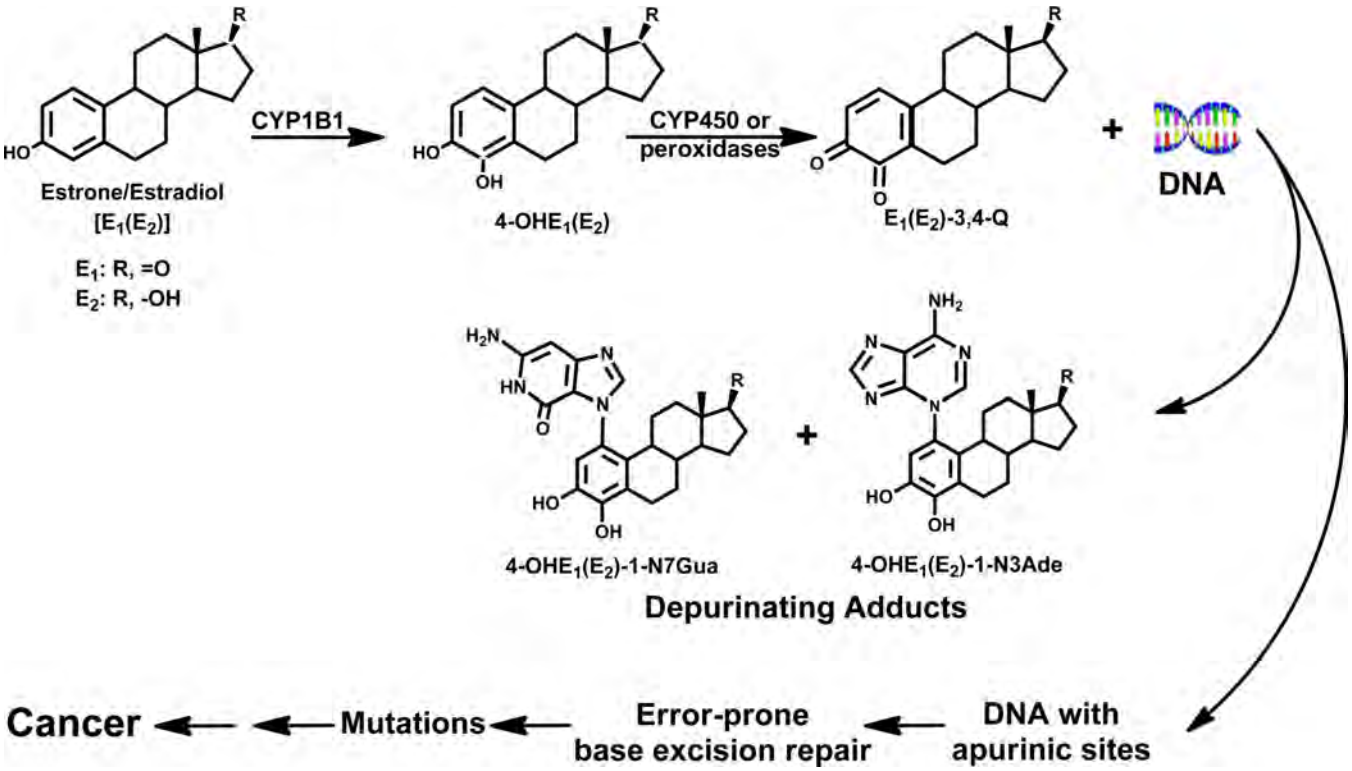

Figure 19.
Predominant metabolic pathway in cancer initiation by estrogens.

NIH-PA Author Manuscript

NIH-PA Author Manuscript

NIH-PA Author Manuscript

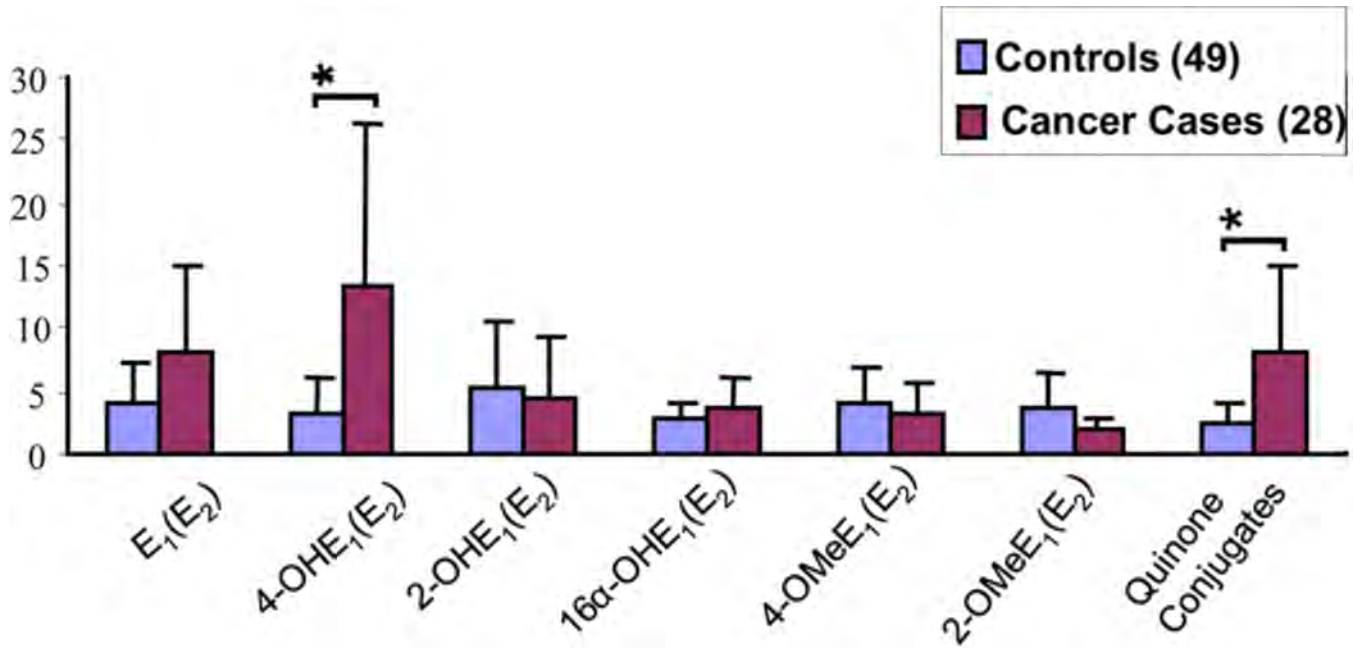

Figure 20.

Relative imbalance of estrogen metabolism in non-tumor breast tissue of women with breast cancer *vs* controls. The level of 4-$OHE_1(E_2)$ was significantly higher in cases compared to controls ($p < 0.01$). Quinone conjugates were 4-$OHE_1(E_2)$-2-NAcCys, 4-$OHE_1(E_2)$-2-Cys, 2-$OHE_1(E_2)$-(1+4)-NAcCys, and 2-$OHE_1(E_2)$-(1+4)-Cys. The levels of quinone conjugates were significantly higher in cases than in controls ($p < 0.003$). *Statistically significant differences were determined using the Wilcoxon rank sum test (Rogan et al., 2003).

NIH-PA Author Manuscript

NIH-PA Author Manuscript

NIH-PA Author Manuscript

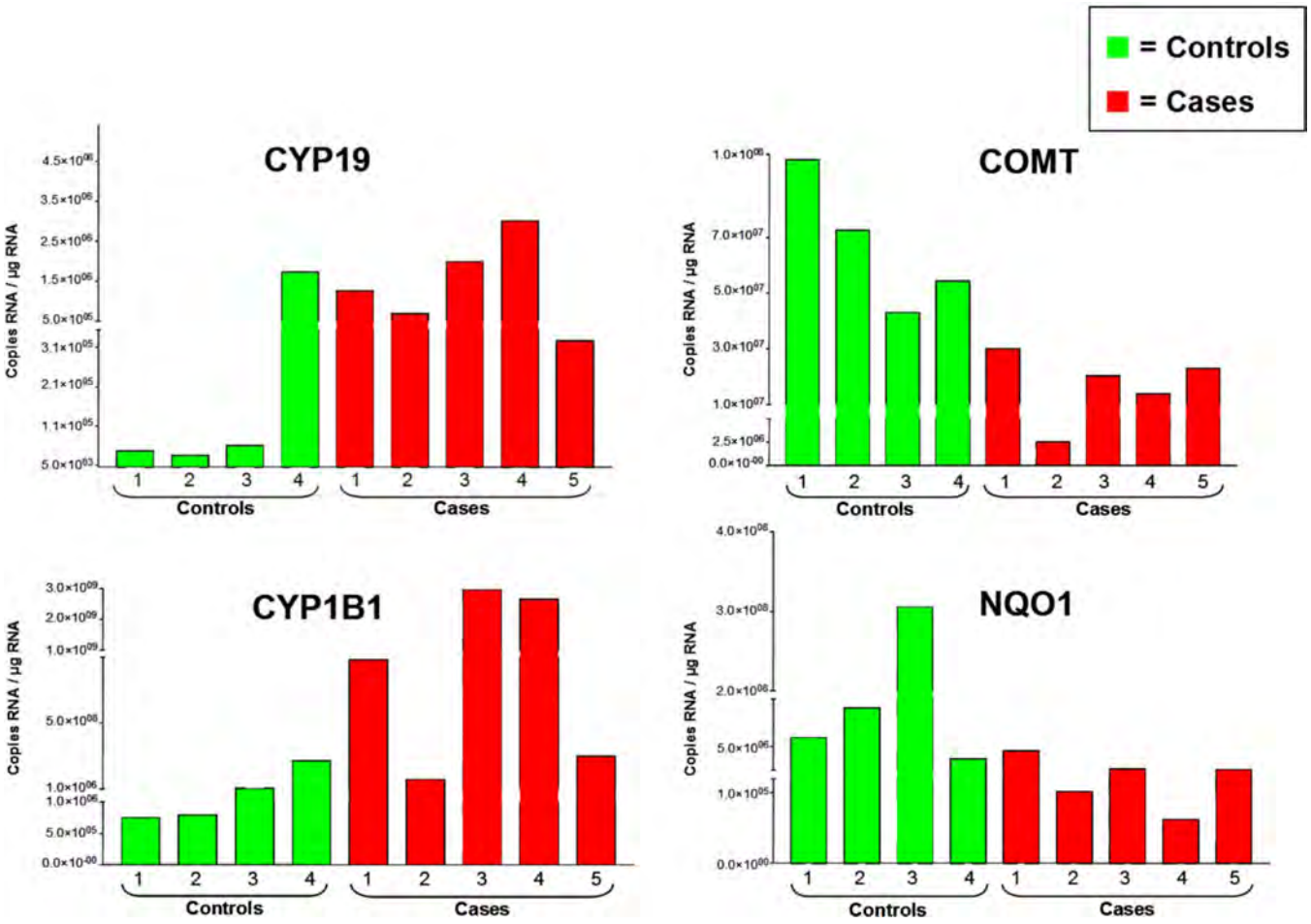

Figure 21.

Expression of estrogen activating (CYP19 and CYP1B1) and protective (COMT and NQO1) enzymes in non-tumor breast tissue from women with breast cancer and control women (undergoing reduction mammoplasty). Steady-state RNA levels of the genes were quantified by TaqMan real-time RT-PCR (Singh et al., 2005).

NIH-PA Author Manuscript
NIH-PA Author Manuscript
NIH-PA Author Manuscript

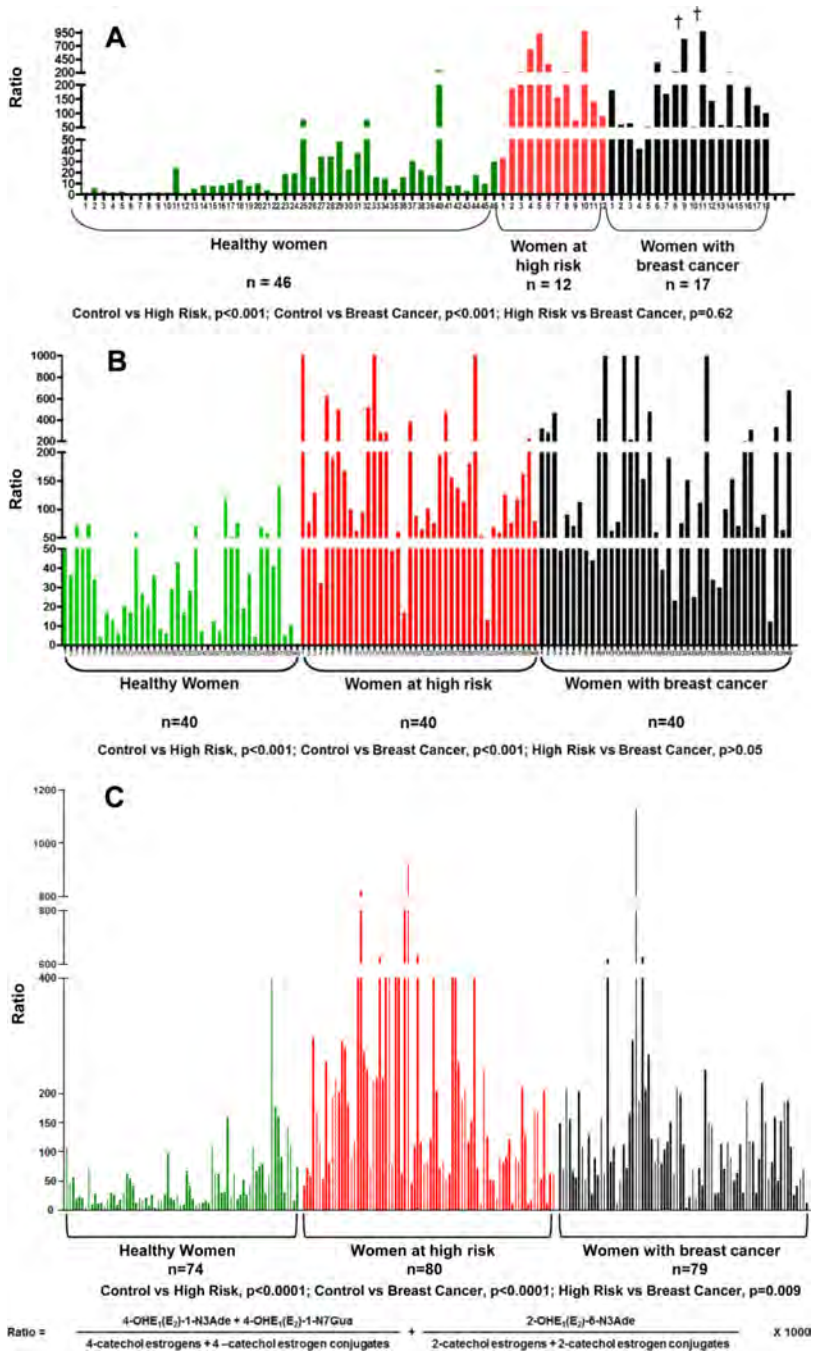

Figure 22.

Ratios of depurinating estrogen-DNA adducts to estrogen metabolites and conjugates in (A) urine of healthy women, high-risk women and women with breast cancer - first study (Gaikwad, et al., 2008); (B) urine of healthy women, high-risk women and women with breast cancer - second study (Gaikwad et al., 2009b) and (C) serum of healthy women, high-risk women and women with breast cancer (Pruthi et al., 2012).

NIH-PA Author Manuscript

NIH-PA Author Manuscript

NIH-PA Author Manuscript

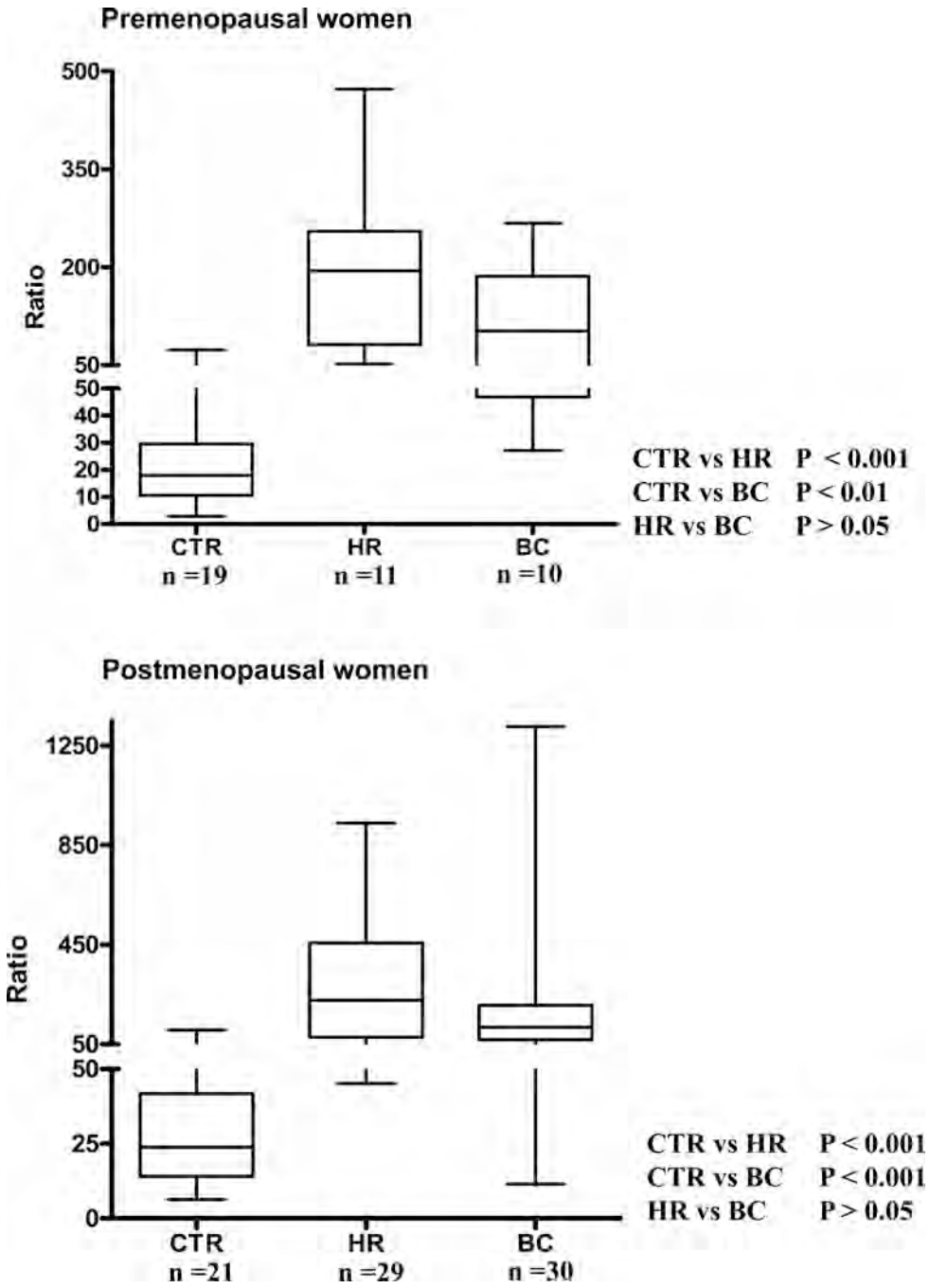

Figure 23.
Comparison of serum ratios in premenopausal women and postmenopausal women (Pruthi et al., 2012).

NIH-PA Author Manuscript

NIH-PA Author Manuscript

NIH-PA Author Manuscript

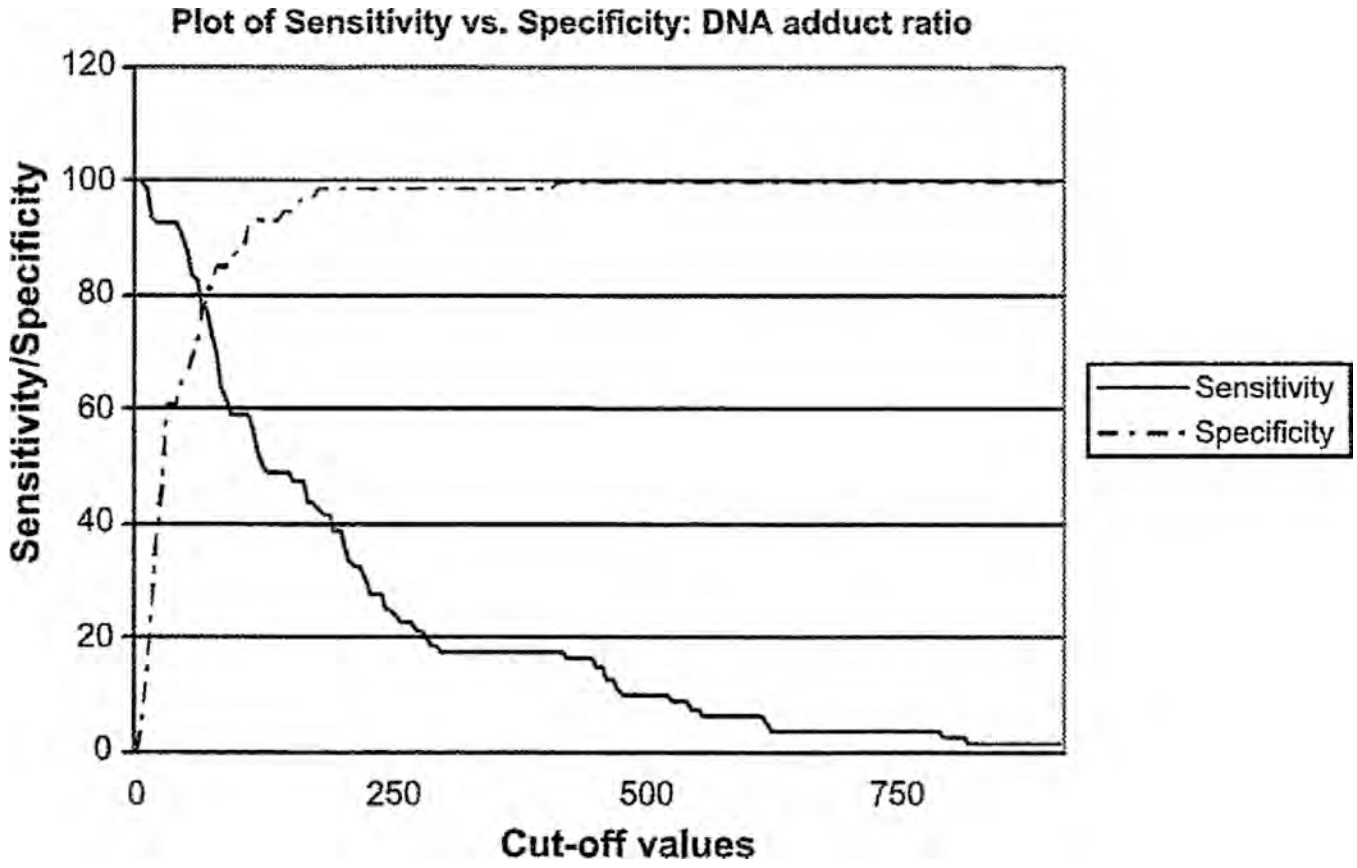

Figure 24.

Plot of sensitivity versus specificity: serum DNA adduct ratio. Sensitivity and specificity plotted against cut-off values between women with low risk of breast cancer (Gail model score ≤ 1.66%) and women with high risk of breast cancer (Gail model score ≥ 1.66%). Note: The two curves cross at a cut-off value of 77 (Pruthi et al., 2012).

NIH-PA Author Manuscript

NIH-PA Author Manuscript

NIH-PA Author Manuscript

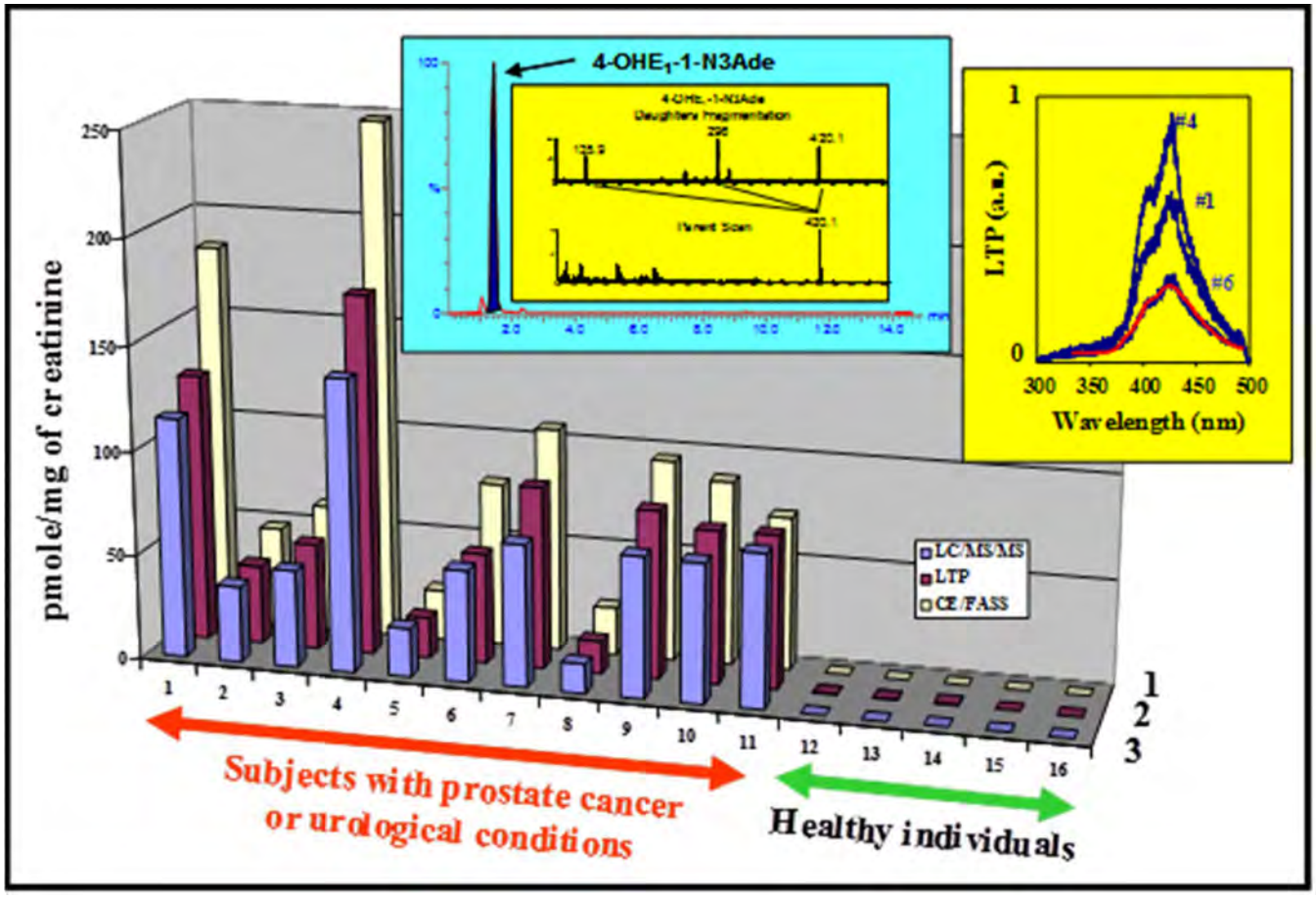

Figure 25.

Identification of the 4-OHE$_1$-1-N3Ade adduct in urine samples from men with prostate cancer or urological conditions and healthy men as controls. Right inset: The LTP spectra labeled 1, 4, and 6 refer to individual samples 1, 4, and 6, respectively; the red spectrum is that of the standard. Left inset: LC/MS/MS identification of the parent compound at *m/z* 420.1, and *m/z* 135.9 and 296 are the fragmentation daughters selected for unequivocal identification of the adduct. LC/MS/MS = HPLC/tandem mass spectrometry, LTP = low temperature phosphorescence, and CE/FASS = capillary electrophoresis with field-amplified sample stacking (Markushin et al., 2006).

NIH-PA Author Manuscript

NIH-PA Author Manuscript

NIH-PA Author Manuscript

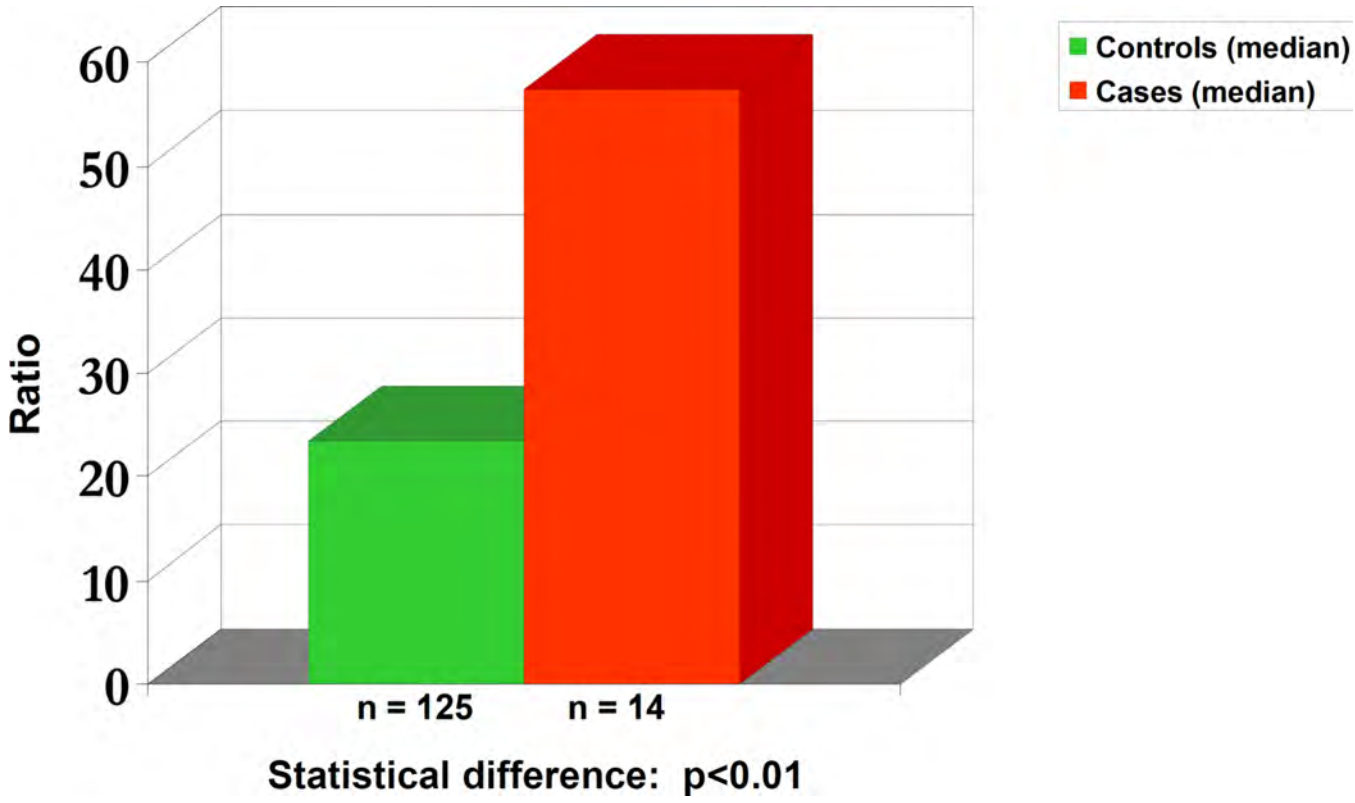

Figure 26.
Average levels of the ratio of estrogen-DNA adducts to estrogen metabolites and conjugates in urine samples from men with and without prostate cancer, $p < 0.001$ (Yang et al., 2009).

NIH-PA Author Manuscript

NIH-PA Author Manuscript

NIH-PA Author Manuscript

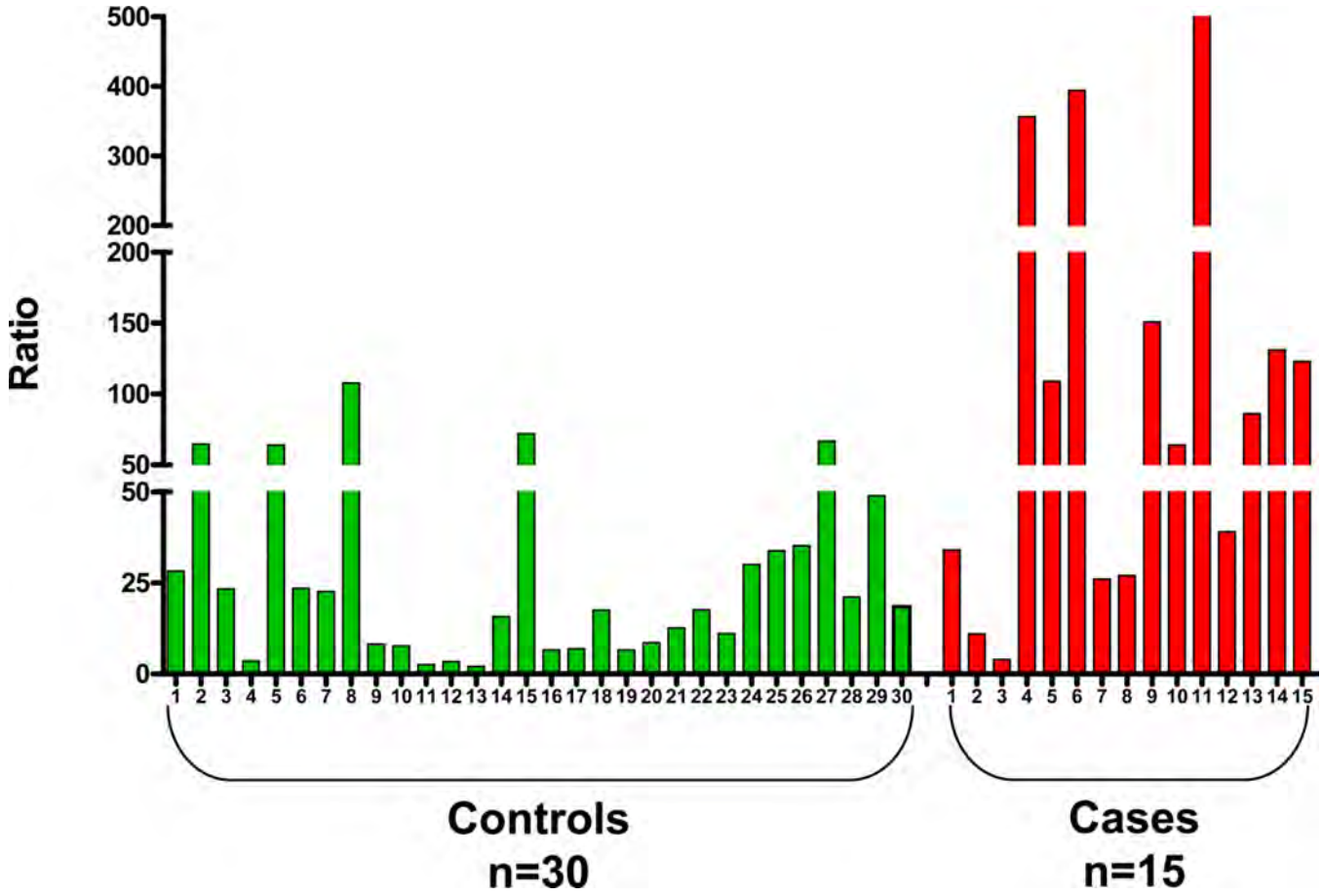

Figure 27.
Individual ratios of depurinating estrogen-DNA adducts to estrogen metabolites and conjugates in urine of healthy control men and men with non-Hodgkin lymphoma (NHL). Healthy controls vs NHL, $p < 0.007$ (Gaikwad et al., 2009a).

NIH-PA Author Manuscript

NIH-PA Author Manuscript

NIH-PA Author Manuscript

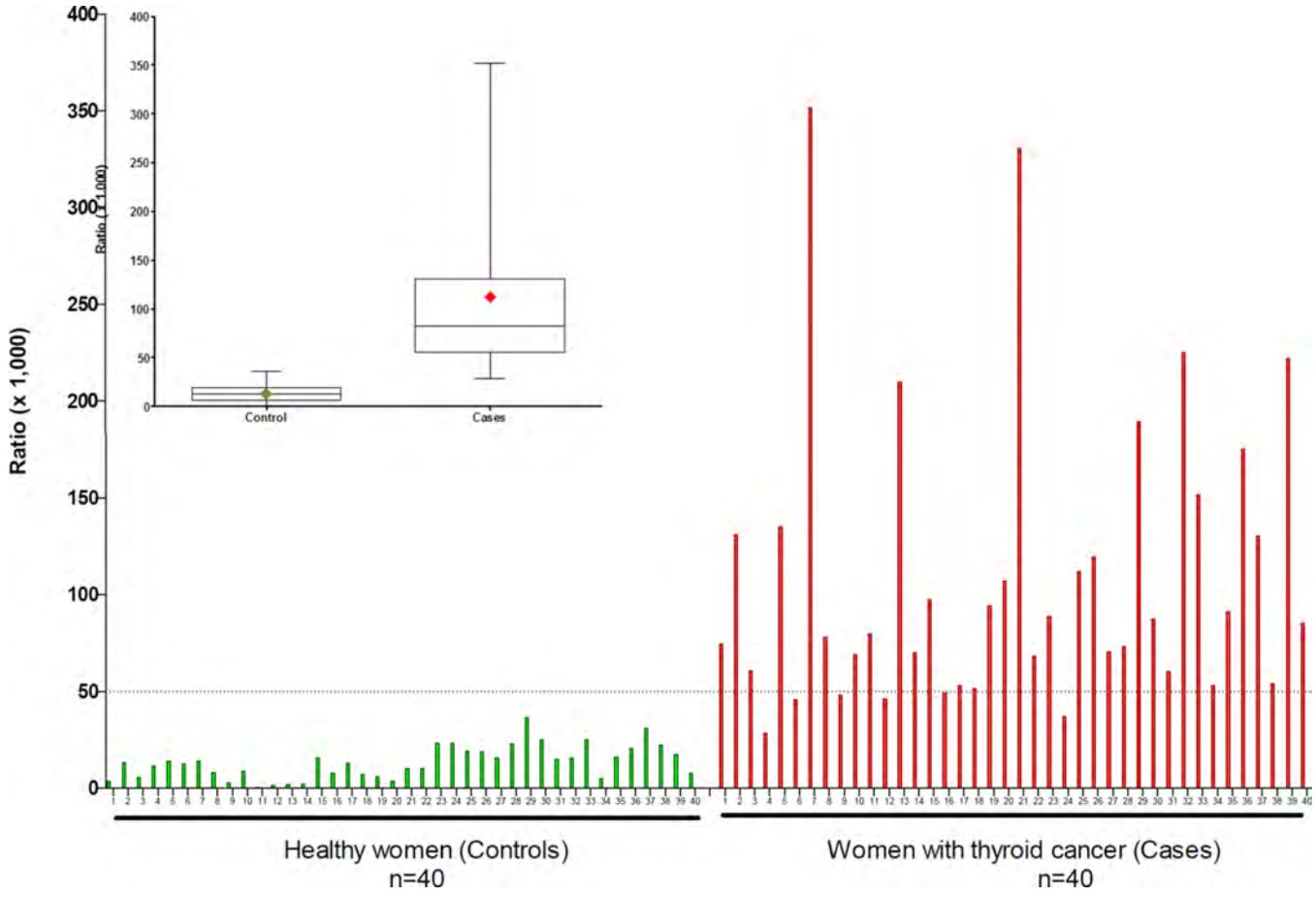

Figure 28.

Ratio of urinary depurinating estrogen-DNA adducts to estrogen metabolites and conjugates for women diagnosed with thyroid cancer (cases) or not diagnosed with cancer (controls). The dotted line representing a ratio of 30 is the cross-over point for sensitivity and specificity of the ratio. Inset: Ratios presented as median values and ranges (min to max). The diamonds represent the mean values ($p < 0.0001$) (Zahid et al., 2013b).

NIH-PA Author Manuscript

NIH-PA Author Manuscript

NIH-PA Author Manuscript

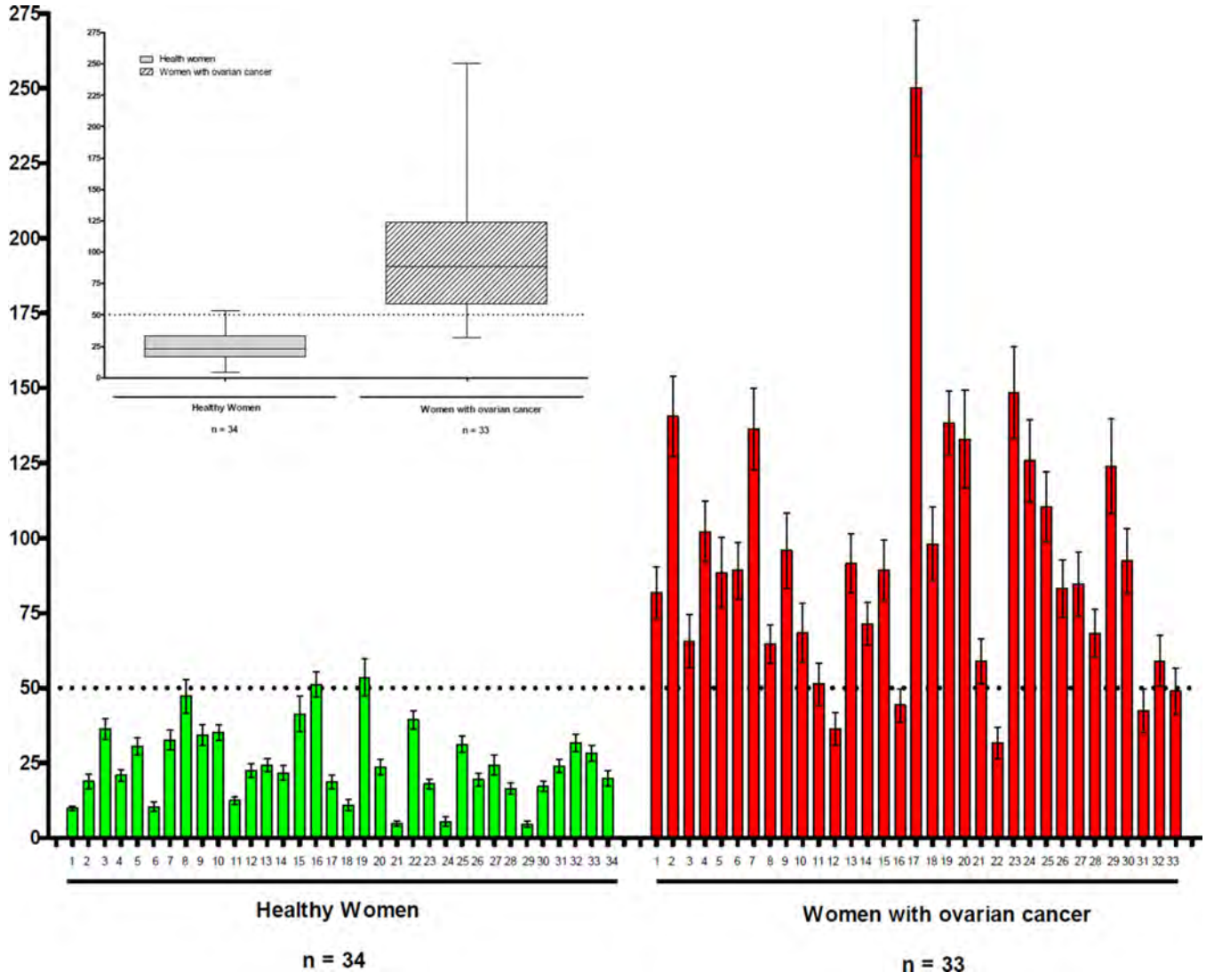

Figure 29.

Ratios of depurinating estrogen-DNA adducts to estrogen metabolites and conjugates in urine samples from healthy control women and women diagnosed with ovarian cancer. The ratios were significantly higher in cases ($p < 0.0001$) (Zahid et al., 2013a).

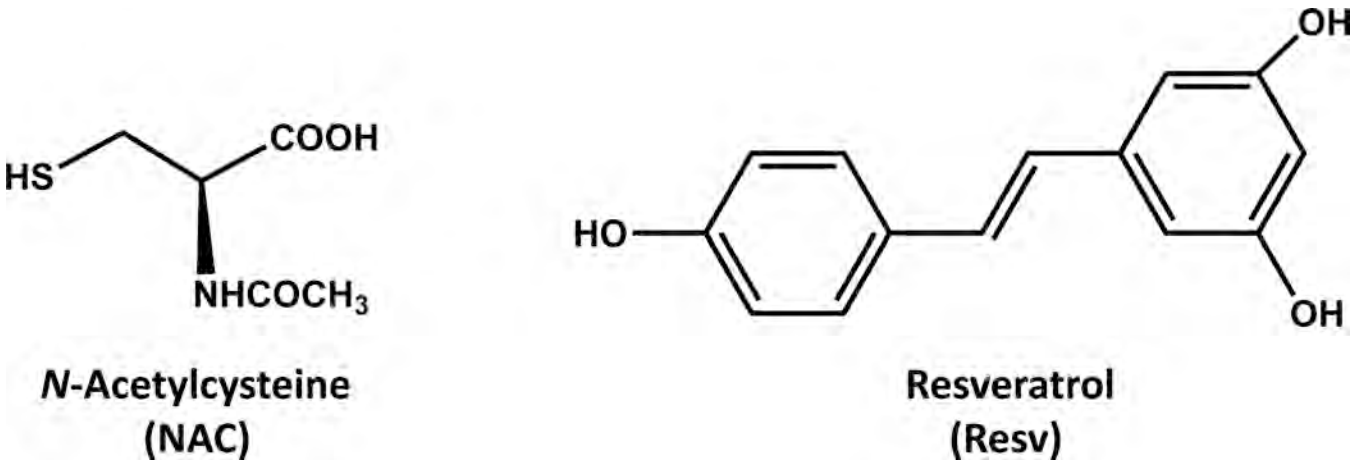

Figure 30.
Structures of *N*-acetylcysteine and resveratrol.

NIH-PA Author Manuscript
NIH-PA Author Manuscript
NIH-PA Author Manuscript

NIH-PA Author Manuscript

NIH-PA Author Manuscript

NIH-PA Author Manuscript

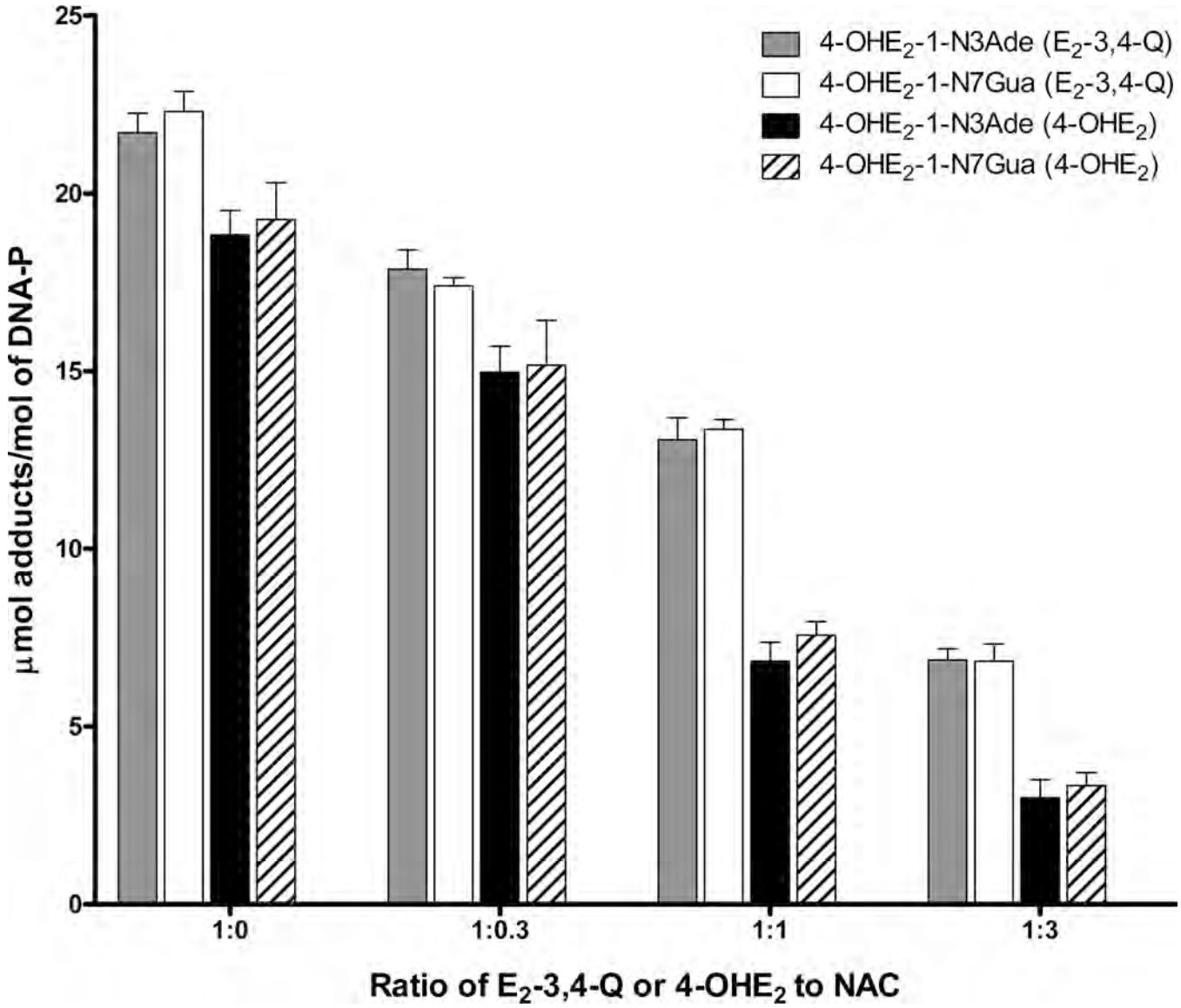

Figure 31.
Effect of NAC on the formation of depurinating adducts obtained by reaction of 87 μM E_2-3,4-Q or LP-activated 4-OHE_2 with DNA. In the presence of NAC, the levels of adducts were lower, with $p < 0.002–0.04$ (Zahid et al., 2007).

NIH-PA Author Manuscript
NIH-PA Author Manuscript
NIH-PA Author Manuscript

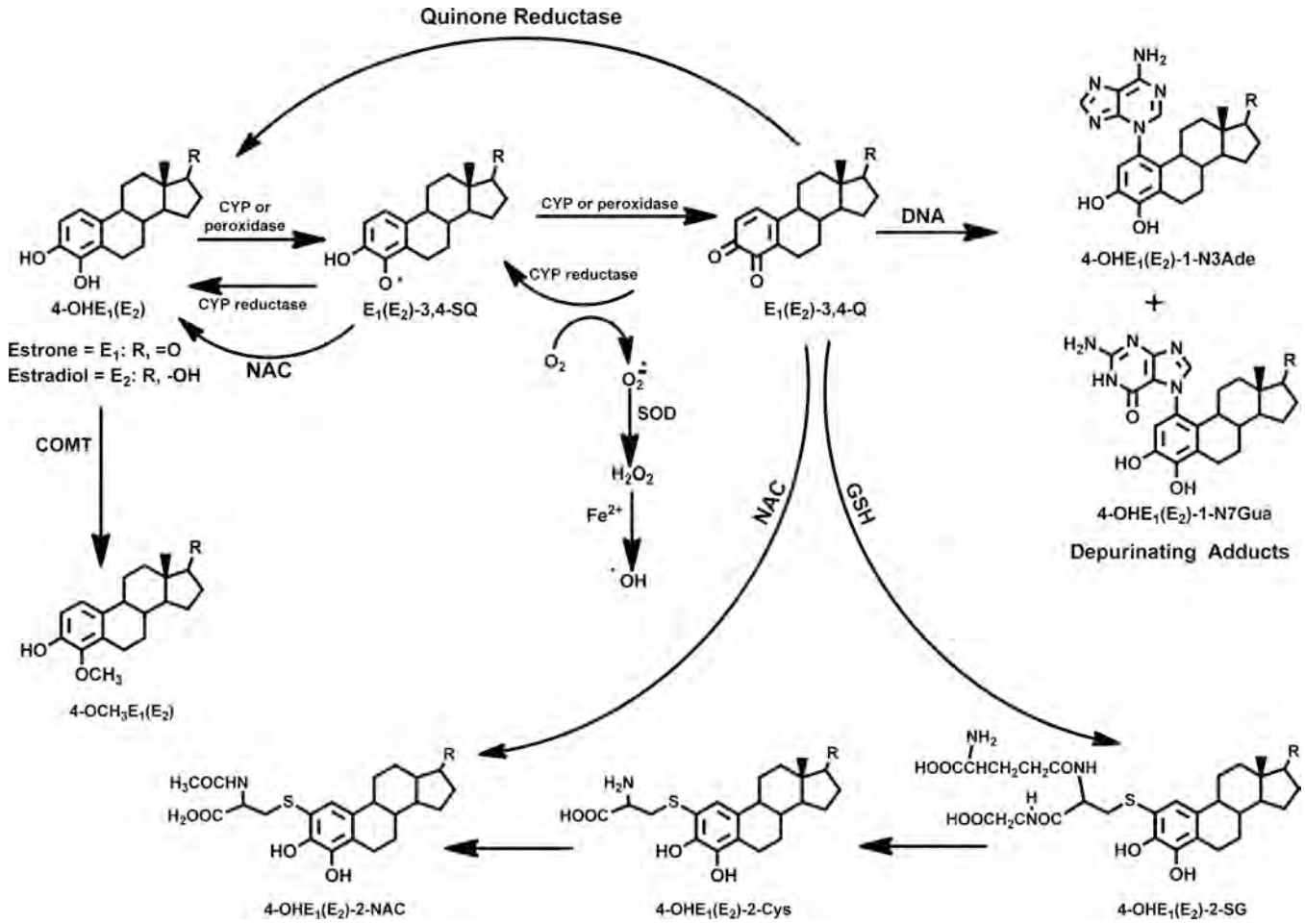

Figure 32.
Metabolic pathway for 4-$OHE_1(E_2)$ in the absence or presence of NAC.

NIH-PA Author Manuscript

NIH-PA Author Manuscript

NIH-PA Author Manuscript

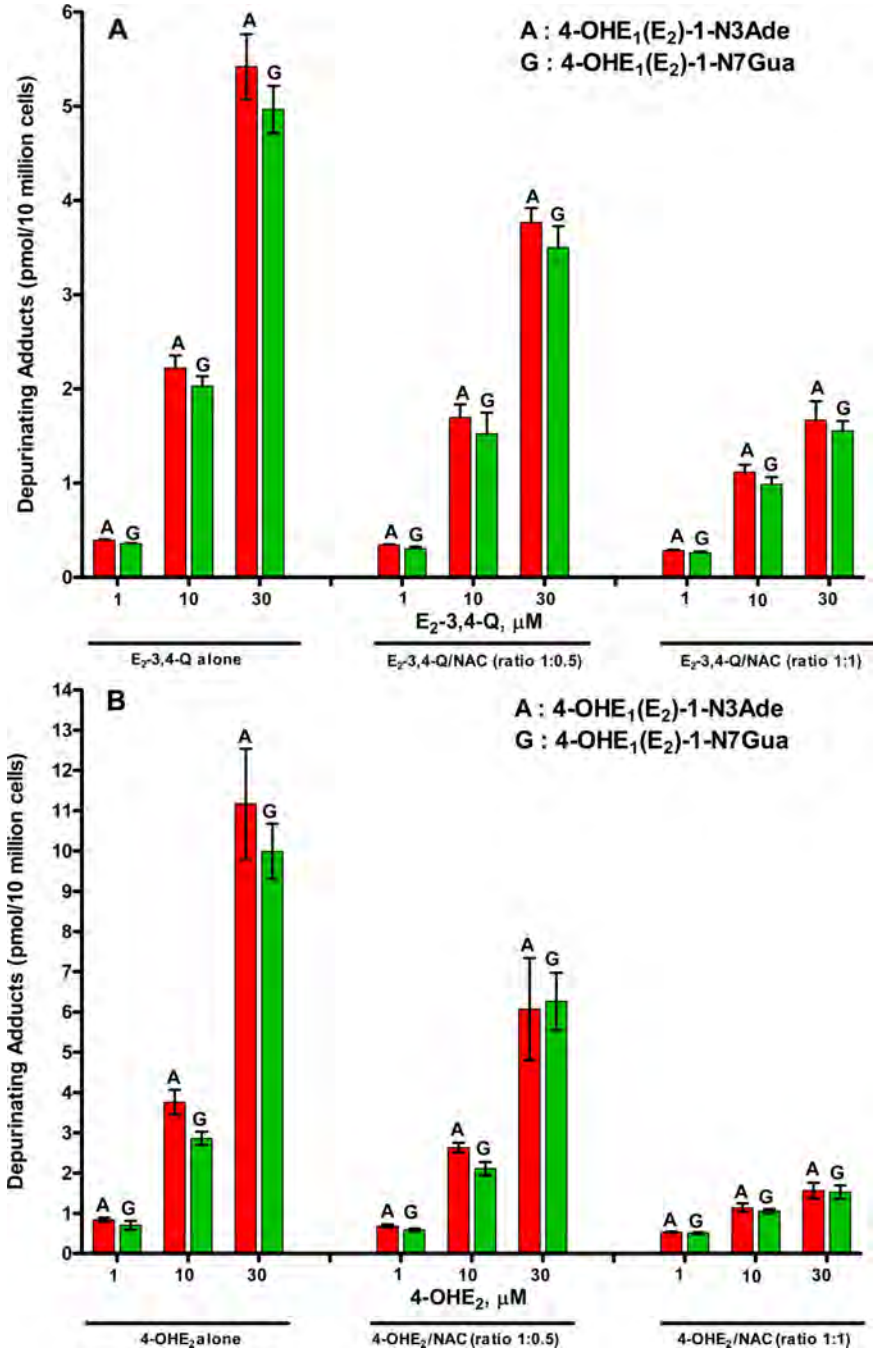

Figure 33.

Effects of NAC on the formation of (A) estrogen-DNA adducts in MCF-10F cells treated with E_2-3,4-Q and (B) estrogen-DNA adducts in MCF-10F cells treated with 4-OHE_2(Zahid et al., 2010a).

NIH-PA Author Manuscript

NIH-PA Author Manuscript

NIH-PA Author Manuscript

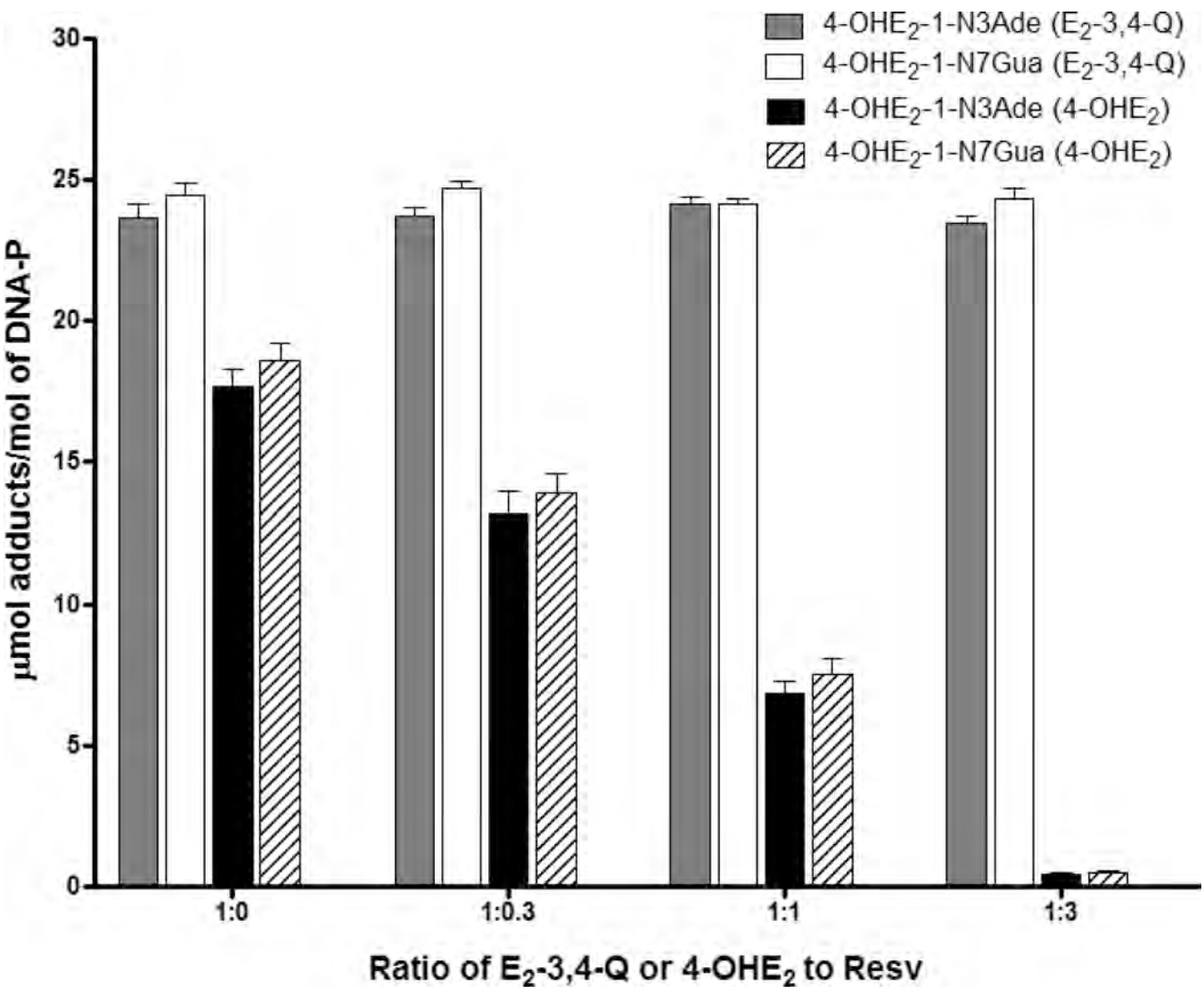

Figure 34.

Effect of Resv on the formation of depurinating adducts obtained by reaction of 87 μM E_2-3,4-Q or LP-activated 4-OHE_2 with DNA. In the presence of Resv, the levels of both adducts formed from 4-OHE_2 were reduced with $p < 0.0003–0.04$ (Zahid et al., 2007).

NIH-PA Author Manuscript

NIH-PA Author Manuscript

NIH-PA Author Manuscript

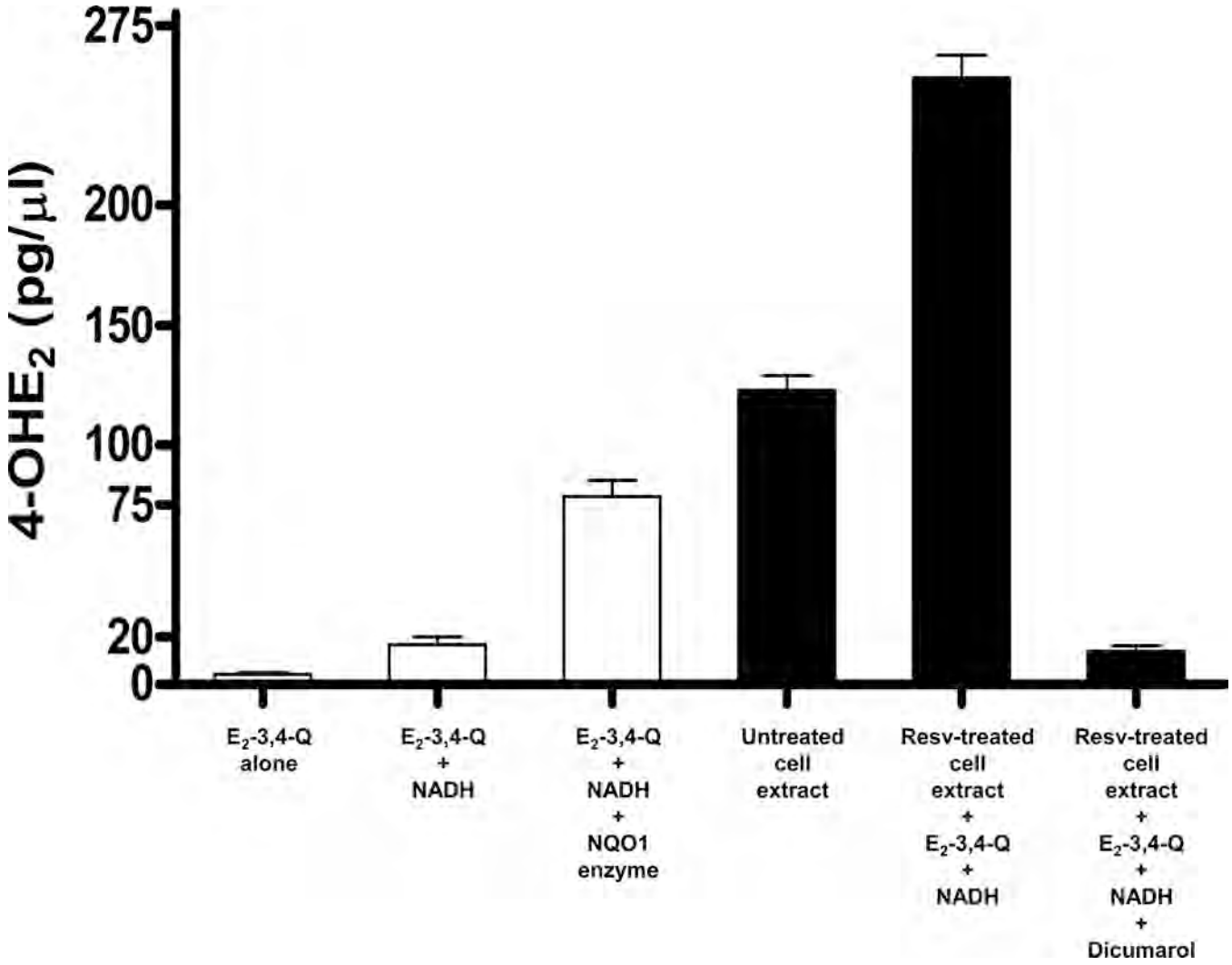

Figure 35.

Induction of NQO1 expression and activity in MCF-10F cells treated with Resv. NQO1 enzymatic activity, the reduction of E_2-3,4-Q to 4-OHE_2, was determined by UPLC-MS/MS. As a positive control, production of 4-OHE_2 by purified recombinant NQO1 incubated with E_2-3,4-Q + NADH was compared to E_2-3,4-Q and NADH without enzyme. The levels of the reaction product, 4-OHE_2, in Resv-treated cells were significantly different from those in the untreated cells, $p < 0.05$ as determined by ANOVA. The inhibition of 4-OHE_2 production by the NQO1-specific inhibitor dicumarol indicates that reduction of E_2-3,4-Q to 4-OHE_2 was by NQO1 (Lu et al., 2008; Zahid et al., 2008).

NIH-PA Author Manuscript

NIH-PA Author Manuscript

NIH-PA Author Manuscript

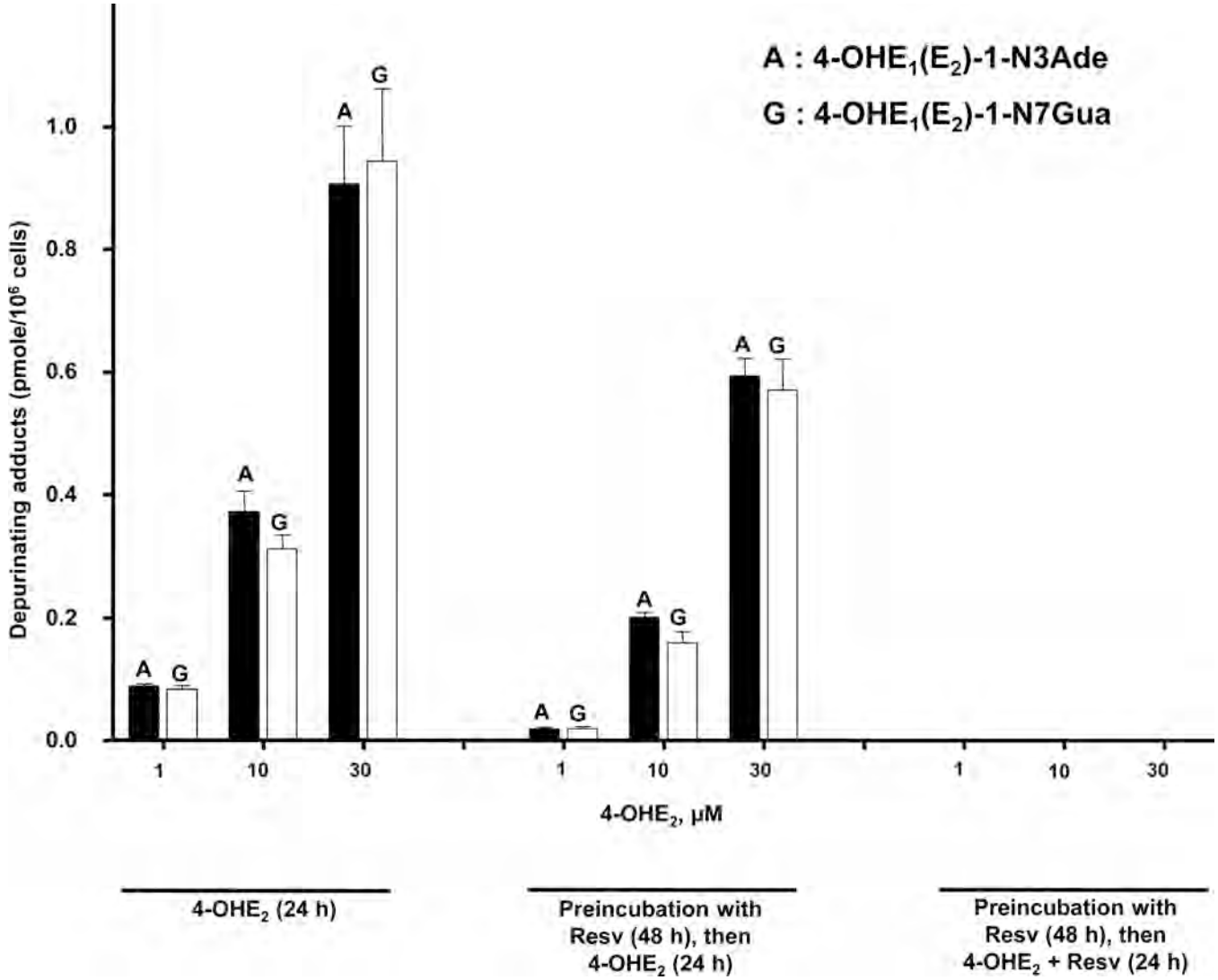

Figure 36.

Levels of depurinating DNA adducts in MCF-10F cells treated with 4-OHE_2 with or without Resv. The levels of DNA adducts in cells pretreated with Resv were significantly lower than those in the cells not pretreated with Resv, $p < 0.05$ as determined by ANOVA. When the cells were pretreated with Resv and fresh Resv was added along with 4-OHE_2, no adducts were detected (Zahid et al., 2008).

NIH-PA Author Manuscript

NIH-PA Author Manuscript

NIH-PA Author Manuscript

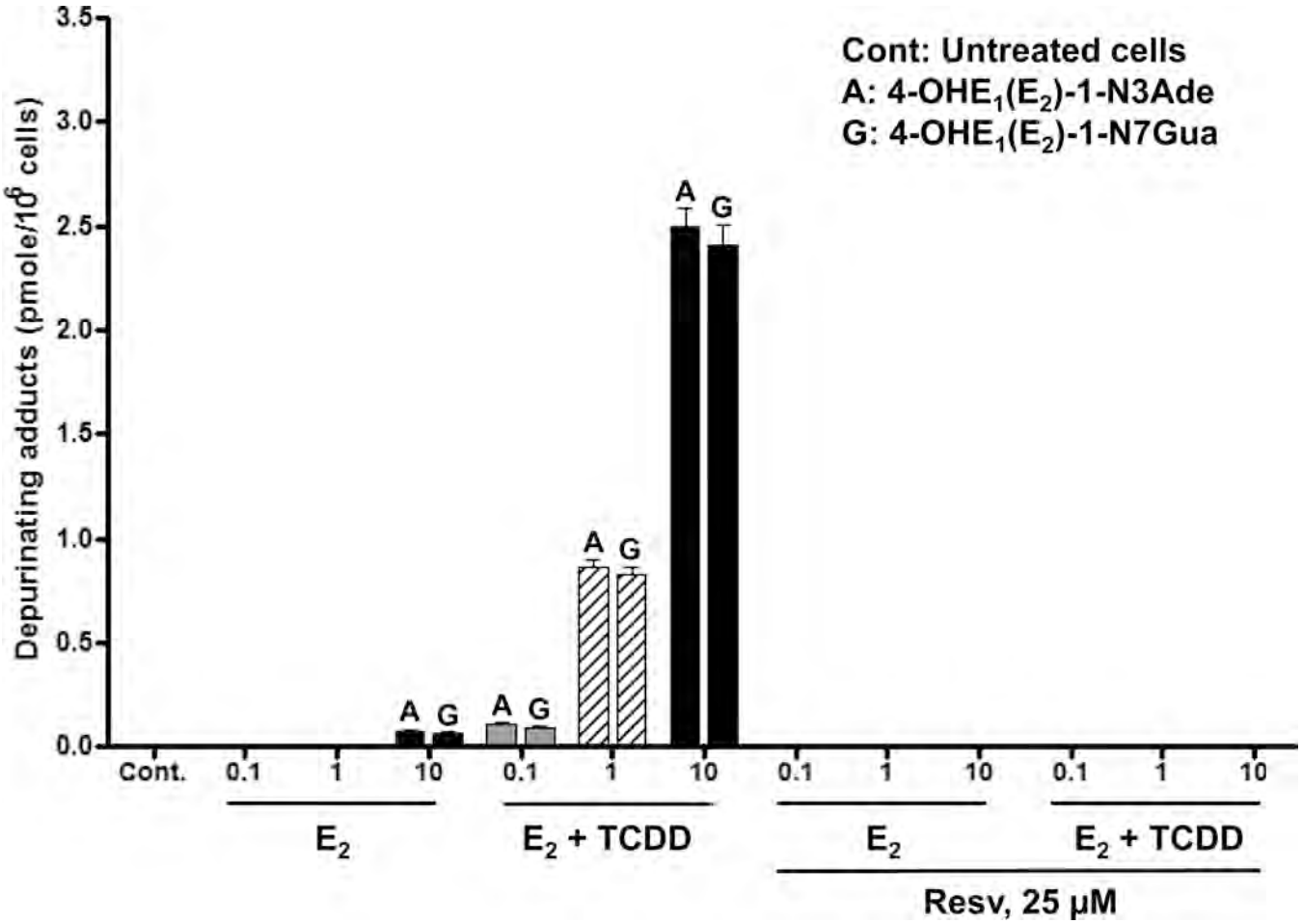

Figure 37.

Levels of depurinating DNA adducts in MCF-10F cells pretreated with TCDD with and without Resv and treated with increasing concentrations of E_2 for 24 h. The levels of DNA adducts in Resv pretreated cells are significantly different from those in the cells not pretreated with Resv, $p < 0.05$ as determined by ANOVA. The DNA adduct levels were corrected for recovery and normalized to cell numbers. *Columns*, mean of triplicate cultures from three experiments; *bars*, SD (Lu et al., 2008).

NIH-PA Author Manuscript
NIH-PA Author Manuscript
NIH-PA Author Manuscript

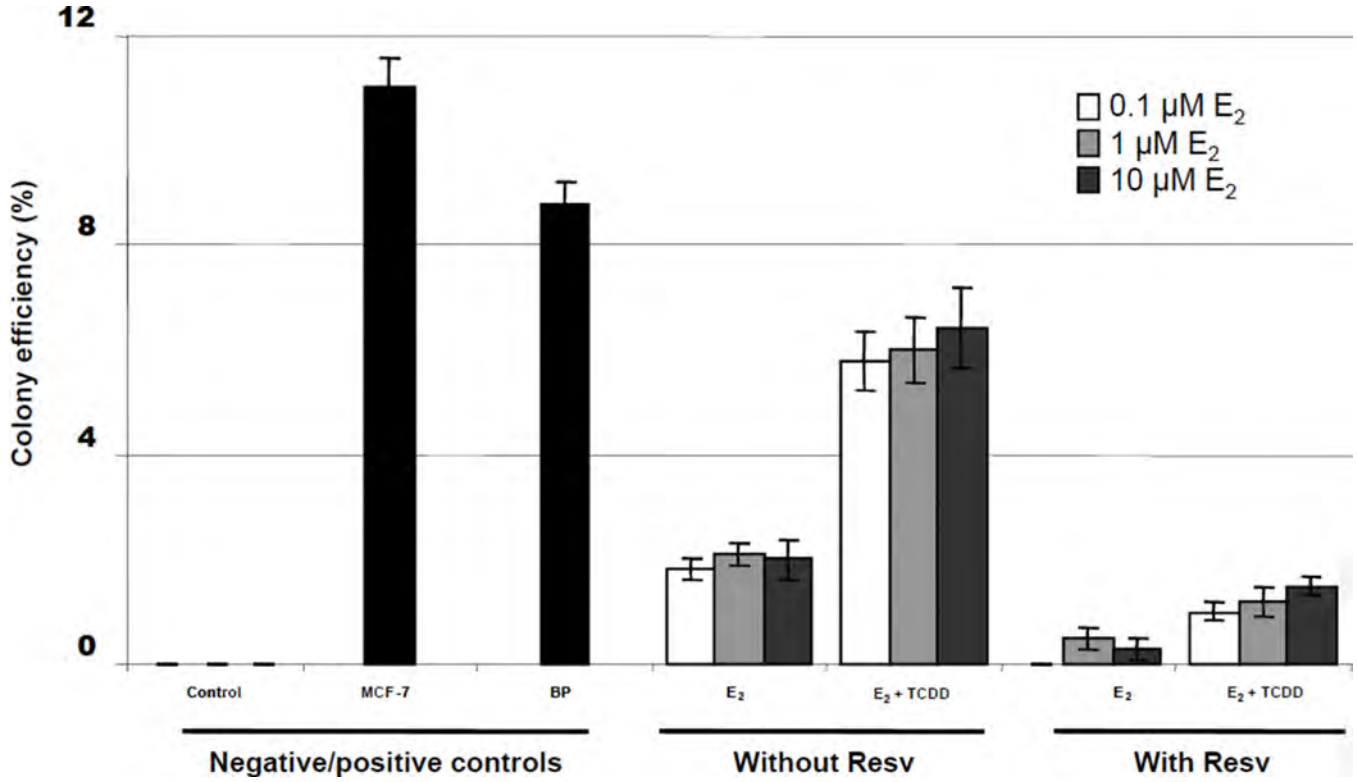

Figure 38.

Antitransformation effects of Resv on E_2-induced transformation of MCF-10F cells. MCF-10F cells were pretreated with TCDD with and without Resv, then treated with E_2. The results are expressed as colony efficiency (%): The number of colonies formed per number of cells plated×100. *Column*, mean of assays from triplicate experiments; *bars*, SD; $p < 0.05$. A negative control was conducted with MCF-10F cells cultured without any treatment. Two positive controls were included. One was cultured MCF-7 cells, which are a transformed cell line. In the other, MCF-10F cells were transformed with benzo[*a*]pyrene (BP) (Lu et al., 2008).

NIH-PA Author Manuscript
NIH-PA Author Manuscript
NIH-PA Author Manuscript

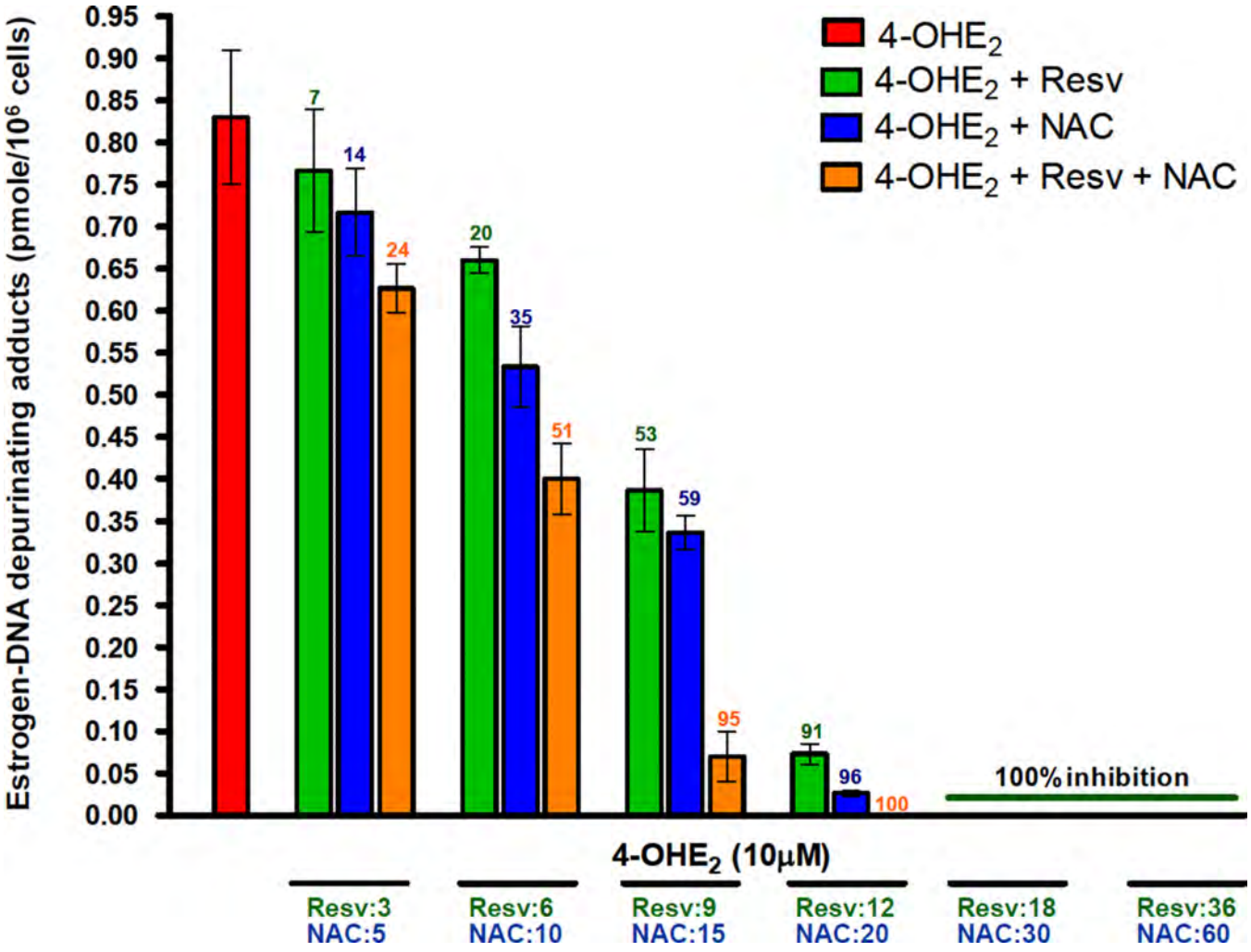

Figure 39.

Effects of NAC, Resv, or NAC + Resv on the formation of depurinating estrogen-DNA adducts in MCF-10F cells treated with 4-OHE_2. The number above each bar indicates the percent inhibition compared to treatment with 4-OHE_2 alone (Zahid et al., 2011a).

NIH-PA Author Manuscript

NIH-PA Author Manuscript

NIH-PA Author Manuscript

Table 1

Carcinogenicity of PAH in mouse skin and rat mammary gland

Compound	IP (eV)[c]	Carcinogenicity[a,b]	
		Mouse skin	Rat mammary gland
Dibenzo[*a*,*l*]pyrene-11,12-dihydrodiol	7.79	+++++	NT
5-Methylchrysene	7.73	+++	-
Dibenz[*a*,*h*]anthracene	7.61	+++	-
Benz[*a*]anthracene	7.54	±	-
Benzo[*a*]pyrene-7,8-dihydrodiol	7.49	++++	++
7-Methylbenz[*a*]anthracene	7.37	+++	±
8-Fluorobenzo[*a*]pyrene	7.32	+	+
7-Fluorobenzo[*a*]pyrene	7.31	++	±
10-Fluorobenzo[*a*]pyrene	7.29	-	+
4-Fluoro-7,12-dimethylbenz[*a*]anthracene	7.29	+	++
Dibenzo[*a*,*l*]pyrene	7.27	+++++	+++++
9-Fluorobenzo[*a*]pyrene	7.26	-	-
2-Fluoro-7,12-dimethylbenz[*a*]anthracene	7.24	+	-
Benzo[*a*]pyrene	7.23	++++	+++
7,12-Dimethylbenz[*a*]anthracene	7.22	+++++	+++++
10-Fluoro-3-methylcholanthrene	7.17	NT	++
8-Fluoro-3-methylcholanthrene	7.14	NT	++
3-Methylcholanthrene	7.12	++++	++++
6-Methylbenzo[*a*]pyrene	7.08	+++	++
1,2,3,4-Tetrahydro-7,12-dimethylbenz[*a*]-anthracene	6.94	+++	+++++

[a] Evaluation of mouse skin carcinogenicity is based on the results from repeated application and/or initiation-promotion obtained in our laboratory. Evaluation of rat mammary gland carcinogenicity is based on the results from intramammillary injection obtained in our laboratory.

[b] Extremely active, +++++; very active, ++++; active, +++; moderately active, ++; weakly active, +; very weakly active ±; inactive, -; not tested, NT.

[c] Determined from the absorption maximum of the charge-transfer complex of each compound with chloranil (Cavalieri et al., 1983), except for DB[*a*,*l*]P-11,12-dihydrodiol, 5-methylchrysene, dibenz[*a*,*h*]anthracene and BP-7,8-dihydrodiol that were calculated from the oxidation potentials of these compounds determined by cyclic voltammetry (Cremonesi et al., 1992).

NIH-PA Author Manuscript

NIH-PA Author Manuscript

NIH-PA Author Manuscript

Table 2

Correlation of depurinating adducts with H-*ras* mutations in mouse skin papillomas[a]

PAH	Major DNA adducts in mouse skin	H-*ras* mutations No. of mutations/No. of mice
DMBA	N7Ade (79%)	4/4 CAA → CTA
DB[*a*,*l*]P	N7Ade (32%)	4/5 CAA → CTA
	N3Ade (49%)	
DB[*a*,*l*]P-11,12-dihydrodiol	N7Ade (75%)	7/7 CAA → CTA
anti-DB[*a*,*l*]PDE	N7Ade (2.0%)	5/5 CAA → CTA
BP	C8Gua + N7Gua (46%)	7/13 GGC → GTC
	N7Ade (25%)	2/13 CAA → CTA

[a] Chakravarti et al., 1995

NIH-PA Author Manuscript
NIH-PA Author Manuscript
NIH-PA Author Manuscript

Table 3

Mutagenicity of E_2-3,4-Quinone

	Depurinating Adducts µmole/mol DNA-P		Stable Adducts µmole/mol DNA-P	H-*ras* mutations	
				A → G	Other
Tissue	**4-OHE$_2$-1-N3Ade**	**4-OHE$_2$-1-N7Gua**		**Total clones**	**Total clones**
SENCAR mouse skin[a]	12.5	12.1	0.004		
6 h				5/29	2/29
12 h				4/30	2/30
1 d				7/50	4/50
3 d				3/40	1/40
ACI rat mammary gland[b]	81	90	0.017		
6 h				16/29	3/29
12 h				14/34	6/34

[a] Chakravarti et al., 2001

[b] Mailander et al., 2006

NIH-PA Author Manuscript

NIH-PA Author Manuscript

NIH-PA Author Manuscript

Table 4

Representative profile of estrogen metabolites, conjugates and DNA adducts in a urine sample from a high-risk woman.[a]

NO.	Compound	pmole/mg creatinine mean, n=2	Total pmole/mg creatinine
1	Androstenedione	1.56	**1.56**
2	Testosterone	0.24	**0.24**
3	E_1 Sulfate	1.81	**1.81**
4	E_2*	5.29	**15.93**
5	E_1*	10.64	
6	2-OHE_2	3.09	**3.15**
7	2-OHE_1	0.05	
8	4-OHE_2	2.64	**2.91**
9	4-OHE_1	0.27	
10	16α-OHE_2	12.12	**38.64**
11	16α-OHE_1	26.52	
12	2-OCH_3E_2	1.95	**49.81**
13	2-OHC_3E_1	47.87	
14	4-OCH_3E_2	0.41	**5.08**
15	4-OCH_3E_1	4.67	
16	2-OH-3-OCH_3E_2	1.91	**10.27**
17	2-OH-3-OCH_3E_1	8.36	
18	2-OHE_2-1-SG	0.17	**3.10**
19	2-OHE_2-4-SG	0.17	
20	2-OHE_1-1-SG	0.49	
21	2-OHE_1-4-SG	0.47	
22	2-OHE_2-1+4-Cys	0.27	
23	2-OHE_1-1-Cys	0.10	
24	2-OHE_1-4-Cys	0.44	
25	2-OHE_2-1-NAcCys	0.07	
26	2-OHE_2-4-NAcCys	0.07	
27	2-OHE_1-1-NAcCys	0.43	
28	2-OHE_1-4-NAcCys	0.43	
29	4-OHE_2-2-SG	0.51	**1.77**
30	4-OHE_1-2-SG	0.50	
31	4-OHE_2-2-Cys	0.13	
32	4-OHE_1-2-Cys	0.06	

NIH-PA Author Manuscript

NIH-PA Author Manuscript

NIH-PA Author Manuscript

NO.	Compound	pmole/mg creatinine mean, n=2	Total pmole/mg creatinine
33	4-OHE_2-2-NAcCys	0.29	
34	4-OHE_1-2-NAcCys	0.28	
35	4-OHE_2-1-N7Gua	0.48	**2.81**
36	4-OHE_1-1-N7Gua	2.33	
37	4-OHE_2-1-N3Ade	137.78	**137.90**
38	4-OHE_1-1-N3Ade	0.13	
39	2-OHE_2-6-N3Ade	0.06	**0.07**
40	2-OHE_1-6-N3Ade	0.02	
		Ratio[b]	**936**

[a] Gaikwad et al., 2008

[b] See Figure 22 for a definition of the ratio.